Feasibility of Solar/Heat Pump Systems for Reducing Conditioning Energy Consumption

by

GREGORY J. MARSICEK JR.

A thesis submitted in partial fulfillment of
the requirements for the degree of

MASTER OF SCIENCE
(MECHANICAL ENGINEERING)

at the

UNIVERSITY OF WISCONSIN – MADISON

2012

Approved by

_____

Professor Sanford A. Klein

_____

Professor Gregory F. Nellis

Date:_____

Abstract

A thermally efficient building model was developed to be used with high efficiency conditioning equipment in an effort to reduce building energy consumption for space heating and cooling. BEopt was used extensively to determine the ideal construction parameters to achieve a low energy building envelope (BEopt, 2012). With a complete set of construction parameters, the building model was created in TRNSYS using the Type 56 Multi-zone Building model (TRNSYS, 2010).

A family of four was assumed to occupy the home, and a schedule was created to model the internal generation from showers, cooking, and occupants. Two locations, Chicago, IL and Dallas, TX were chosen to simulate the building models. These locations were chosen because Chicago represents a heating dominated location while Dallas represents a cooling dominated location.

To meet the calculated building load, several different options were considered. The first was an air-source heat pump. A sizing methodology was created for the heat pump based on the ability to meet the building load and life cycle costs. When the air-source heat pump system was compared to a conventional system, consisting of a high efficiency natural gas furnace and SEER 16 air conditioning system, the results found that the heat pump system consumes 10% more source energy and has higher life cycle costs. For a cooling dominated location, the heat pump outperforms the conventional system, both in terms of energy and economic savings. A geothermal heat pump is used in the cold climate case as well. This system had significant source energy savings (28%) over the conventional system and higher life cycle costs.

Two solar systems were also used, a photovoltaic system and solar thermal heating system. The photovoltaic system was roof mounted and was determined to be a better investment than the solar thermal heating system, as it saved more source energy at lower life cycle costs.

Acknowledgements

This research was made possible by many people, which I will attempt to summarize in the following paragraphs.

I would first like to thank the National Institute of Standards and Technology (NIST) for their sponsoring of this research. I would like to thank Dr. Piotr Domanski for reviewing my research and offering many suggestions. In addition, I would like to thank Harrison Skye for hosting me (along with the rest of the Net-Zero buildings team at NIST) during my trip to present and tour the facility in Gaithersburg, MD.

I am thankful for the time and effort invested by my advisors, Professors Sanford Klein and Greg Nellis. Both Greg and Sandy have provided an unlimited supply of knowledge that has made this research possible. The proofing of my progress reports and thesis helped me improve my technical writing skills. They also taught excellent classes, which were by far my favorite courses during my college career. Beyond research and class, there was always sound advice given and relaxing conversations had about sports, photography, running or current events. I also would like to thank Doug Reindl for serving on my thesis committee. In addition, my undergraduate assistant, Cody Eaton, provided much needed help with building load calculations.

I'd also like to give special thanks to Sandy. During my undergraduate Thermodynamics course, he offered guidance that shaped me into the engineer I am today. Without the experience gained and relationship formed during that semester, I would not be in the position I am in now. I will be forever grateful for the opportunity he provided me.

In addition, I would like to thank all of my old Solar Energy Lab-mates. I am thankful that Ty Neises took me on as an undergraduate assistant. This turned out to be the start of a great friendship for Ty and I. I also met Will through Ty, and the three of us were able to enjoy many runs to picnic point or through the arboretum and workouts on the track. A special thanks to Will for coaching me to a PR in the Crazylegs 8K (and to Ty for training with me). See you guys in Colorado! Mandy, you were my last remaining 1337 friend. Thank you for answering all my questions throughout my time here and for laughing with me when I attended conferences that I didn't pay for (but insisted that I did pay). Also, I hope Ty, Will and I didn't drive you crazy during your time in 1337.

When Ty and Will left new students came; Ser Eric of the Alar, Rogelio (Row-Jelly-O), Russ, Diego, Brad K, Ser Bradley of the Moore and Nevzat. Thanks for spending your days with me, both at the SEL and at Union South. I will certainly miss you all, but hopefully we will meet up again in the future (maybe for season 6 of Game of Thrones or for some QQ).

Finally, I would like to thank my family and friends for your support throughout my 20 years of education. My parents have always provided encouragement, especially when the road was tough and I was in need. I'd most of all like to thank Lauren and our cats Hank and Henrietta for their day to day support. You always were there to enjoy the good times with me but were also there to put a smile on my face after a long day.

Table of Contents

List of Figures

List of Tables

Nomenclature

A	area (m^2)
a_0	intercept of collector efficiency (-)
a_1	negative of the 1st order coefficient in the collector efficiency equation (kJ/hr-m^2-K)
a_2	negative of the 2nd order coefficient in the collector efficiency equation (kJ/hr-m^2-K^2)
b_0	negative of the 1st order coefficient in the incident angle modifier curve fit equation (-)
b_1	negative of the 2nd order coefficient in the incident angle modifier curve fit equation (-)
$\dot{C}$	capacitance rate (kJ/hr-K)
C	cost ($)
DD	degree day (°C-day)
Er	percent error (%)
E	incident solar radiation (W/m^2)
f	fraction (-)
F	correction factor (-)
F_R	collector heat removal factor (-)
$\dot{g}$	internal generation (kJ/hr)
h	enthalpy (kJ/kg)
I_T	solar radiation incident on the collector (kJ/hr-m^2)
$K(\tau\alpha)$	incidence angle modifier (-)
$\dot{L}$	building load (kJ/hr)
L	energy consumption (kW-hr)
LCC	life cycle cost ($)
M	manufacturer predicted value
$\dot{m}$	mass flow rate (kg/hr)
P	power (W)
P_1	ratio of life-cycle fuel costs (-)
P_2	ratio of owning cost to initial cost (-)
Q	heat (kJ)
$\dot{Q}$	heat, rate (kJ/hr)

T	temperature (K)
TT	TRNSYS Type predicted value
U	heat transfer coefficient (kJ/hr-m^2-K)
U_L	overall collector heat loss coefficient
U_{LT}	thermal loss coefficient dependency on T (kJ/hr-m^2-K^2)
UA	conductance (kJ/hr-K)
W	work (kJ)
$\dot{W}$	power (kJ/hr)

Acronyms

AFUE	Annual Fuel Utilization Efficiency
DOE	Department of Energy
E+	EnergyPlus
EER	Energy Efficiency Ratio
ERC	Energy Rate Control
HVAC	Heating, Ventilating, and Air-Conditioning
IDB	Indoor Dry Bulb
IWB	Indoor Wet Bulb
NIST	National Institute of Technology and Standards
NREL	National Renewable Energy Laboratory
ODB	Outdoor Dry Bulb
PLF	Part Load Factor
PLR	Part Load Ratio
PV	Photovoltaic
SAM	System Advisor Model
SEER	Season Energy Efficiency Rating
SHGC	Solar Heat Gain Coefficient
TESS	Thermal Energy System Specialists
TLC	Temperature Level Control
TRNSYS	Transient System Simulation Tool

Greek Letters

ε	heat exchanger effectiveness (-)
η	efficiency (-)
$(\tau\alpha)_n$	product of the cover transmittance and the absorber absorptance at normal incidence (-)

Subscripts

air,in	air inlet conditions (heat exchanger)
amb	ambient conditions
av	average conditions
b	building
c	collector
cycling	cycling conditions
TotalIncident	total incident radiation
H,I	hot inlet of heat exchanger
M	module
r	refrigerant
ss	steady state conditions
TempCorr	temperature correction
u	useful energy
w	window
water,in	water inlet conditions (heat exchanger)

1. Introduction

1.1 Project Background

Building research efforts have been focused on finding the optimal path to net-zero residential building operation. The incentive for this research is the significant energy consumption associated with the housing sector and the growing concern about the availability and carbon content associated with the consumption of fossil fuels. For 2010, the United States Department of Energy reported that the residential sector contributed to 22% of the United States' total energy consumption, seen in Figure 1.1.

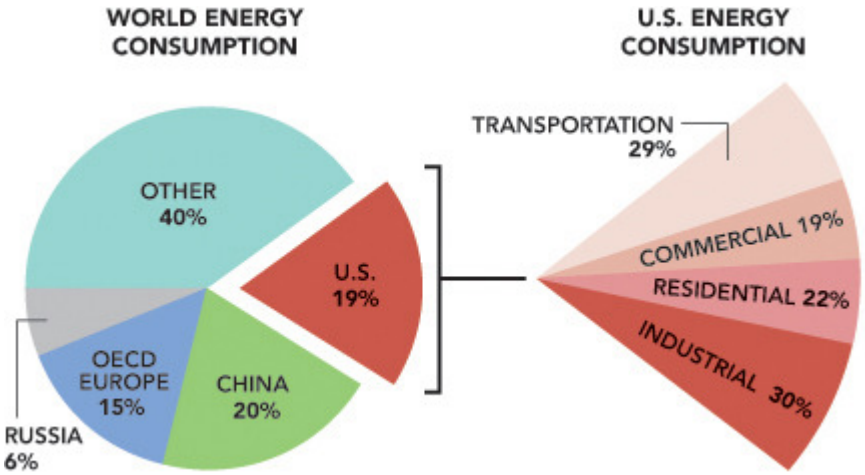

Figure 1.1: Energy consumption by sector in the United States (U.S. Department of Energy, 2012).

In addition to a high current demand, the residential sector has shown throughout history to have an increasing demand for energy, seen in Figure 1.2. This is understandable, as over the past century there has been an increase in the number of appliances present in the average home as well as an increasing population. It is expected that this energy demand will contribute to a growth in energy demand in the future.

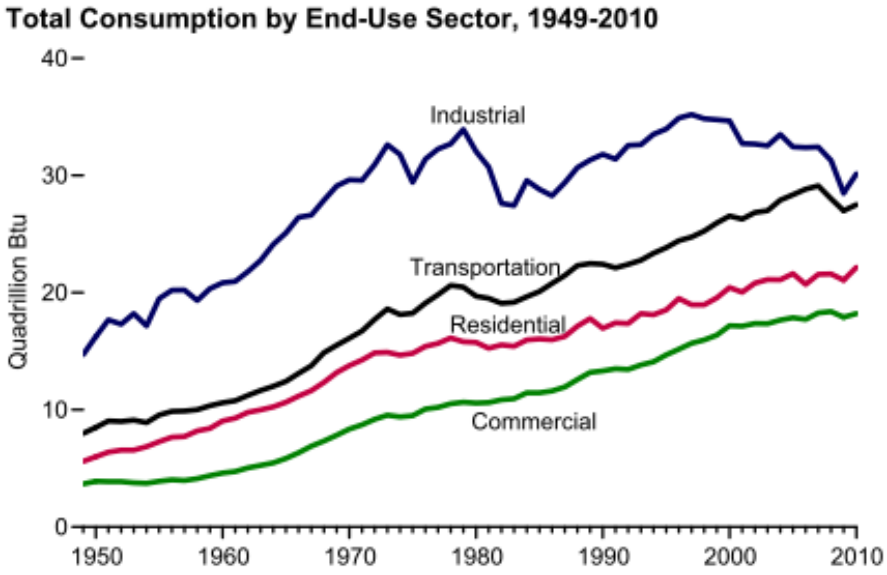

Figure 1.2: Historical energy demand trends by sector for the United States (U.S. Energy Information Administration, 2010).

If the goal is to reduce the amount of energy consumption of the United States, it is clear that focusing on the residential sector will make an impact. According to the U.S. Department of Energy, 50% of all energy consumed by residential homes is contributed to space heating and cooling (U.S. Department of Energy, 2012). In order to realistically achieve net-zero operation, in which the building produces as much energy as it consumes annually, the energy requirement for heating and cooling must be controlled. This research will evaluate using heat pumps and solar energy to reduce the condition requirements, as compared to a conventional system consisting of a natural gas furnace and air conditioner.

1.2 Net-Zero Literature Review

A net-zero building can be defined simply as a building that generates as much energy as it consumes over the course of a year. There are two primary ways to evaluate a building's energy consumption. The first method is based on a site energy basis. Site energy can be easily determined by referring to the building's utility bills, which often

list the total energy consumption of both electricity (kW-hr) and natural gas (therms). However, this does not take into account the energy expense of electricity, from the generation and distribution. A source energy net-zero building produces as much energy as it consumes on a source energy basis, which considers how the energy consumed on site is extracted, produced/generated and distributed. (Crawley, 2009)

Many net-zero buildings exist in the United States that are either occupied or used as test facilities. One case study is a Habitat for Humanity home in Denver, Colorado (Christensen, et al., 2008). This construction is of interest because it is in a climate location that can have a significant heating requirement. The construction is a 1,280 ft^2, 3 bedroom home, which features a ductless natural gas furnace located in the main living area and small electric baseboard strip heaters in the bedrooms. This home has an efficient thermal envelope, utilizing double stud walls (two 2x4 wall joined together, each with R13 insulation) and low conductance windows (u-value = 0.30 Btu/hr-F-ft^2). A 4 kW photovoltaic (PV) array provides ample electricity generation which offsets electricity consumed by appliances, lights and baseboard strip heaters. It was found that this home produced 24% more source energy than it consumed over the course of a year (by returning excess electricity generation to the grid). However, it was noted that the energy savings can vary greatly depending on occupant behavior and yearly climate conditions, as in the second year the home produced 12% more source energy than it consumed. It is possible that the home may not meet net-zero with extreme weather conditions or abnormal occupant behavior.

In colder climates, net-zero implementation is much more difficult due to the large heating loads. In Massachusetts, several net-zero homes ranging from 1100 to 2600 ft^2

have been built that utilize mini-split air-source heat pump systems (Bergey, 2011). These systems eliminate the requirement for ductwork, which lowers building costs. Like the previous net-zero home in Denver, these homes are very thermally efficient. However, most houses have large PV arrays, on the order of 7.6 kW, normally limited by roof size.

The EcoTerra house near Montreal, Canada uses a different design to achieve net-zero operation (O'Brien, 2010). This 2,476 ft^2 home uses building integrated photovoltaic array with thermal recovery to produce electricity and meet the building heating load. Air is drawn behind the PV array and warmed to provide space heating to the home. In addition, a geothermal heat pump system is used to supplement the solar system.

1.3 Research Motivation

This stated goal to find economically feasible ways to achieve net-zero operation for residential homes requires the research of various methods to condition a home and the economic consequences. A net-zero test facility has been constructed in Gaithersburg, Maryland at the National Institute of Technology (NIST) campus, shown in Figure 1.3.

Figure 1.3: This is a Google SketchUp model of the net-zero home located in Gaithersburg, MD. This home will be used as a test facility and as a demonstration to the general public.

The project objective is to evaluate the performance of a net-zero home through this test facility. This home will also validate previous building energy and ventilation models (NIST, 2011). Like the net-zero test home, this research uses a home that looks, feels, and operates like a high quality home that United States citizen's are accustomed to.

The primary objective of this research will be to investigate the feasibility of using a heat pump and solar energy to reduce the energy consumption required for building conditioning, primarily in cold climate cases where the heating load dominates the total building energy consumption. Both air-source and ground source heat pump systems are investigated along with photovoltaics and solar thermal for space heating. These systems are evaluated against a conventional system consisting of a natural gas furnace and air conditioner to determine the benefit (or drawback) in terms of energy and economic savings.

1.4 Thesis Outline

This report closely follows the path that the research took. First, a building model was constructed with the Transient System Simulation Tool software (TRNSYS, 2010). This 2,200 ft^2 building model was a thermally efficient design, based on information gathered from parametric simulations in BEopt, a simulation program distributed by the National Renewable Energy Laboratory (BEopt, 2012). The outline of this process is found in Chapter 2. With a completed building model, the research shifted to preparing models for air-source and ground-source heat pumps, photovoltaic array and solar thermal heating system (with storage). These models are described in detail in Chapter 1. The simulation results from the building model and conditioning equipment models are

discussed in Chapter 4. Conclusions and recommendations for the future of net-zero research and discussion are presented in Chapter 5.

2. Building Model

This chapter will discuss the development of a building model that will be simulated using weather conditions associated with various locations (i.e. climate zones). First, two different simulation tools will be discussed, BEopt and TRNSYS, in the context of how they were used for this research. Then, a comparison of the TRNSYS and DOE-2.2 simulation programs will be made for verification. Lastly, the building model developed for this project will be outlined and the various locations investigated are discussed.

2.1 BEopt and BEoptE+

BEopt is an optimization program distributed by the National Renewable Energy Laboratory (NREL) that is used in conjunction with TRNSYS and DOE-2.2. TRNSYS is used to calculate the solar loads for photovoltaics and solar domestic hot water heating system. DOE-2.2 is responsible for simulating the building envelope, lighting, occupant loads and heating and cooling loads. When a simulation is performed, initial BEopt parameters are input to TRNSYS and DOE-2.2. The results using these parameters are reported to BEopt and the BEopt program makes parameter adjustments that are returned to TRNSYS and DOE-2.2 for another simulation (Christensen et al., 2006). BEopt allows a user to easily create a building envelope and outfit it with various construction parameters, as seen in Figure 2.1 and Figure 2.2.

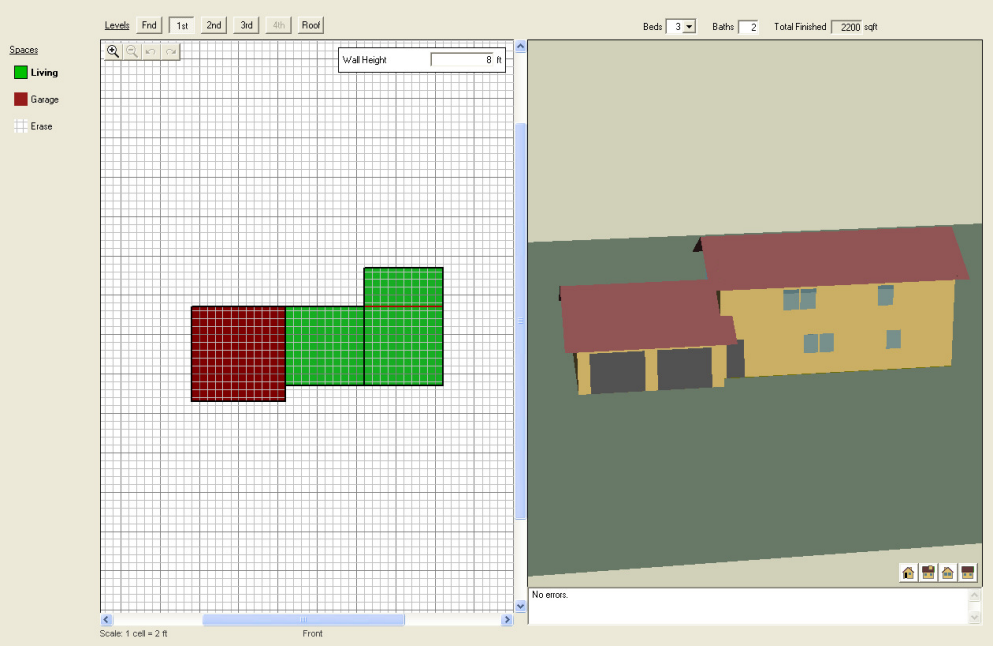

Figure 2.1: The building construction screen in BEopt. Buildings are easily created by clicking and dragging on the grid.

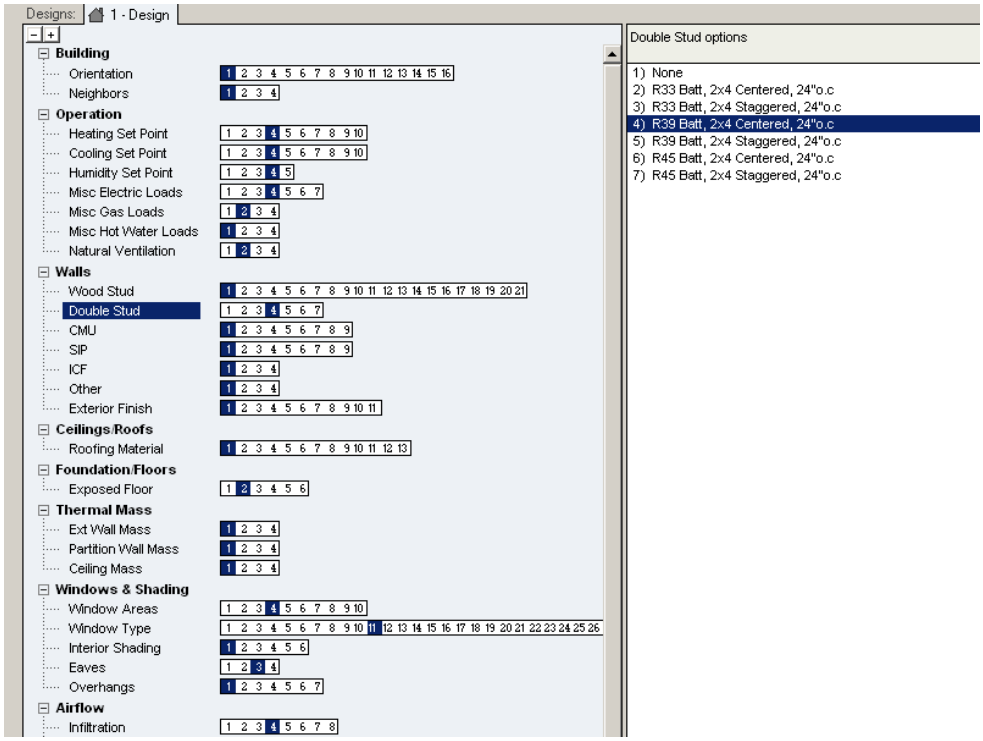

Figure 2.2: BEopt building parameters screen where insulation and window type can be assigned to the building.

Recently, NREL has switched from DOE-2.2 to EnergyPlus (E+) for hourly building simulation and the program title has been changed to BEoptE+ (however this report will

refer to BEoptE+ as BEopt). There are no other major interface changes that differ from the DOE-2.2 versions of BEopt. E+ allows for more detailed building simulations ranging from stratified zone air modeling to the ability to simulate time steps less than one hour (Hong et al., 2008). A drawback to using E+ (as opposed to DOE-2.2) is that simulation time is greatly increased, causing optimizations that require many iterations to be time consuming. More options for building parameters have been added to BEopt, such as geothermal heat pumps or the possibility to add performance degradation to unmaintained heating, ventilating and air conditioning (HVAC) equipment.

The primary reason for using BEopt was to perform parametric simulations to determine what parameters yield an energy efficient house. An optimal house design will be selected based on BEopt, and both economic data (capital costs, etc.) and engineering data (thermal conductivity, etc.) will be referenced for the TRNSYS simulations.

2.1.1 BEopt Parametric Simulations

The design of the residential home has the objective of being both aesthetically pleasing to homeowners and also suitable for the installation of efficient conditioning equipment. For a family consisting of two adults and two children, 2,200 ft^2 of finished floor area was used. In addition, half of the basement area was unfinished and unconditioned, which was assumed to be used for storage. An unfinished two car garage (24 ft by 24 ft) was included in the model as well. The front view (pointing south-east) and the back view (pointing north-west) are shown in Figure 2.3. These drawings of the home come from Google SketchUp (Google SketchUp 8, 2011).

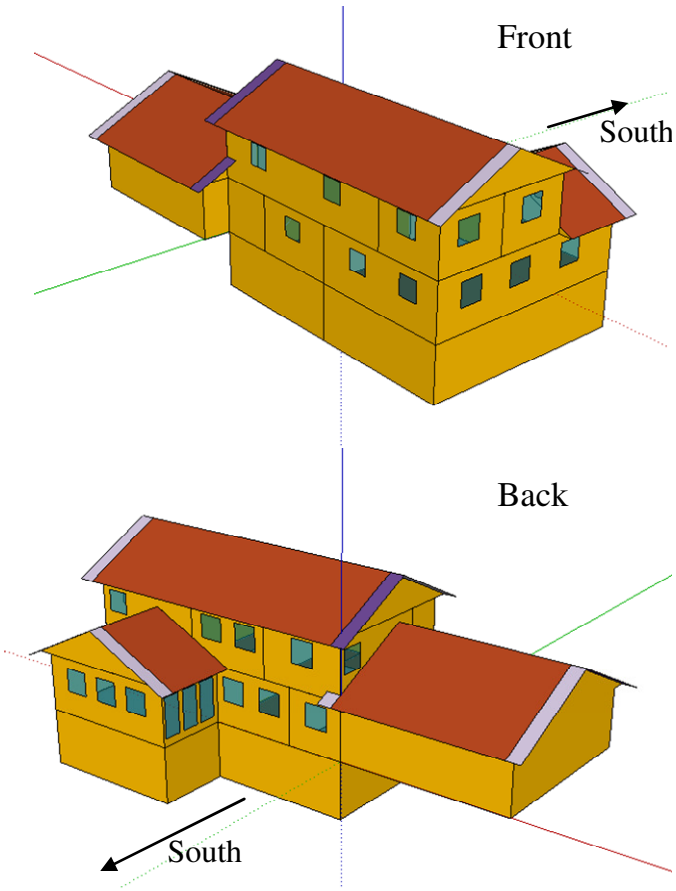

Figure 2.3: Front and rear view of the residential home. This model is shown in Google SketchUp. The model was imported into TRNSYS using the TRNSYS3d Plugin. The "back view" is the south facing portion of the building.

With a building envelope defined, the next step was to run simulations to determine what building parameters should be used (insulation, window type, etc). Parametric simulations were run for the heating dominated climate location of Chicago, Illinois. While this location is heating dominated, it does have large peak cooling loads, as temperatures during the cooling season can reach nearly 40°C. The weather file used was an Energy+ format (.epw) for O'Hare International Airport.

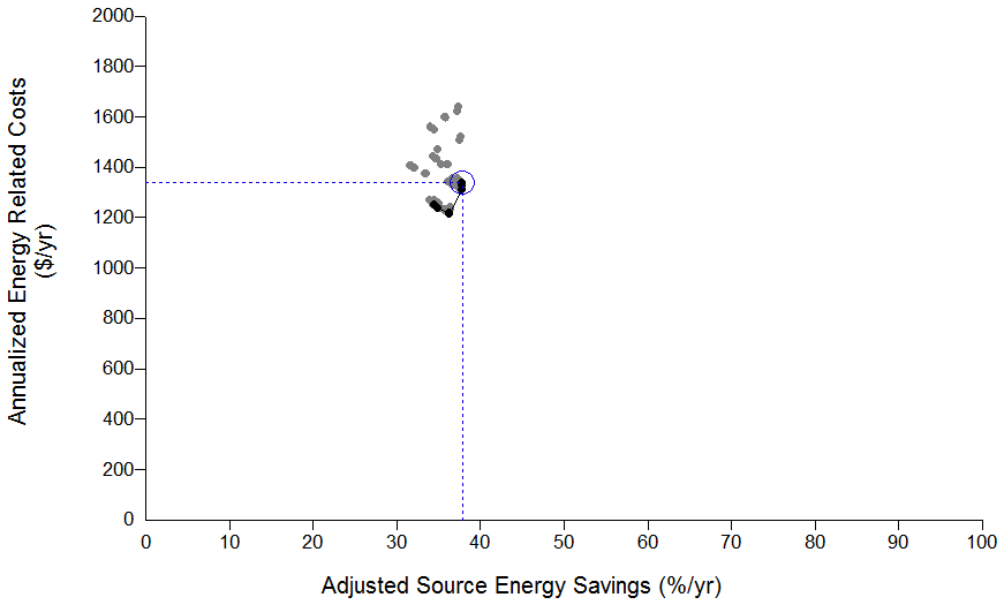

Figure 2.4: BEopt parametric simulation results. Each point is a unique building simulation. The largest energy savings point is highlighted.

Figure 2.4 shows the BEopt parametric simulation results on an energy costs vs. source energy savings plot. Each data point on this plot represents a building simulation, each with different parameters. The basis for this plot is the Building American Baseline home, representative of the average residential house. The Building America House Simulation Protocol is designed to promote the reduction of energy consumption in residential homes, released by the United States Department of Energy (BAHSP, 2010). It includes information such as average lighting usage, water usage and many other occupant related data. It also discusses the B10 Benchmark home, which is used as a baseline to evaluate energy efficient house designs. Data points on Figure 2.4 to the right of 0% source energy savings represent saving more source energy than the baseline home. The largest source energy saving building design (38% source energy savings) was chosen for this research and will be defined in the following section.

2.2 Transient System Simulation Tool (TRNSYS)

The primary tool used for this research was TRNSYS. TRNSYS is a robust simulation tool that contains many models, or Types, for HVAC and other building related equipment. These Types require the user to designate parameters, such as rated capacity or efficiency, which do not change throughout the course of the simulation. The inputs may vary at each time step and the outputs are calculated based on the Type's source code. These Types make TRNSYS easy to use, in that models for each piece of equipment do not need to be developed from scratch.

2.2.1 Type 56 Multi-zone Building

The Type 56 Multi-Zone Building was used to model the thermally efficient building defined by BEopt. This model allows the user to create a building envelope consisting of thermal zones. The thermal zones can represent a single room in a home and these can then interact with other thermal zones or rooms. The more thermal zones that a model has, the more computationally intensive the model becomes as each thermal zone has its own set of calculations for thermal gains and losses.

The Type 56 Multi-Zone Building has two different simulation methods: Energy Rate Control (ERC) and Temperature Level Control (TLC). Simulations that use TLC mimic the function of a real building, in that the temperature is allowed to float in response to the actual operation of the conditioning equipment and building load. For example, this simulation would require a control strategy that would monitor the zone temperature and determine when conditioning is required. With a TLC simulation, small time steps must be used which increases the simulation time. The TLC simulation will be used in a comfort analysis to determine the effects of having a properly tuned air delivery system.

An air delivery system controls the amount of air delivered to each room. Improper tuning leads to over or under conditioned rooms and occupant discomfort. In addition, this also may lead to excess energy consumption. These results are found in Chapter 4 of this thesis.

An ERC simulation on the other hand does not allow the temperature to float. By setting the zone temperature, TRNSYS will calculate the load required to meet this set point, based on equation (2.1), where $\dot{L}$ is the load required to meet the building set point T_{house}. Generation (solar gains, internal generation, etc) is represented by $\dot{g}$, UA_b is the building conductance and T_{amb} is the ambient temperature

$$\dot{L} = \dot{g} + UA_b \left(T_{house} - T_{amb} \right) \tag{2.1}$$

It should be noted that equation (2.1) does not account for the transient operation of the heating or cooling equipment that meet the load. However, the benefit of ERC is that the building model can be simulated once and a load file can be written for use later with the conditioning equipment, thereby saving computational effort.

The following sections will outline the details of the thermally efficient home found from the parametric simulations in BEopt. These details are implemented in to the TRNSYS model using TRNSYS3d, a Google SketchUp plug-in (TRANSSOLAR, 2010). This building model will be used in conjunction with a heat pump in an effort to reduce the energy required to meet the building load.

2.2.2 Construction Characteristics

The envelope construction parameters are defined in Table 2.1. As stated previously, BEopt contains engineering specifics (thermal conductivity, density, etc) for all of these materials. These data were used for the creation of the building model in TRNSYS. One other note to make is that this same building is used for all climate zones in the United States, with the exception of the window type as discussed in the subsequent section.

Table 2.1: Building construction parameters for the thermally efficient home.

General		
	Total Finished Floor Area	2200 ft2
	Beds	3
	Baths	2
Walls		
	Double Stud	R45 batts, 2x4 Centered, 24"o.c
	Exterior Finish	Grey Vinyl
	Interzonal Walls	R-19 Batts, 2x6, 24"o.c.
Ceilings/Roofs		
	Unfinished Attic	Roof R38 Fiberglass + 3.5" Rigid Ins
	Finished Roof	R19 Fiberglass
	Roofing Material	Asphalt Shingles, Dark
Foundation/Floors		
	Finished Basement	4ft R5 Rigid, 8’ walls
	Unfinished Basement	Wall 4ft R5 Rigid
	Interzonal Floor	R13 Fiberglass
	Exposed Floor	20% Exposed
Thermal Mass		
	Floor Mass	Wood Surface
	Ext Wall Mass	2 x 5/8" Drywall
	Partition Wall Mass	2 x 5/8" Drywall
	Ceiling Mass	2 x 5/8" Ceiling Drywall
Windows & Shading		
	Interior Shading	Summer = 0.5, Winter = 0.95
	Eaves	2 ft
Airflow		
	Airchanges Per Hour	0.5

2.2.3 Window Selection

Window selection for the building was based on the climate that the building is located in. One of the primary factors associated with window design is the Solar Heat Gain Coefficient (SHGC). A low SHGC means that very little solar radiation is transmitted through the window into the home. This would be ideal for a cooling dominated location, as reducing the solar gain through the window will reduce the cooling load. However, in a heating dominated location, a higher SHGC would be beneficial, as the solar gains will reduce the heating load (EWC, 2012).

In addition, the heat transfer coefficient of the window (i.e., the U-Value, measured in W/m^2-K) is important in a heating dominated climate. Equation (2.2) defines the conduction through a window.

$$\dot{Q}_w = U_w A_w \left(T_{indoor} - T_{outdoor} \right) \tag{2.2}$$

As seen in the definition of conduction through a window (where $\dot{Q}_w$ is the rate of heat transfer, A_w is the window area, and T_{indoor} and $T_{outdoor}$ are the indoor and outdoor temperatures) a low U_w value will reduce the heat transfer through the window. In a cold climate, during the heating season it is normal for the temperature difference between the indoor and outdoor temperatures to reach 30°C to 40°C. For warmer climates, the temperature difference during the cooling season is more often 10°C to 20°C, putting less emphasis on the U-value of the window and more emphasis on the SHGC. Table 2.2 summarizes the two windows used in this research.

Table 2.2: Window parameters vary by location.

Climate Type	U-Value [W/m2-K]	SHGC [-]
Cold	0.91	0.61
Warm	2.79	0.379

2.2.4 Internal Gains and Occupant Behavior

Another important aspect of a building is the occupant behavior and the internal gains from the occupants and appliances. The building chosen for this research is occupied on a daily basis by two adults and two children. A simple schedule was used which takes into account common tasks such as cooking, sleeping and bathroom use. Table 2.3 presents the sensible gains from various appliances.

Table 2.3: Sensible internal gains for the building, sourced from BEopt and E+. These gains were used in a simple schedule that included daily cooking, showering, sleeping, etc.

Gain Type	Sensible [kJ/hr]
Basement Lighting	371.21
Bathtub Gain	51.48
Clothes Dryer	177.98
Clothes Washer	66.9
Cooking Range	324.6
Dishwasher	137.73
Refrigerator	410
Lighting	1670.6
Basement Electronics	329.9
Living Electronics	1484.5
Shower	200
Sink	52.83
Person	216

Note that the latent gains are not considered. It is assumed that the conditioning equipment, if properly sized, will be able to control the humidity within the house and that additionally, a dehumidifier or humidifier will be present for extreme weather conditions or occupant behaviors.

The occupants are also assumed to be energy conscious, taking advantage of temperature set-backs or step-ups, depending on the season. During transition months such as in early spring, the occupants are assumed to open the windows even if the afternoon temperatures cause the building temperature to increase beyond the cooling set point. Occupants are also assumed to open the windows when the outdoor temperature is either below the cooling set point or above the heating set point. Table 2.4 and Table 2.5 show the heating and cooling set points for both weekdays and weekends.

Table 2.4: This table presents the cooling set points for weekdays and weekends.

Weekday Cooling		Weekend Cooling	
Time of Day [hr]	**Set Point [C]**	**Time of Day [hr]**	**Set Point [C]**
0	22.78	0	22.78
7	22.78	24	22.78
7	24.44	-	-
16	24.44	-	-
16	22.78	-	-
24	22.78	-	-

Table 2.5: This table presents the heating set points for the weekdays and weekends.

Weekday Heating		Weekend Heating	
Time of Day [hr]	**Set Point [C]**	**Time of Day [hr]**	**Set Point [C]**
0	18.33	0	18.33
7	18.33	8	18.33
7	16.67	8	20
16	16.67	23	20
16	20	23	18.33
22	20	24	18.33
22	18.33	-	-
24	18.33	-	-

2.2.5 Ground Temperature

Average monthly ground temperatures were used for building simulations in TRNSYS. The ground temperatures were again obtained from BEopt. BEopt, references the

Kusuda and Achenbach (1965) model for predicting ground temperatures based on air temperatures and soil type. This prediction method is also used by DOE-2.2. Figure 2.5 shows the average ground temperatures for Chicago, Illinois.

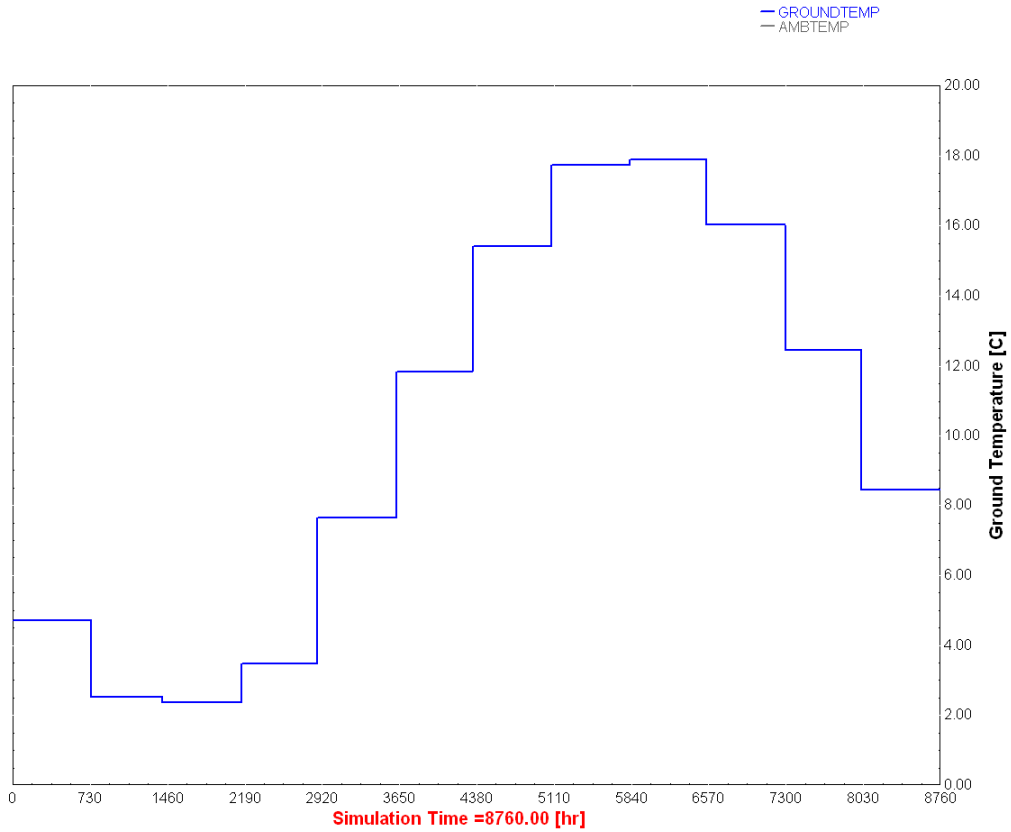

Figure 2.5: Monthly average ground temperatures for Chicago, IL (read from the right y-axis). These were predicted using the Kusuda and Achenbach method.

2.3 EnergyPlus and TRNSYS Building Model Comparison

Prior to modeling the efficient home, a 500 ft^2 single room building was constructed in TRNSYS to verify its simulated characteristics against a similar E+ model. This building model contained no windows or internal generation and was an uninsulated slab on grade construction. Both simulations calculated the amount of energy required to maintain a set point of 20°C, thus neither considered potential transient effects associated with HVAC equipment. The results from these simulations are seen in Table 2.6

Table 2.6: Comparison of results for the 500 ft^2 building.

	Energy+		TRNSYS		Percent Error	
Month	Heat [GJ]	Cool [GJ]	Heat [GJ]	Cool [GJ]	Heat [%]	Cool [%]
January	6.129	0	6.083	0	-0.75	0.00
February	4.99	0	4.982	0.001	-0.16	0.00
March	3.785	0.043	3.729	0.099	-1.48	130.23
April	2.388	0.44	2.193	0.69	-8.17	56.82
May	1.051	1.198	0.949	1.598	-9.71	33.39
June	0.266	1.883	0.22	2.542	-17.29	35.00
July	0.071	2.66	0.044	3.503	-38.03	31.69
August	0.141	2.148	0.104	2.828	-26.24	31.66
September	0.426	1.345	0.391	1.742	-8.22	29.52
October	1.531	0.29	1.518	0.457	-0.85	57.59
November	3.175	0.03	3.084	0.055	-2.87	83.33
December	5.624	0	5.69	0	1.17	0.00
Total	29.577	10.037	28.987	13.516	-1.99	34.66

The results seen in Table 2.6 show that the heating load results for both TRNSYS and E+ are in agreement. The cooling loads do not agree as well as the heating load (34% error), however this will not be investigated further, as it is outside the scope of this project. The premise of this research is to determine how a heat pump compares to a conventional system, on both an energy and economic scale.

2.4 Summary

At this point, the research has established an efficient building model in TRNSYS, using the Type 56 Multi-zone building model. The building is 2,200 ft^2 and has two adult and two children occupants. This model has referenced BEopt for not only the design, but also for characteristics such as engineering values (specific heat, density) for construction parameters and ground temperatures. Window selection is based on climate type.

The results of the building simulation will be covered in the Chapter 4. The TLC simulation method, which mimics the function of a real conditioning system and building, was used to analyze the effects of a properly tuned air delivery system. An

ERC simulation method, which reduces computational effort by creating a building loads file, was used for comparing the heat pump system to the conventional natural gas furnace system.

It is important to remember that the objective of this research is to compare the performance of a heat pump system (with possible solar assistance) and a conventional system consisting of a natural gas furnace and air conditioner. Whether this specific building model is the most possible efficient design is not of concern. For example, if future building techniques allow for a 2,200 ft^2 building to have 20% less conditioning energy requirement than the building used for this research, it could then be assumed that this building is a 2,600 ft^2 model. This will not change the outcome of the heat pump and conventional system analysis.

3. Heating, Air Conditioning and Solar Models

The objective of this research is to find ways to reduce the amount of energy required for conditioning. To meet this objective it is necessary to consider alternative heating, ventilating, and air-conditioning (HVAC) equipment. Models of each of these HVAC components are developed and used to determine energy use in different climates. One method is to use an air-source heat pump system, which will be covered first in this chapter followed by a geothermal heat pump system. A solar thermal heating and photovoltaics will also be discussed.

3.1 The Conventional Conditioning System

In order to assess the benefits or drawbacks of the proposed HVAC equipment, a baseline system must be defined for comparisons. Current trends are that northern climates utilize natural gas furnaces for heating and vapor compression air conditioners for cooling. The baseline system will use a 90% efficiency natural gas furnace. For example, if 45 MJ energy is required to maintain the building set point, then at 90% efficiency, 50 MJ (0.4739 therms) of fuel would be required to operate the natural gas furnace and maintain the building set point. Furnaces achieving high efficiencies such as 90% are often termed condensing furnaces in the current market.

Natural gas is inexpensive fuel and its cost is still trending downward at this time, which has further increased the popularity of these systems for heating requirements. In addition, the capital costs for furnaces are very low, as seen in Table 3.1. It is unlikely that the majority of consumers will use a life cycle costs analysis to compare alternative

systems, implying that more often than not they choose the system that has the lowest upfront cost. As will be seen later, heat pumps have significantly higher capital costs.

Table 3.1: Capital costs for natural gas furnaces (BEopt, 2012).

Furnace Pricing		Gas, AFUE 78%	Gas, AFUE 92.5%
Per kBtu Cost	[$/kBtuh]	$13.63	$31.17
30 kBtu/hr	[$]	$409	$935
40 kBtu/hr	[$]	$546	$1,247
50 kBtu/hr	[$]	$682	$1,559
60 kBtu/hr	[$]	$818	$1,871
70 kBtu/hr	[$]	$955	$2,183
80 kBtu/hr	[$]	$1,091	$2,494
90 kBtu/hr	[$]	$1,228	$2,806

The air conditioner selected for the baseline system is a SEER 16 model, with a single speed compressor. A Seasonal Energy Efficiency Rating (SEER) of 16 is deemed to be high efficiency, as the federally mandated minimum is 13 and units qualifying for the EnergyStar rating start at a SEER of 14 (Consumer Energy Center, 2012). This model and terminology will be covered in the air-source heat pump section, as the air-conditioner model and air-source heat pump model are both vapor compression cycles operating in the same manner.

3.2 Air-Source Heat Pump

One of the primary drawbacks to the conventional natural gas system is that it requires the use of a non-renewable fuel. If the primary goal is to achieve net-zero operation, the residential home should avoid using natural gas, if possible. This can be accomplished with an electricity-driven heat pump which provides heating and cooling. By using electricity to heat or cool the home, it is possible to avoid using a non renewable fuel, since the electricity could be generated by a renewable source such as hydro, solar or

wind, or offset on site by photovoltaics. Unfortunately, a drawback to the heat pump system is the high capital cost, especially when compared to a natural gas furnace. Capital costs for a variety of heat pump efficiencies and rated capacities can be found in Table 3.2.

Table 3.2: Capital costs for a variety of heat pump systems (BEopt, 2012).

Heat Pump Pricing		SEER 13. HSPF 7.7	SEER 14. HSPF 8.2	SEER 16. HSPF 8.6	SEER 18. HSPF 9.3
Per kBtu Cost	[$/kBtuh]	$115	$124	$140	$156
Per ton Cost	[$/ton]	$1,384	$1,482	$1,679	$1,876
0.5 tons	[$]	$692	$741	$840	$938
1.0 tons	[$]	$1,384	$1,482	$1,679	$1,876
1.5 tons	[$]	$2,076	$2,223	$2,518	$2,813
2.0 tons	[$]	$2,767	$2,964	$3,358	$3,751
2.5 tons	[$]	$3,459	$3,705	$4,197	$4,689
3.0 tons	[$]	$4,151	$4,446	$5,037	$5,627
3.5 tons	[$]	$4,843	$5,187	$5,876	$6,565
4.0 tons	[$]	$5,535	$5,928	$6,716	$7,502
5.0 tons	[$]	$6,919	$7,411	$8,395	$9,378

3.2.1 Air-Source Heat Pump Operation

Prior to discussing the model of the heat pump, it is important to understand the operating characteristics of a heat pump. Heat pump operation is based on the vapor compression cycle, where a working fluid is either heated or cooled through thermodynamic phase change to provide conditioning. There are four main components that make up the vapor compression cycle. An outline of a simple heat pump operating in heating mode begins at state 1, seen in Figure 3.1.

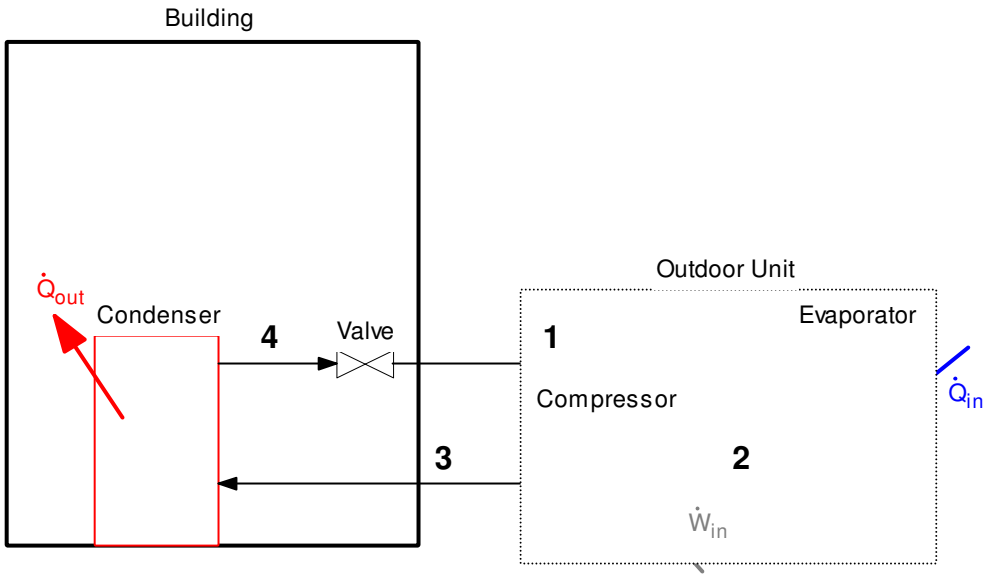

Figure 3.1: Air-source heat pump operating in heating mode. The compressor and evaporator are packaged together and located in the ambient environment.

At state 1, a liquid and vapor working fluid (e.g. R-410A) enters the evaporator at low pressure and temperature. This fluid is passed to the evaporator, which is a heat exchanger located in the ambient outdoor environment to absorb energy (via heat transfer) causing a phase change of the working fluid from liquid to vapor. The vapor at state 2 enters the compressor where it is compressed to a high temperature and pressure; state 3. The working fluid at state 3 enters a heat exchanger located indoors where it condenses as it gives up its heat at a high temperature and pressure. It rejects energy to the indoor environment (via heat transfer), causing the indoor space to be heated. The working fluid exits the condenser as a liquid at high pressure but at a lower temperature than state 3. This high pressure and low temperature liquid is isenthalpically expanded through a valve where the temperature and pressure are lowered further to state 1. For cooling operation, the flow can be reversed, in which the evaporating and condensing operations take place in opposite locations. During cooling, the evaporation process

occurs within the home, absorbing energy (causing cooling) from the indoor air into the refrigerant.

3.2.2 Heat Pump Performance Measures

The performance of a heat pump is most commonly measured by the Coefficient of Performance (COP). The COP is a thermodynamic 1st law efficiency, defined by equation (3.1).

$$COP = \frac{Q_{conditioning}}{W_{input}} \tag{3.1}$$

Currently, heat pumps are capable of operating with an instantaneous COP in the range of 3 to 5, or in other terms, for every kW-hr of electricity supplied to operate the heat pump (W_{input}), 3 to 5 kW-hr of conditioning energy is provided to the living space ($Q_{conditioning}$). However, heat pumps are sensitive to the operating conditions, where cold weather conditions can causes instantaneous COP's to range from 1-2. These effects will be discussed in the following section.

Another common way of representing the COP is the Energy Efficiency Ratio (EER), which is simply the COP converted from dimensionless units to units of BTU/W-hr. EER values tend to range from 10 to 17, found simply by converting the COP range stated above. One issue with the COP or EER is that it is only useful for looking at an instant in time. For example, a heat pump that is operating with a COP of 5 will only do so at a given set of operating conditions (outdoor temperature, indoor temperature). Therefore, an efficiency measure was defined to take into account the varying operating conditions, and thus varying performance of the heat pump system. This performance

measure is called the Seasonal Energy Efficiency Rating (SEER) which has units of BTU/W-hr. The SEER value is a seasonal average which attempts to give consumers an indication of how the heat pump will actually operate over the course of a cooling season. The SEER value is calculated by measuring the EER at various operating conditions and averaging the values (AHRI, 2011). It is convenient to use the SEER value as a label to compare heat pumps. For example, a SEER 16 heat pump is less efficient than a SEER 18 heat pump. However, it should be noted that SEER values do not indicate what the performance of a heat pump (COP or EER) is at a specific set of operating conditions.

The performance of the heat pump is dependent on many factors such as the operating conditions, compressor efficiency and heat exchanger sizes. A low efficiency compressor will consume more energy for the same amount of pressure increase than a high efficiency compressor. Smaller or less efficient heat exchangers will limit the amount heat transfer possible. However, by improving each of these components and thus the performance of the heat pump, the capital cost of the heat pump will also increase.

3.2.3 Heat Pump Cold Climate Performance Issues

Unlike the natural gas furnace, the heat pump is a much more complex system where performance is highly dependent on operating conditions. A major obstacle with a heat pump is operation during cold weather conditions. Figure 3.2 shows a qualitative plot of heat pump capacity and building load vs. outdoor air temperature.

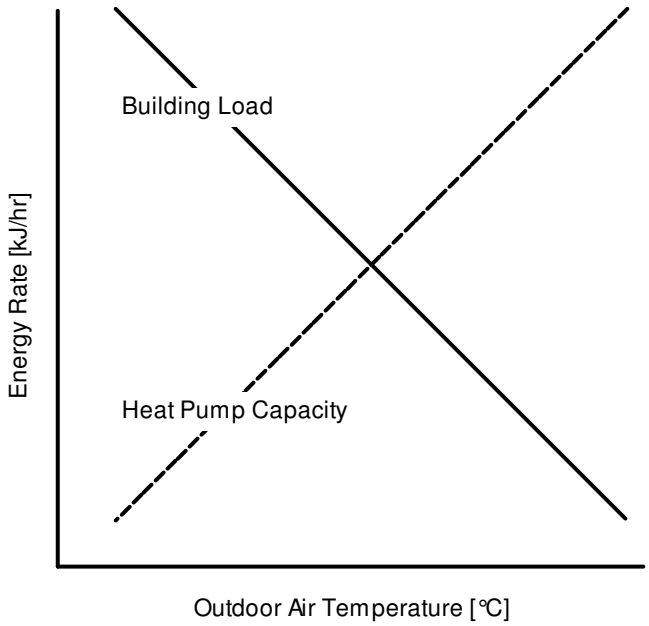

Figure 3.2: Building load and heat pump capacity vs. outdoor temperature.

The solid building load line shows that as the outdoor air temperature drops, the building load increases. This demand can be approximately expressed by equation (3.2) (Klein, S.A. and Nellis, G., 2012).

$$\dot{Q}_b = UA_b \left(T_{base} - T_{amb} \right) \tag{3.2}$$

The base temperature, T_{base}, is the outdoor temperature where the building has no load requirement. For heating applications, T_{base} is lower than the desired building set point temperature by an amount dependent primarily on the internal gains of the building. The building conductance, which is an indication of the building's thermal efficiency, is defined as UA_b. As the ambient temperature (T_{amb}) decreases, $\dot{Q}_b$ will increase.

An ideal HVAC system would be able to provide the required heating load at any operating condition at its highest efficiency. However, as seen in Figure 3.2, the heat pump capacity decreases as the building load increases. As the outdoor temperature

drops the refrigerant at state 2 (Figure 3.1) undergoes a increase in specific volume. This is problematic, because as the vapor enters the compressor at a lower specific volume, the mass flow rate is decreased, which is directly related to the amount of capacity available, seen in equation (3.3). As the mass flow rate of refrigerant drops, the rate of heat transfer in the condenser decreases, which reduces heating capacity.

$$\dot{Q}_{condenser} = \dot{m}_r \left(h_3 - h_4 \right) \tag{3.3}$$

In addition, when the temperature approaches the freezing point of water, another issue can arise on the outdoor unit's heat exchanger. Since the evaporator is colder than the outdoor air, it is possible that the surfaces of the evaporator will be below the dew point of the ambient air, causing ice build up on the evaporator and reducing the effectiveness of the heat exchanger. One solution to this problem is to use electric resistance heating to periodically melt the ice that builds up on the evaporator, which will reduce the COP of the system.

Although the COP and the capacity of a heat pump decrease as the outdoor temperature is reduced, using a heat pump in a cold climate is still a possibility and the methods to achieve this are seen in Figure 3.3. The black dot at the intersection of the building load and capacity lines represents the "balance point" temperature. At this outdoor temperature, the heat pump is capable exactly meeting the building load.

However, if the temperature decreases, the heat pump capacity drops below the required building load and an auxiliary heating source must be used or the building load will not be met resulting in occupant discomfort. Auxiliary heating can come in several forms, most commonly electric resistance heating or natural gas combustion. The heat pump

modeled in this research utilizes resistance heating, to avoid consuming a non renewable energy source such as natural gas. A disadvantage to using resistance heating is that the COP of this process is 1, which decreases the efficiency of the overall process (heat pump plus auxiliary heat).

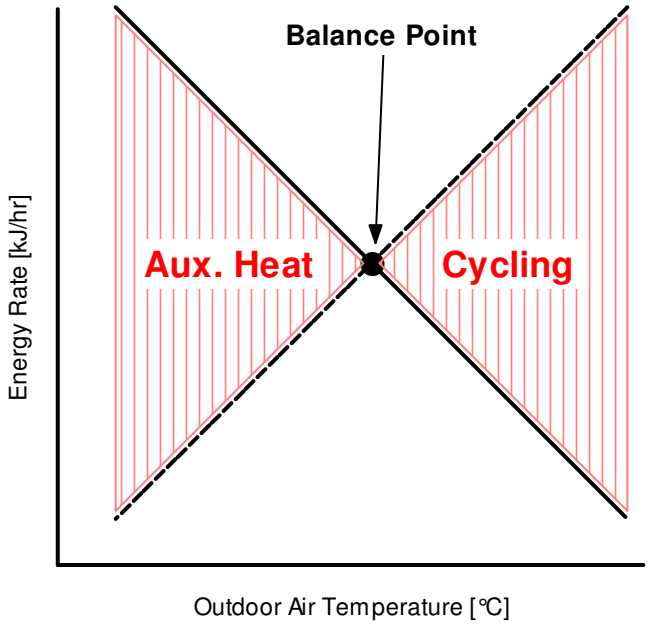

Figure 3.3: Auxiliary heating and cycling regions for an air-source heat pump during cold climate conditions.

Another problem exists if the temperature increases above the balance point. In this situation, the heat pump is over-sized for the required building load. In order to prevent overheating of the conditioned zone, the heat pump must be cycled, or turned on and off to reduce the amount of energy that is delivered over a time period. Cycling also comes with a performance penalty. When a heat pump is operating at steady state, a high pressure side of the cycle is established (states 3 and 4). However, when the heat pump is turned off, this pressure eventually will equalize at a lower value. If the heat pump is required to provide conditioning, energy is required to return to steady state operating conditions with high pressure after the compressor.

One option that exists to help increase the performance of the heat pump is to utilize a two-stage compressor. This compressor has the ability to operate at two different speeds, thus the ability to provide two different capacities, as shown in Figure 3.4, where the low stage can be used to reduce cycling losses and the high stage is used to reduce the amount of auxiliary heat required.

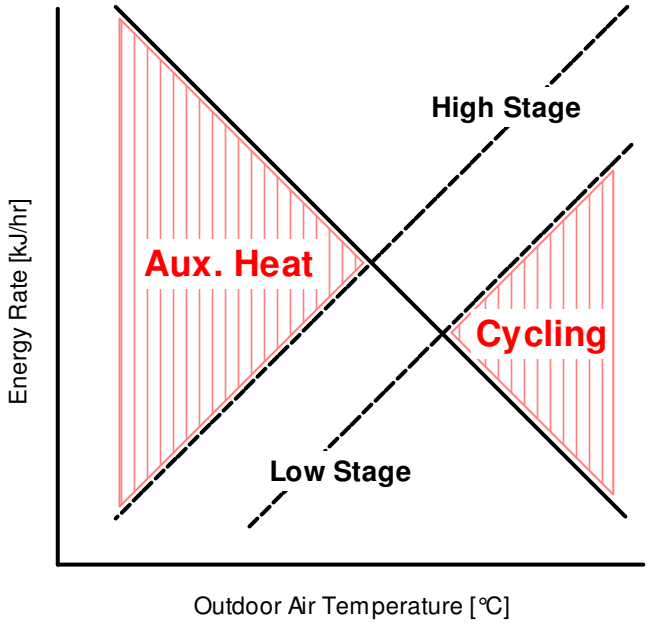

Figure 3.4: Two stage heat pump capacity and building load vs. outdoor temperature.

3.2.4 Type 922 Air-Source Heat Pump Model

Thermal Energy System Specialists have created an air-source heat pump model; Type 922 (TESS, 2009). This Type models a two stage air-source heat pump by using a data lookup approach that relies on a compilation of manufacturer's performance data to create data lookup files. By entering the specifications of the heat pump at the design condition, this type will interpolate these data files to attain the capacity and power at any condition. In addition, the data files are normalized, so that one set of data files can be used to represent a wide range of heat pump efficiencies and capacities.

ASHP_Normalized_Cooling_LowSpeed.dat - Notepad

File Edit Format View Help

```
0.917   1.000   1.167                 !Normalized volumetric flow rate
15.000  17.222  19.444  21.667        !Indoor wet bulb (C)
22.222  23.889  25.556  26.667        !Indoor dry bulb (C)
29.444  35.000  40.556  46.111        !Outdoor dry bulb
0.9579  1.0039  0.9008                !Total, sensible and power ratios @ .917, 15.000, 22.222, 29.444
0.9097  0.9837  1.0153                !Total, sensible and power ratios @ .917, 15.000, 22.222, 35.000
0.8562  0.9567  1.1145                !Total, sensible and power ratios @ .917, 15.000, 22.222, 40.556
0.7974  0.9230  1.1908                !Total, sensible and power ratios @ .917, 15.000, 22.222, 46.111
0.9579  1.1252  0.9008                !Total, sensible and power ratios @ .917, 15.000, 23.889, 29.444
0.9097  1.1050  1.0153                !Total, sensible and power ratios @ .917, 15.000, 23.889, 35.000
0.8562  1.0780  1.1145                !Total, sensible and power ratios @ .917, 15.000, 23.889, 40.556
```

Figure 3.5: Normalized data file for the Type 922 Air-Source Heat Pump. This type interpolates to find the capacity and power at the given operating conditions.

Figure 3.5 shows the normalized data file used by Type 922. The normalized condition is when the total, sensible and power ratios are 1 (columns 1, 2 and 3, respectively). For this data file, the normalized condition is at an indoor dry bulb temperature (IDB) of 26.67°C, outdoor dry bulb (ODB) of 35°C and indoor wet bulb (IWB) of 19.44°C. From the manufacturer's chart, Figure 3.6, the total and sensible cooling capacity and power are recorded at these conditions and are parameters for the type.

			Outdoor Ambient Temperature																							
			65ºF				75ºF				85ºF				95ºF				105ºF				115ºF			
			Entering Indoor Wet Bulb Temperature																							
IDB	Airflow		59	63	67	71	59	63	67	71	59	63	67	71	59	63	67	71	59	63	67	71	59	63	67	71
80	956	MBh	25.7	26.2	28.0	29.9	25.1	25.6	27.4	29.2	24.5	25.0	26.7	28.5	23.9	24.4	26.0	27.8	22.7	23.2	24.7	26.5	21.0	21.5	22.9	24.5
		S/T	0.95	0.90	0.73	0.54	1.00	0.93	0.75	0.56	1.00	0.95	0.77	0.58	1.00	1.00	0.80	0.60	1.00	1.00	0.83	0.62	1.00	1.00	0.84	0.63
		ΔT	24	23	20	16	24	23	20	16	24	23	20	16	23	23	20	16	22	22	20	16	20	21	18	15
		kW	1.36	1.39	1.44	1.49	1.48	1.51	1.56	1.62	1.58	1.61	1.67	1.73	1.66	1.70	1.76	1.83	1.74	1.78	1.84	1.91	1.80	1.85	1.91	1.98
		Amps	5.4	5.5	5.7	5.9	5.9	6.0	6.2	6.4	6.4	6.5	6.7	7.0	6.8	7.0	7.2	7.5	7.2	7.4	7.7	8.0	7.7	7.9	8.1	8.4
		Hi PR	213	229	242	253	239	257	272	284	272	293	309	322	310	333	352	367	349	375	396	413	385	415	438	457
		Lo PR	113	120	131	140	119	127	138	147	124	132	144	153	130	138	151	161	136	145	158	169	141	150	164	175
	850	MBh	24.9	25.4	27.2	29.1	24.3	24.9	26.6	28.4	23.7	24.3	25.9	27.7	23.2	23.7	**25.3**	27.0	22.0	22.5	24.0	25.7	20.4	20.8	22.3	23.8
		S/T	0.91	0.85	0.69	0.52	0.94	0.88	0.72	0.54	0.97	0.91	0.74	0.55	1.00	0.94	**0.76**	0.57	1.00	0.97	0.79	0.59	1.00	0.98	0.80	0.60
		ΔT	25	23	20	16	25	24	21	17	25	24	21	17	25	24	**21**	17	24	24	21	16	22	22	19	15
		kW	1.35	1.38	1.43	1.48	1.46	1.50	1.55	1.60	1.56	1.60	1.65	1.71	1.65	1.69	**1.75**	1.81	1.72	1.76	1.83	1.89	1.79	1.83	1.89	1.96
		Amps	5.4	5.5	5.7	5.9	5.8	5.9	6.1	6.4	6.3	6.5	6.7	6.9	6.7	6.9	**7.1**	7.4	7.2	7.3	7.6	7.9	7.6	7.8	8.0	8.4
		Hi PR	211	227	240	250	237	255	269	281	269	290	306	319	307	330	**349**	364	345	371	392	409	381	410	433	452
		Lo PR	112	119	130	138	118	126	137	146	123	131	143	152	129	137	**150**	159	135	144	157	167	140	149	162	173
	744	MBh	23.0	23.5	25.1	26.8	22.5	22.9	24.5	26.2	21.9	22.4	23.9	25.6	21.4	21.8	23.3	25.0	20.3	20.8	22.2	23.7	18.8	19.2	20.5	22.0
		S/T	0.88	0.82	0.67	0.50	0.91	0.85	0.69	0.52	0.93	0.87	0.71	0.53	0.96	0.90	0.73	0.55	1.00	0.94	0.76	0.57	1.01	0.94	0.77	0.57
		ΔT	25	24	21	17	25	24	21	17	25	24	21	17	25	24	21	17	25	24	21	17	23	22	20	16
		kW	1.32	1.35	1.39	1.44	1.43	1.46	1.51	1.56	1.52	1.56	1.61	1.67	1.61	1.64	1.70	1.76	1.68	1.72	1.78	1.84	1.74	1.78	1.84	1.91
		Amps	5.2	5.3	5.5	5.7	5.6	5.8	6.0	6.2	6.1	6.3	6.5	6.7	6.5	6.7	6.9	7.2	7.0	7.1	7.4	7.7	7.4	7.6	7.8	8.1
		Hi PR	205	220	233	243	230	247	261	272	261	281	297	310	298	320	338	353	335	360	380	397	370	398	420	438
		Lo PR	108	115	126	134	115	122	133	142	119	127	138	147	125	133	145	155	131	139	152	162	136	144	157	168

Figure 3.6: Performance data chart for a Goodman two stage SEER 18 air-source heat pump (Goodman, 2011).

3.2.5 Type 922 Air-Source Heat Pump Model Modifications

Two main issues were encountered with the Type 922 heat pump model. First, the heat pump model did not include a part load factor penalty to account for cycling. To

implement a part load factor penalty, this research follows the guidelines presented in "Residential Equipment Part Load Curves for Use in DOE-2" (Henderson et al., 1999).

To determine compressor power required from cycling, the part load factor must be determined. The part load factor is a function of the fraction of time, *f*, the heat pump must run, which is calculated in equation (3.4).

$$f = \min\left(1, \frac{\dot{Q}_b}{\dot{Q}_{condenser}}\right) \tag{3.4}$$

The building load was calculated by using energy rate control and determining the load to maintain the set temperature at each time step throughout the year. The condenser heat transfer, $\dot{Q}_{condenser}$, is calculated by the Type 922 model. If the heat pump is unable to meet the building load, *f* will be 1 and in addition, the auxiliary heaters must be activated to meet the remaining load. If $\dot{Q}_{condenser}$ is greater than the building load, fraction of time the heat pump must run, *f*, will be less than 1. The part load factor (PLF) is determined from its relationship with the fraction of time the heat pump runs, as shown in equation (3.5).

$$PLF = 0.75 + 0.45f - 0.2f^2 \tag{3.5}$$

Equation (3.5) is a simplification of the PLF equation presented by Henderson. A comparison of the two equations is seen in Figure 3.7. This simplification helps avoid infinitesimally small part load factors that could unrealistically impact the calculation of the compressor power.

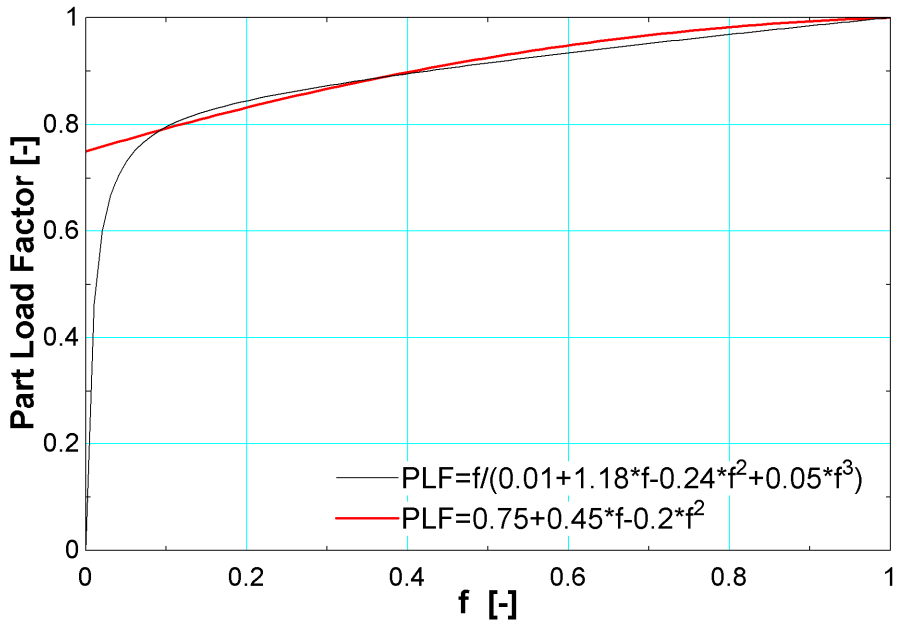

Figure 3.7: Comparison of part load factor curves.

With the part load factor calculated, the cycling compressor power and delivered capacity can be determined for part-load conditions. Equation (3.6) calculates the power to operate the heat pump during cycling situations, $\dot{W}_{cycling}$. The steady state power is denoted by $\dot{W}_{ss}$.

$$\dot{W}_{cycling} = \frac{\dot{W}_{ss}}{PLF} f \tag{3.6}$$

The fraction of capacity delivered, $\dot{Q}_{cycling}$, is calculated using equation (3.7). In this equation, $\dot{Q}_{ss}$ represents the steady state capacity.

$$\dot{Q}_{cycling} = \dot{Q}_{ss} f \tag{3.7}$$

The other issue with the Type 922 heat pump was that it was intended for use with temperature level control, in which the heat pump is operated based on a control signal

from a thermostat and delivers conditioned air to be mixed with the room temperature air. However, many of the simulations done for this research have used the energy rate control method in order to greatly reduce simulation time. The Fortran code in the Type 922 heat pump model was modified and renamed to Type 229.

The first added calculation in the Type 229 code determines the heat pump cooling capacity in both the high and low stages, which is shown in the following code.

```
C     CALCULATE COOLING PERFORMANCE IN HIGH AND LOW STAGES
       IF(COOLING_SEASON.GE.1)THEN
             NX=4
             NVAL(4)=N_LPS
             NVAL(3)=N_WB_IN_C
             NVAL(2)=N_DB_IN_C
             NVAL(1)=N_DB_OUT_C
             NY=3
             X(1)=T_SINK
             X(2)=T_IN
             X(3)=WB_IN
              X(4)=LPS_AIR_HI/LPS_RATED_AIR_HI
             CALL DYNAMICDATA(LU_COOL_HI,NX,NVAL,NY,X,Y,INFO,*43)
             CALL LINKCK('TYPE 229','DYNAMICDATADATA  ',1,99)
43           IF(ErrorFound()) RETURN 1
             Q_TOTAL_C_HIGH=RATED_TOT_C_HI*Y(1)
             Q_SENSIBLE_C_HIGH=RATED_SENS_C_HI*Y(2)
             POWER_DATA_C_HIGH=RATED_POW_C_HI*Y(3)
```

The code first checks whether the heat pump is operating in cooling mode, and if it is not then it skips all cooling mode calculations and moves to the heating mode calculations. This is done with the conditional statement `IF(COOLING_SEASON.GE.1)`.

Following this check, the cooling capacity and power for the high stage are determined when the Type 229 model interpolates the normalized data files that were discussed previously. The interpolation parameters are based on the given weather conditions `(T_IN, T_SINK, WB_IN)`, which are the indoor and outdoor dry bulb temperatures

and indoor wet bulb temperature. This same process is repeated to determine the cooling capacity and power for the low stage (shown below).

```
            NX=4
            NVAL(4)=N_LPS
            NVAL(3)=N_WB_IN_C
            NVAL(2)=N_DB_IN_C
            NVAL(1)=N_DB_OUT_C
            NY=3
            X(1)=T_SINK
            X(2)=T_IN
            X(3)=WB_IN
             X(4)=LPS_AIR_LOW/LPS_RATED_AIR_LOW
            CALL DYNAMICDATA(LU_COOL_LOW,NX,NVAL,NY,X,Y,INFO,*45)
            CALL LINKCK('TYPE 229','DYNAMICDATADATA  ',1,99)
45          IF(ErrorFound()) RETURN 1
            Q_TOTAL_C_LOW=RATED_TOT_C_LOW*Y(1)
            Q_SENSIBLE_C_LOW=RATED_SENS_C_LOW*Y(2)
            POWER_DATA_C_LOW=RATED_POW_C_LOW*Y(3)
```

With the high and low stage cooling capacity and power determined, the Type 229 heat pump uses the building load to select which stage should be operated. Since the high and low stages are simply a change in compressor speed, it is not possible to run both the high and low stage simultaneously. For example, the compressor could either operate in the low stage at 500 RPM, or switch to the high stage at 750 RPM which will increase the available capacity.

```
C    DETERMINE WHICH STAGE OF COOLING TO RUN BASED ON COOLING
PERFORMANCE
      IF(BUILDING_LOAD.LT.MIN_LOAD) THEN
          Y_COOL_LOW=0
          Y_COOL_HI=0
      ELSE IF((Q_TOTAL_C_LOW.GE.BUILDING_LOAD).AND.(STAGE.EQ.2))THEN
          Y_COOL_LOW=1
          Y_COOL_HI=0
      ELSE
          Y_COOL_HI=1
          Y_COOL_LOW=0
      ENDIF
```

A check is first made to determine if the building load is less than the minimum load; a minimum load is set to prevent the heat pump from running to meet a small load that in

reality would not cause the occupant to operate the cooling equipment or would fall within the thermostat dead band. For this house, it was determined that a building load of 500 kJ/hr represented a temperature change of 2°C over 1 hour.

It is assumed that the heat pump would not run if the house temperature would drop less than 2°C over a 1 hour time step, and thus, any load less than 500 kJ/hr will not be met by the heat pump. The second check used is to determine if the heat pump is a one or two stage model. If it is a single stage model then the heat pump will only operate in the high stage. If it is a two stage model, the heat pump will attempt to use the low stage capacity to meet the building load. If the low stage capacity is smaller than the building load, then the high stage is chosen.

With the correct stage selected, the heat pump must then determine if any cycling will occur to meet the load. This check is done using the part load factor calculations.

```
      IF((COOLING_SEASON.EQ.1).AND.(BUILDING_LOAD.GT.MIN_LOAD))THEN
         POWER_COMPRESSOR_SS=DMAX1(0.,(POWER_DATA-POWER_FAN_I-
POWER_FAN_O))
         ONE=1.0
         IF(PART_LOAD.EQ.1) THEN
         FRAC=MIN(ONE,(BUILDING_LOAD/Q_TOTAL_C))
         ELSEIF(PART_LOAD.EQ.0)THEN
         FRAC=1.0
         ENDIF

         PLR=0.75+0.45*FRAC-0.2*FRAC**2
         POWER_COMPRESSOR=POWER_COMPRESSOR_SS/PLR

         Q_TOTAL_C=Q_TOTAL_C*FRAC

      ENDIF
```

The part load factor again checks to determine that the heat pump is operating in cooling mode and also whether the building load at the given time step is larger than the minimum load. If these conditions are met, the type will determine the steady state

compressor power (which does not include the fan power). The type will then determine if the part load factor has been disabled. One of the features of the Type 229 is the ability to disable the part load factor, which is done by setting the part load parameter to 0. If the part load factor has been disabled, the type will use the steady state compressor power. If it has not been disabled, the type will then calculate the part load factor and modify the compressor power to account for cycling as outlined previously.

This same process is used for the heating mode of the model. The only significant difference is the auxiliary heating capacity is calculated when the heat pump is unable to meet the heating load.

```
C       DETERMINE IF AND HOW MUCH AUX HEATING IS REQUIRED
         IF((BUILDING_LOAD.GT.Q_TOTAL_H).AND.(HEATING_SEASON.GE.1))
THEN
             Q_AUX=BUILDING_LOAD-Q_TOTAL_H
         ELSE
             Q_AUX=0
         ENDIF
```

This calculation simply subtracts the heat pump capacity from the building load to determine how much auxiliary energy is required to meet the building load completely. If the capacity is larger than the building load, the auxiliary energy required is set to zero.

Problems were also encountered in the interpretation of the normalized data in the Type 229 model. It was found that when the operating conditions fell outside of the range supplied in the normalized data, this code would not extrapolate to find the capacity and power values. For example, the lowest indoor temperature in the data file was 21.11°C, and the indoor temperature operating condition supplied for interpolation was 18°C, the Type 229 would incorrectly return the capacity results for 21.11°C. Using a polynomial

curve fit to the normalized data, capacity and power data at lower temperature indoor dry bulb temperatures were added to the data file to allow for interpolation for these situations.

It was also found that the manufacturers do not provide data for operation when the outdoor temperature falls below -13.9°C. The manufacturer states that extrapolation should not be used predict the performance below this temperature. This control decision is typical in the operation of heat pumps, as many mechanical issues could arise in the operation of heat pumps at very cold conditions. Thus, when the outdoor temperature falls below -13.9°C the heat pump is disabled and the heating load is met with strip heaters.

3.2.6 Type 229 Air Source Heat Pump Validation (Cooling Mode)

To ensure that the type will reliably reproduce the manufacturer's performance data, a comparison was preformed between two manufacturers, Goodman and Carrier, from which performance data was provided. The SEER ratings for the Goodman and Carrier heat pumps were 18 and 16.5, respectively. It should be again noted that the SEER value does not indicate the performance of the heat pump at a specific operating condition. It is simply a label to compare heat pumps; for example, at the same operating conditions, the SEER 16.5 system should perform worse than the SEER 18 system.

The reported steady state results from the TRNSYS type were plotted with the manufacturer's steady state data for both heating and cooling operation. Figure A.1 through Figure A.3 in Appendix A present the results for various operating conditions for a 3 Ton Goodman SEER 18 two-stage heat pump. Each point corresponds to the capacity

or power at specific operating conditions (outdoor dry bulb temperature, indoor wet bulb temperature and indoor dry bulb temperature). Points falling on the 45^{o} line represent agreement with the manufacturer's data.

The percent error for these data were on average 2.8% for the total capacity, 4.7% for the sensible capacity and 5.4% for the cooling power. Percent error is calculated using equation (3.8)

$$Er = \frac{TT - M}{M} \bullet 100 \tag{3.8}$$

where the Type's prediction is *TT*, the manufacturer's reported value is *M* and *Er* is the percent error. The ability for the type to accurately model various SEER rated heat pumps was also important. A 2 ton Carrier SEER 16.5 two-stage heat pump was used to check the model's accuracy, shown in Appendix A, Figure A.4 through Figure A.6. As with the SEER 18 comparison, each data point represents a specific steady state operating condition defined by the outdoor dry bulb temperature, indoor wet bulb temperature and indoor dry bulb temperature.

Similarly to the SEER 18 results, the SEER 16.5 cooling performance is modeled accurately by the Type 229 heat pump. The total capacity, sensible capacity and power average percent error was 2.3%, 2.9% and 3.4%, respectively. The magnitude of the error in the cooling performance was judged to be acceptable by running a simulation using the manufacturer's data in the data file and comparing to the results from a simulation using the normalized file. This simulation utilized a building loads file

calculated from the building model discussed in Chapter 2 and for Chicago, IL. The electrical consumption comparison for cooling dominated months are shown in Table 3.3.

Table 3.3: Error in the energy consumption during summer months due to inaccuracies in the heat pump cooling capacity. These power values are solely the power required to run the HVAC equipment. The heat pump simulated was a SEER 19 Carrier 3 Ton unit.

Cooling Dominated Month	TRNSYS [kW-hr]	Manufacturer's Data [kW-hr]	Error [%]
June	63.9	60.2	6.1
July	224.1	229.9	2.5
August	84.2	86.1	2.2

It is important to note that it is not possible to accurately represent data from various manufacturers using a normalized file, as there is some performance variation. Figure A.7 through Figure A.9 in Appendix A show the normalized values for several capacities and SEER values.

3.2.7 Type 229 Air Source Heat Pump Validation (Heating Mode)

The next step was to ensure that the model would accurately represent the heating performance of the heat pump. Figure A.10 through Figure A.13 of Appendix A show the results from comparing the TRNSYS data to the manufacturer's data for both a SEER18 and SEER16.5 heat pump. Again, each data point represents a specific operating condition, specified by the indoor dry bulb temperature and outdoor dry bulb temperature.

These results show that the Type 229 heat pump struggles to accurately represent manufacturer's data for heating. This is due to the normalized data file not accurately following the manufacturer's performance trends. For the SEER 18 system, the average percent error for heating capacity and power was 30.8% and 20.5%. The SEER 16.5 experienced similar results, where the average percent error was 18.9% and 21.0%.

In an attempt to improve the heating accuracy, new data files were constructed by normalizing to a 5 ton Carrier SEER 16.5 data file. The difference between the original data file and revised data file are shown in Appendix A, Figure A.14 through Figure A.21, for the high stage. A view of this error is seen in Figure A.30 through Figure A.33, also located in Appendix A, where the capacities and power are plotted versus outdoor temperature.

With the new data files, the error in the capacity ranged from 3% to 5.2% (depending on the capacity) for the high stage of the SEER 18 heat pump. The average percent error in power values was approximately 3.5% for the SEER 18 heat pump. For the SEER 16.5 heat pump, the high stage capacity average error for reproducing the manufacturer's data ranged from 1.4% to 3.6%. The power average error for the SEER 16.5 heat pump was reduced to a range from 1% to 4.4%. This revised data file reproduces the manufacturer's data much more accurately than the original normalized file for the high stage. Next, the low stage of the heat pump model was investigated to improve the model's accuracy. In addition to the original results, these revised results are presented in Figure A.22 through Figure A.29 of Appendix A. An alternate view of this error is seen in Figure A.34 through Figure A.37, found in Appendix A. These plots show slight improvement by using the revised file over a range of outdoor temperatures for various SEER ratings and capacities.

Trying to improve the low stage model performance by creating a new normalized data file yielded only slightly improved results. For the SEER 18 heat pump, the average capacity error ranged from 7.8% to 10.2%. The power average error was reduced to a range of 0.83% to 2.6%. The SEER 16.5 heat pump had slightly lower average capacity

error values, ranging from 2.3% to 8%. The power average error was 2.79%, with a peak point of 13.1% for a 2 ton 16.5 SEER heat pump.

The errors reported in the plots of Appendix A represent operating steady-state operating conditions. However, the heat pump will be operated over a range of conditions. Since the capacity and power error tends to be largest when the temperature is cold, the impact on the calculated auxiliary energy for a heating season may be larger than seen for steady-state operation. To assess the impact of this error on the total energy consumption for heating, a simulation was run utilizing the actual manufacturer's heating performance data for a 3 ton SEER 19 heat pump. The building loads file for this simulation was calculated using the building model described in Chapter 2, using a location of Chicago, IL. These results are found in Table 3.4.

Table 3.4: Error in the energy consumption during winter months due to inaccuracies in the heat pump heating capacity. These power values are solely the power required to run the HVAC equipment. The heat pump simulated was a SEER 18 Goodman 3 Ton unit.

Heating Dominated Month	TRNSYS [kW-hr]	Manufacturer's Data [kW-hr]	Error [%]
January	2306	2354.3	2.1
February	1780	1848.1	3.7
November	987.1	1019.6	3.2
December	1940	2012.8	3.6

The difficulty in attempting to normalize all of the heating data is shown in Figure A.38 and Figure A.39. While the normalized data file will accurately represent most capacities and SEER ratings at a given operating condition, there are variations and exceptions in reported manufacturers' data that are not easily reproduced.

3.3 Ground Source Heat Pump System

One problem that was seen with the air-source heat pump was a decrease in both capacity and performance (COP) during cold ambient conditions. There are alternatives to avoid these detrimental operating conditions. One alternative is to use a ground source heat pump system that uses the ground as a sink or source for heat. The benefit to this system is that the ground temperature remains relatively constant over the course of the year. For a location such as Fargo, North Dakota, the ground temperature is relatively constant at approximately 8°C (North Dakota State University, 2012). On the other hand, the air temperatures for Fargo have ranged from -44.44°C to 41.11°C (National Weather Service, 2012).

However, there are two primary disadvantages to the ground source heat pump system. First, in many cases, these systems have higher first costs relative to air-source heat pumps that may not present an economic return. Ground source heat exchangers can be implemented in several ways, as shown in Figure 3.8. The vertical loop system tends to have high capital costs due to the drilling process required for installing the bore field. Alternatives to the vertical bore field are horizontal or slinky systems. These systems require trenches to be dug and therefore avoid the use of costly drilling machinery. Horizontal systems can be nearly half as expensive as vertical systems, however, in both cases, prices fluctuate depending on the local excavation market.

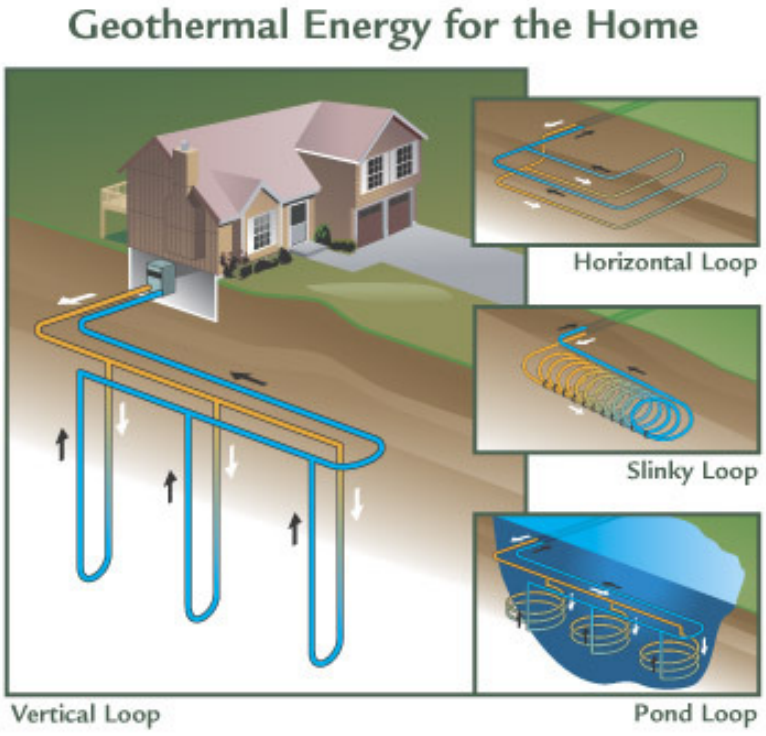

Figure 3.8: Various ground source systems for residential use (Kansas City Power & Light, 2012).

The other disadvantage of the geothermal heat pump system is space requirements. Unlike an air-source heat pump or natural gas furnace system, the ground source heat pump system requires space for a bore field to be drilled or a horizontal/slinky system to be installed. This makes the ground source system suitable for suburban or rural locations, but perhaps not so for small urban buildings. The remainder of this section will outline the liquid source heat pump and ground heat exchanger models.

3.3.1 Type 919 Liquid Source Heat Pump

Like the air source heat pump model, the Type 919 Liquid Source Heat Pump was created by TESS (TESS, 2010). This model operates in the same manner as the Type 922 Air-Source Heat Pump model in that they both use the data look up approach. The model uses two sets of normalized data files created from Trane 4 ton water source heat pump data. The Type 919 was also intended for use with a temperature level control

simulation. The modifications made to the Fortran code so it could be easily compatible with an energy rate control simulation are covered in the next section.

3.3.2 Type 919 Liquid Source Heat Pump Modifications

To adapt the Type 919 to an energy rate control simulation, several adjustments were made to the source code. The first change was to create a method to turn the heat pump on if the building load was greater than 500 kJ/hr (indicating a temperature change of more than 2°C), which is documented in the following lines of code. In addition, this code determines whether the heat pump should be cooling or heating by checking the values of the schedule inputs `heat_season` and `cool_season`. If heating or cooling is required, `onsig_h` or `onsig_c` will be set to 1. If no conditioning is required, both `onsig_h` and `onsig_c` are set to 0 and the heat pump does not run during that time step.

```
! Determine if the heat pump is on or off
       If (building_load < 500.) Then
           onsig_c = 0.
           onsig_h = 0.
           onsig_aux1 = 0.
           onsig_aux2 = 0.
           onsig_fan = 0.
       ElseIf ((building_load > 500.).AND.(heat_season ==
1.).AND.(cool_season ==
       0.)) Then
           onsig_h = 1.
           onsig_c = 0.
       ElseIf ((building_load > 500.).AND.(cool_season == 1.)) Then
           onsig_c = 1.
           onsig_h = 0.
       EndIf
```

If conditioning is required, the type will calculate the available capacity at the current operating conditions by interpolating the data file to find the capacity and power at the given operating conditions. However, the type also must calculate how much auxiliary energy (for heating) or cycling is required to meet the load, since it is rare that the heat

pump operates at the balance point. This process is shown for the cooling mode in the following code.

```
! Calculate the part load factor penalty
   If (building_load < q_tot_c) Then
       power_compressor_ss = power_compressor
       one = 1.0
       frac = MIN(one,(building_load/q_tot_c))
       PLR = 0.75+0.45*frac-0.2*frac**2
       power_compressor = power_compressor_ss*frac/PLR
       q_tot_c=q_tot_c*frac
   EndIf
```

If the building load, `building_load`, is less than the available cooling capacity, `q_tot_c`, the heat pump will cycle and the part load factor penalty is applied (Henderson et al., 1999). Note, in this code the part load factor is labeled part load ratio, `PLR`.

If the heat pump is in heating mode, this same part load factor penalty is applied. However, if the heat pump cannot meet the building load, the model will determine the amount of auxiliary heating required (`q_aux`). Both of these steps are seen in the following lines of code.

```
! Calculate Aux heat or part load factor
    If (building_load > q_tot_h) Then
        q_aux = building_load-q_tot_h
    ElseIf (building_load < q_tot_h) Then
        power_compressor_ss = power_compressor
        one = 1.0
        frac = MIN(one,(building_load/q_tot_h))
        PLR = 0.75+0.45*frac-0.2*frac**2
        power_compressor = power_compressor_ss*frac/PLR
        q_tot_h=q_tot_h*frac
        q_aux = 0.
    EndIf
```

Initially it is determined if the building load, `building_load`, is greater than the available heating capacity, `q_dot_h`. If this is the case, the amount of auxiliary heating, `q_aux`, required is the difference between the building load and the available heating

capacity. If the building load is less than the heating capacity, then the cycling penalty is applied and the auxiliary heating is set to 0.

With these modifications, the Type 919 heat pump model was renamed to Type 230. Given the building load, the model decides whether conditioning equipment should be operated, and if so, the model calculates the power required to meet the load, taking into account any auxiliary heating or cycling effects.

3.3.3 Type 230 Liquid Source Heat Pump Validation

Prior to simulating the heat pump with the building load and running an economic analysis, it was important to validate the model. Similar to the air-source model, the liquid source heat pump was compared to manufacturer's performance data. For the Type 230 liquid source heat pump, manufacturer's data from ClimateMaster for an EER 20 single stage model was used for comparison. To make the comparison, the capacity and power were plotted at various operating conditions to determine the accuracy of the normalized data file. For the cooling mode, the total, sensible and power data is shown in Figure 3.9 through Figure 3.11. In each of these plots, points falling on the diagonal indicate that the TRNSYS model is in agreement with the ClimateMaster data. The dashed lines indicate a plus or minus 5% error.

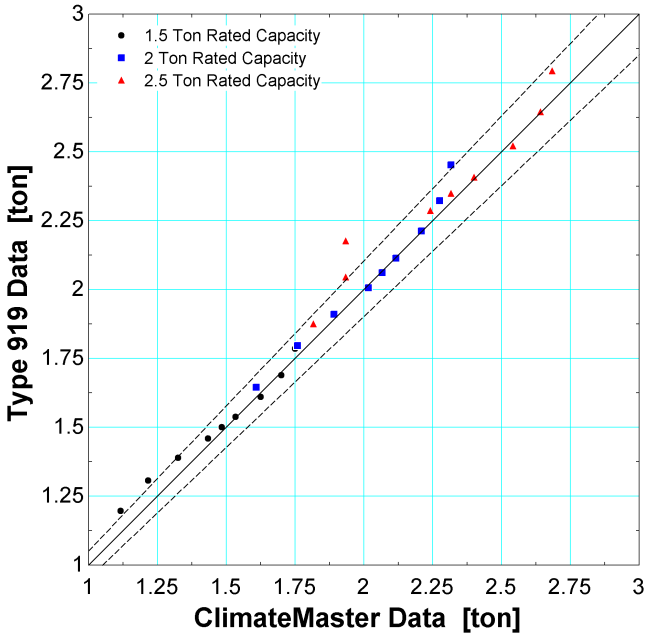

Figure 3.9: Comparison of total cooling capacity results for the TRNSYS model and the ClimateMaster Data. Points falling on the 45° diagonal are in perfect agreement. One outlier had a 12.5% error, while the majority of the data fell within 5%.

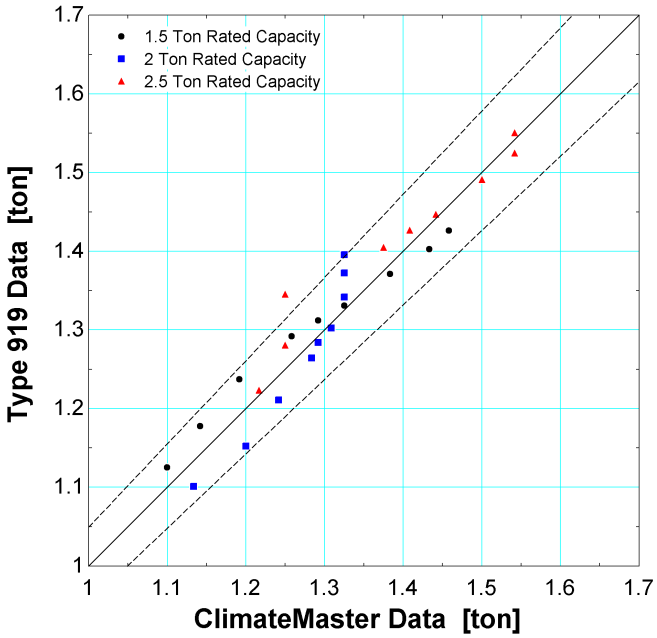

Figure 3.10: Comparison of sensible cooling capacity results for the TRNSYS model and the ClimateMaster Data. Points falling on the 45° diagonal are in perfect agreement. The dashed lines represent a percent error of 5%. The outliers are no greater than 7.6% error.

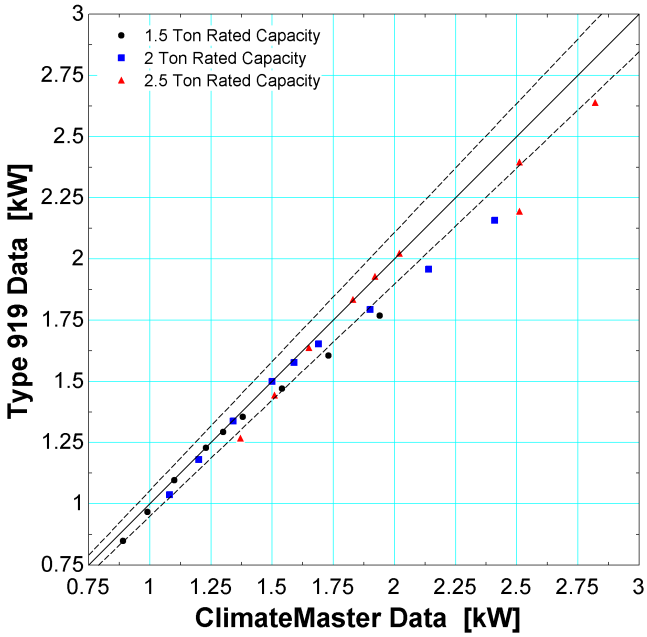

Figure 3.11: Comparison of cooling power consumption results for the TRNSYS model and the ClimateMaster Data. Points falling on the 45° diagonal are in perfect agreement. The dashed lines represent a percent error of 5%. The greatest error found was 12%.

From these data the heat pump model has shown to accurately reproduce the ClimateMaster data within 5%, excluding several outliers, which is sufficient accuracy for this research. The next set of data involved validating the heating mode of the heat pump model, seen in Figure 3.12 and Figure 3.13.

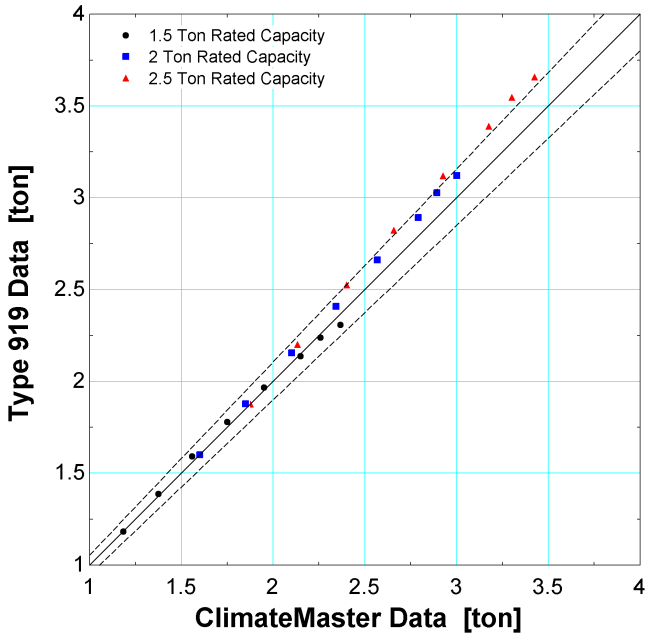

Figure 3.12: Comparison of power consumption results for the TRNSYS model and the ClimateMaster Data. Points falling on the 45° diagonal are in perfect agreement. The dashed lines represent a percent error of 5%. The greatest error found was 6.9%.

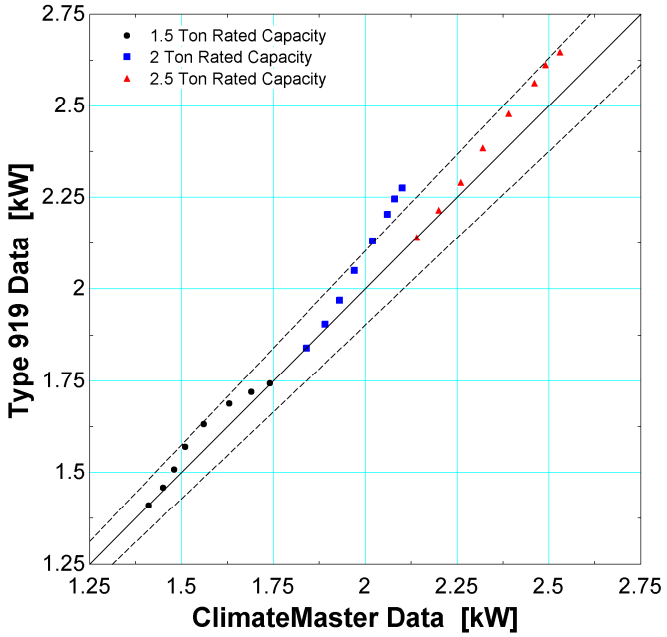

Figure 3.13: Comparison of power consumption results for the TRNSYS model and the ClimateMaster Data. Points falling on the 45° diagonal are in perfect agreement. The dashed lines represent a percent error of 5%. The greatest error found was 7.7%.

For the heating results, the majority of data points fall within the 5% error range, and the outliers do not exceed a percent error of 7.7%. Again, as with the cooling mode, the heating mode validation was deemed acceptable for this research, as the error was within 5%, aside from several outliers. With a validated model, the heat pump is now ready for simulation with the building loads file to determine the amount of energy required to condition the home and the economic impact of using the geothermal system. The next section will cover the u-tube ground heat exchanger.

3.3.4 Type 557a Vertical U-Tube Ground Heat Exchanger

The mathematical model for the vertical u-tube heat exchanger was written by Göran Hellström (1989). Thermal Energy System Specialists have implemented this model into TRNSYS Type 557a (TESS, 2010). This is a robust model that allows many of the heat exchanger parameters to be adjusted. These parameters are presented in Table 3.5 on the following page. This model has inputs of fluid temperature and flow rate, which are transient outputs of the Type 230 liquid source heat pump model. The outputs from this model, fluid temperature and flow rate, are connected to the fluid inlet of the Type 230 liquid source heat pump.

Table 3.5: This table lists the adjustable parameters for the Type 557a vertical u-tube ground heat exchanger.

Parameter	Value	Units
Number of Boreholes	2	-
Borehole Depth	133.375	m
Borehole Spacing	4.806	m
Header Depth	1	m
Number of Boreholes in Series	1	-
Number of Radial Regions	1	-
Number of Vertical Regions	10	-
Storage Thermal Conductivity	4.68	kJ/hr-m-K
Storage Heat Capacity	1764	kJ/m3-K
Initial Surface Temperature	7.96	°C
Initial Thermal Gradient	0	°C/m
Insulation Indicator	No Insulation	
Number of U-Tubes per bore	1	-
Borehole Radius	0.102	m
Outer Radius of U-Tube Pipe	0.017	m
Inner Radius of U-Tube Pipe	0.014	m
Center-to-Center Half Distance	0.025	m
Fill Thermal Conductivity	4.68	kJ/hr-m-K
Pipe Thermal Conductivity	1.512	kJ/hr-m-K
Gap Thermal Conductivity	5.04	kJ/hr-m-K
Gap Thickness	0	m
Reference Borehole Flow Rate	144	kg/hr
Reference Temperature	30	°C
Fluid Specific Heat	4.19	kJ/kg-K
Fluid Density	1000	kg/m3
Number of Simulation Years	1	-
Maximum Storage Temperature	100	°C
Number of Preheating Years	0	-
Maximum Preheat Temperature	30	°C
Minimum Preheat Temperature	10	°C
Preheat Phase Delay	90	day
Average Air Temperature	7.96	°C
Amplitude of Air Temperature	13.32	delta°C
Air Temperature Phase Delay	234	day
Number Ground Layers	1	-
Thermal Conductivity of Layer	4.68	kJ/hr-m-K
Heat Capacity of Layer	1764	
Thickness of Layer	1000	m
Inlet Fluid Temperature	20	°C
Inlet Flow Rate	0	kg/hr
Temperature on Top of Storage	20	°C
Air Temperature	20	°C
Circulation Switch	Center to Border	-

The design of the system was determined from BEopt (BEoptE+, 2012), which suggests that the sizing of the ground loop should be 106.7 m/ton. This size agrees with recommendations from ASHRAE (ASHRAE, 2007). For example, for a heat pump with a rated capacity of 1 ton, a 53.35 m bore hole should be drilled, as the total U-tube length would be twice the size, or 106.7 m. With ground heat exchangers, the length required can vary greatly depending on soil type and conditions. For example, if a large underground aquifer will have much different heat transfer characteristics than clay soil.

3.4 Photovoltaic System

A photovoltaic (PV) system allows for solar energy to be converted to electricity which can be used on site or potentially sold to the utility. The latter situation varies by location, as some utilities will not purchase electricity. In addition, purchase rates can vary greatly across the United States, which can change the economic outlook for photovoltaics. These programs are subject to change as they increase in popularity. As the number of participants in the program increases, the amount of electricity put on the grid will reach a maximum and utilities may limit or stop its purchasing of energy from consumers. (Myers, 2010).

Various PV systems exist each with their own advantages and disadvantages. For example, a rack mounted system will operate with a higher efficiency than a comparable roof mounted system because the rack mounted system will have better natural cooling. However, the rack mounted system requires ground space, which not all consumers have. This research focused on a simple close roof mounted system to help gain an

understanding of whether photovoltaics help the heat pump system provide more source energy and economic savings over the conventional system previously described.

The System Advisor Model (SAM), a solar design program distributed by NREL (2011), was utilized to calculate the monthly amount of electricity produced by the PV panels. A simple efficiency model was used, shown in equation (3.9).

$$P_M = E_{TotalIncident} \bullet A_M \bullet \eta_M \bullet F_{TempCorr} \tag{3.9}$$

This equation calculates the amount of power produced (P_M) based on the incident radiation ($E_{TotalIncident}$), module area (A_M), collector efficiency (η_M) and a temperature correction factor ($F_{TempCorr}$). This panel has a constant efficiency of 13.5% regardless of the radiation level, however does have a temperature correction factor ($F_{TempCorr}$) which adjusts the collector efficiency based on temperature. This model has the ability to be easily scaled. For example, using equation (3.9) with a 1 m^2 panel at 13.5% efficiency exposed to 800 W/m^2 incident radiation, the panel will produce 108 W of power. If the panel is doubled in size to 2 m^2, the panel will then produce 216 W of power. While this calculation neglected the temperature correction factor, including it would not have changed the result that the panel area and power produced are scalable as the temperature correction factor is independent of collector area.

While this method will not be as accurate as some of the more detailed models, it will provide results and trends that indicate whether PV is a benefit when used in conjunction with the heat pump system. SAM also allows for the PV system to be derated, which takes in to account various inefficiencies in the PV system. While derating is considered,

no performance degradation over time is considered. These derating inefficiencies are outlined in Table 3.6.

Table 3.6: Derating of the PV system. This accounts for inefficiencies in the wiring, transformer, etc. These values were the default suggestions in SAM.

Derate	Percentage
Mismatch	98
Diodes and Connections	99.5
DC Wiring	98
Soiling	92
Sun Tracking	96
Nameplate	95
Total Pre-Inverter Derate	80.2
AC Wiring	99
Transformer	100
Total Post-Inverter Derate	99
Total Derate Factor	79.4

To calculate the diffuse incident radiation from the weather file supplied total and beam data, the Reindl model was used (Duffie and Beckman, 2006). When a simulation is run, SAM reports the amount of electricity generated per month by the system, in kW-hr. It is assumed that the utility would purchase all excess electricity from the house at any time at the same rate the customer purchases electricity at (0.14 $/kW-hr).

3.5 Solar Thermal Heating System

The solar thermal system is another method (in addition to a photovoltaic system) to utilize the radiation provided from the sun to push towards lower building energy consumption. The solar thermal system considered here uses flat plate collectors to transfer thermal energy to a working fluid, often water or glycol. One option is to immediately use this thermal energy by heating domestic hot water or heat exchanging with air to reduce the building load. However, unlike PV, the solar thermal system is not capable of simply selling thermal energy to the utility during periods where the building

does not require thermal energy. Therefore, a storage tank is required in order to store thermal energy so that it is available at times when it is required. An advantage of the solar thermal system is that it allows easy and inexpensive energy storage on site and therefore remains free from a grid connection; unlike PV, which requires a grid connection to sell back excess energy (unless battery storage is used). The system that is simulated in this research is shown in Figure 3.14.

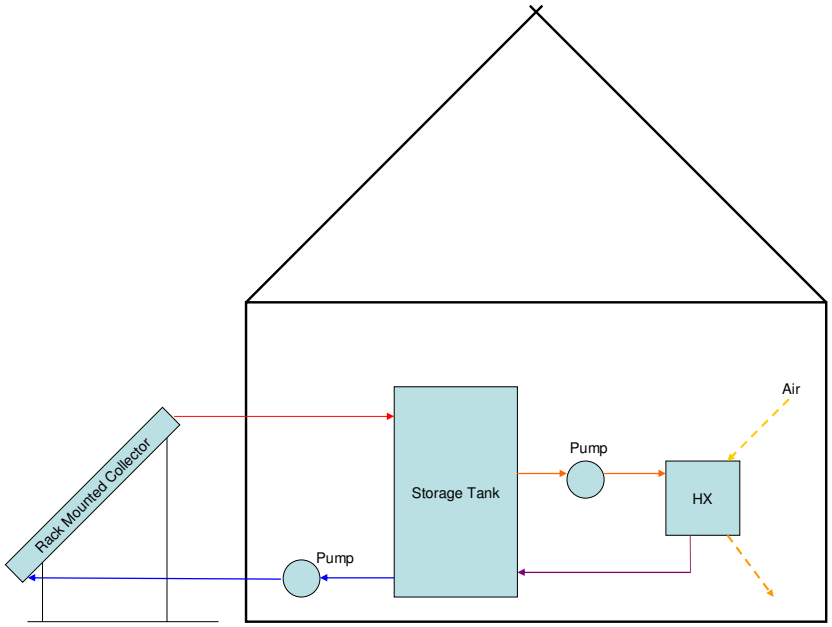

Figure 3.14: This figure shows the rack mounted solar thermal heating system. This system includes a collector-side pump and a heat exchanger side pump, which both may operate at different times.

The thermal solar system uses a stratified storage tank with no internal auxiliary heating. Auxiliary tank heating, possibly provided with a second tank or an instant heater, would be required if the tank was providing domestic hot water to ensure hot water is available when solar radiation is unavailable. A heat exchanger transfers the thermal energy from the hot water to the room air, reducing the building load.

The tank is assumed to be located in the conditioned space of the basement, where the thermal losses will provide heating to the house. Initial simulations look only at the ability to provide thermal energy to reduce the building heating load and thus do not account for the tank's ability to heat domestic hot water. Without the ability to heat hot water, the system is unusable during the cooling season. The results in Chapter 4 will show that for a cold climate location, the ability to heat the hot water load will not change the results. The following sections will outline each component and the model characteristics.

3.5.1 Collector Model and Parameters

The thermal collector chosen to represent solar thermal system is a single-glazed selective-surface flat plate collector manufactured by Alternate Energy Technologies (model AE-50). Performance parameters for this and most other solar collectors are provided by the Solar Rating and Certification Corporation (SRCC, 2012). The AE-50 collector was selected as it displays average performance characteristics for most collectors available today. For reference, the SRCC report sheet on this collector can be found in Appendix B. Table 3.7 summarizes the construction characteristics of collector.

Table 3.7: This table show the Alternate Technologies AI-50 collector construction specifications.

Specification	Value
Aperture Area	4.40 [m^2]
Fluid Capacity	6.4 [L]
Absorber Material	Tube: Copper Plate: Copper Fin
Absorber Coating	Selective
Insulation (Side/Back)	Polyisocyanurate

Simulating this collector in TRNSYS required the use of the Type 1b flat plate collector model. The model parameters include the efficiency and incidence angle modifier equations. Equation (3.10) is the efficiency of the collector.

$$\eta_c = F_R(\tau\alpha)_n - F_R U_L \frac{(T_{inlet} - T_{amb})}{I_T} - F_R U_{L/T} \frac{(T_{inlet} - T_{amb})^2}{I_T} = a_0 - a_1 \frac{\Delta T}{I_T} - a_2 \frac{\Delta T^2}{I_T} \quad (3.10)$$

The coefficients for this collector are as follows: $a_0 = 0.691$, $a_1 = 3.396$ W/m^2-C, and $a_2 = 0.01968$ W/m^2-C^2. Coefficient a_2 ($F_R U_{L/T}$) accounts for the linear dependency of U_L versus T_{inlet} -T_{amb} (Duffie and Beckman, 2006). Figure 3.15 plots the incidence angle modifier K(τα). For this collector, b_0=0.194 and b_1=0.006.

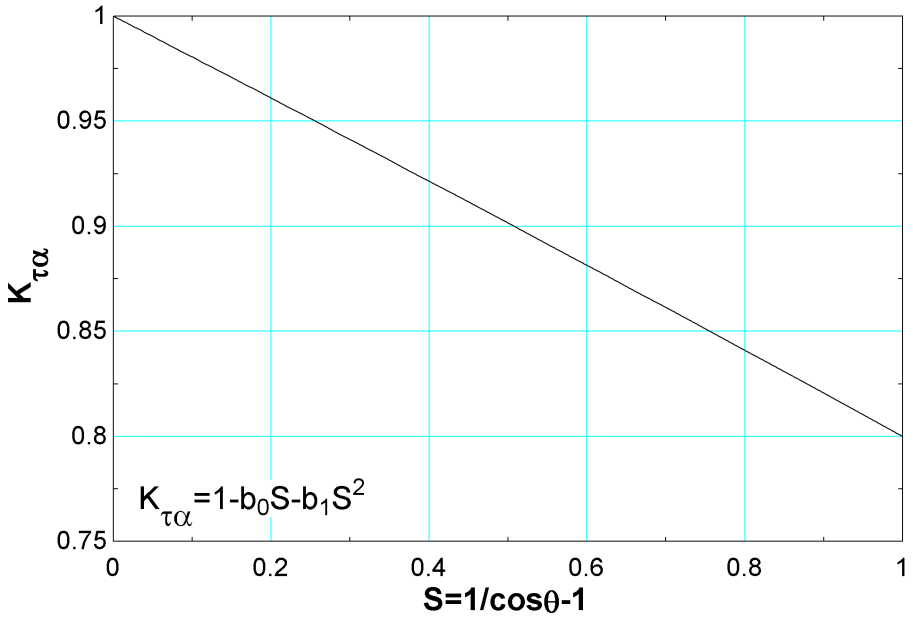

Figure 3.15: K(τα) as a function of incidence angle (θ) and S (1/cosθ-1).

While the collector could be mounted on the roof with a slope of 26.5° at an azimuth of 0° (south-facing) this orientation will not yield optimal performance in the winter months. A rack-mounted collector at a 60° slope will collect more thermal energy (for

the Chicago location). The optimal collector slope will vary from location to location. The Type 1b collector has outputs of temperature, flow rate and useful energy gain.

3.5.2 Pumps and Control

There are two pumps in this system, one for the collector loop and one for the heat exchanger loop. Both are modeled using the Type 3b Pump and run on independent control schemes. The collector loop pump is controlled using an on/off differential controller. The control scheme monitors the cold outlet temperature of the tank (the bottom node) and the hot outlet temperature of the collector. If the collector has the ability to raise the temperature of the water, the controller will run the pump. The control loop for the heat exchanger runs in a similar manner. The controller checks that the tank outlet (the top node) is above 30°C so that running the system will create comfortable heat transfer to the room. It also determines whether there is a building load at the current time step. If there is no load or the tank outlet temperature is too low then the controller remains off. Both controllers will turn off if the fluid temperature reaches 100°C.

3.5.3 Thermal Storage Tank

The storage medium is a simple, thermally insulated tank. In TRNSYS, Type 4c is the tank model used, which represents a multi-node stratified tank with the option of auxiliary heaters. If the tank temperature drops below 30°C, the tank is unable to provide thermal energy to building. Any thermal losses during the heating season can be considered to be beneficial as the tank environment is the conditioned living space. The model is capable of representing the tank with a variable number of tank segments or nodes. Increasing the number of nodes improves the ability to accurately model the

thermal stratification in the storage tank, which asymptotically improves system performance. The effect of number of nodes on the results will be shown in Chapter 4. The tank model records the inlet and outlet temperatures along with the energy received from the source, which is delivered to the load and lost through the tank walls.

3.5.4 Heat Exchanger

The TRNSYS Type 91 constant effectiveness heat exchanger (independent of configuration) is used to model the thermal exchange between the air and hot water. The specific heat of both the water and air are assumed to be constant at 4.19 and 1 kJ/kg-K, respectively. The heat exchanger model records inlet and outlet temperatures along with the energy transferred. The energy transferred is determined from minimum capacitance stream, shown by equation (3.11).

$$\dot{Q}_{\max} = \dot{C}_{\min}\left(T_{h,i} - T_{c,i}\right) \tag{3.11}$$

The actual heat transfer is then calculated with equation (3.12).

$$Q = \varepsilon \bullet Q_{\max} \tag{3.12}$$

Part of the solar design process requires that the load heat exchanger avoids becoming highly resistive to heat transfer. A poorly designed heat transfer process will result in higher tank temperatures and a reduction in the efficiency and collector useful energy gain. An ideal operating range is defined by equation (3.13), where ε_L is the heat exchanger effectiveness, $(UA)_h$ is the building conductance, and $C_{\min}$ is the minimum capacitance rate.

$$1 < \frac{\varepsilon_L C_{\min}}{(UA)_h} < 5 \tag{3.13}$$

For the heat exchanger, the effectiveness is held constant at 0.95, the maximum air flow rate is 1000 kg/hr (approx. 500 cfm) and the water flow rate is 500 kg/hr. In this heat exchanger, the air has the minimum capacitance rate and controls the heat exchanger effectiveness. Due to the energy rate control simulation method, the building load at every time step is known and the energy delivered to the room should never exceed the amount required by the room. This situation differs from reality in that a real system would allow temperature fluctuations (delivering more or less energy than required). Thus, the air is driven by a variable speed fan, so that it can be slowed to reduce the maximum amount of energy delivered to the heat exchanger. The amount of energy delivered to the room is determined at each time step calculated by equation (3.14).

$$\dot{q} = \dot{q}_{\max} \varepsilon = \dot{C}_{\min} (T_{water,in} - T_{air,in}) \varepsilon \tag{3.14}$$

If the heat transfer to the air is greater than the building load, then only a fraction of the energy is needed, which is calculated by equation (3.15).

$$Fraction = MIN\left(\frac{BuildingLoad}{\dot{q}}, 1 \right) \tag{3.15}$$

This fraction, between 0 and 1, is multiplied by the flow rate of the air. Reducing the flow of the air will reduce the amount of energy transferred to the room. The way this system is simulated deviates from the actual workings of a solar thermal system. More than likely, the system would not utilize a variable speed fan due to increased cost and

the ability to deliver more energy than the building requires (temperature is allowed to fluctuate unlike an ERC simulation).

4. Results

This chapter will discuss and analyze the results from the various simulations and models discussed in this thesis. First the building model results will be discussed. These results, which are loads files, were then used to simulate the various heat pumps and solar equipment.

4.1 Building Model

This section will present the energy rate control simulation results for the building model discussed in Chapter 2. The primary locations of interest are cold climates, where the heating load dominates the energy consumption of the building. Achieving reduced energy consumption in locations such as San Francisco, California is less interesting, because the climate type is very temperate, and the number of conditioning hours required is small. However, reducing the conditioning energy requirement for locations such as Chicago, Illinois are more interesting, as it is possible for monthly average temperatures to be as low as -10°C during heating months. Another location of interest is a cooling dominated climate, such as Dallas, Texas, where the cooling loads dominate the conditioning energy requirement. Traditionally, air-source heat pumps are common in areas where the heating loads are small and temperate.

Chicago, IL is reported to have approximately 3,465 annual heating degree days measured at a base temperature of 18°C (Degree Days, 2012). Heating and cooling degree days characterize an environment in terms of conditioning requirements. Degree days are calculated by using equation (4.1) (Duffie and Beckman, 2006).

$$DD = \sum_{mo} \left(T_{base} - T_{av} \right)^{+} \tag{4.1}$$

A degree day takes the difference between the daily average ambient temperature, T_{av}, and the base temperature, T_{base} (18°C), and multiplies it by the time step (1 day). Cooling degree days are calculated in the same manner, except that the ambient temperature must be higher than the base temperature.

A heating and cooling schedule was created for the Chicago location. This schedule prevented the equipment from heating and cooling in the same day. For example, using the energy rate control simulation, it was possible for a slight cooling load to be present during the day and a heating load to be present at night, especially in the spring and fall months. It was decided that most occupants in the spring and fall do not mind when the temperature increases slightly over the set point, and thus, they would not require cooling for a few hours of the afternoon. Table 4.1 on the following page shows the heating and cooling monthly schedule for the Chicago location. For example, in May, no cooling is provided even if the house temperature increases over the set point. This table may not be valid for extreme weather years, where there are significantly more cooling or heating days, but for the average weather data being used for this research, this schedule is appropriate. Using the construction parameters presented in Chapter 2, the energy rate control simulation was run and the following monthly building conditioning requirements were totaled, as seen in Table 4.2.

Table 4.1: This table shows the heating and cooling months for the Chicago location. H - Heating, C - Cooling.

Month	Mode
Jan	H
Feb	H
Mar	H
Apr	H
May	H
Jun	C
Jul	C
Aug	C
Sep	C
Oct	H
Nov	H
Dec	H

Table 4.2: Monthly conditioning energy requirement for Chicago, IL. These values do not include HVAC inefficiencies. They represent the ideal amount of energy required to meet the building set point.

Month	Energy Req. [GJ]
Jan	8.77
Feb	7.07
Mar	4.99
Apr	2.95
May	0.65
Jun	1.9
Jul	3.64
Aug	2.18
Sep	0.89
Oct	0.82
Nov	4.02
Dec	8.23

The energy requirement in Table 4.2 is the exact amount of energy required to maintain the building set point. The calculation does not include the efficiency of any conditioning equipment. A data file was created which contains the building load in kJ/hr at 15 minute time steps that will be used when simulating the conditioning equipment.

For this house, the amount of energy required to maintain the building set point during the heating months was 37.5 GJ while the total cooling requirement is 8.61 GJ. The heating energy requirement represents 81.3% of the total conditioning energy that must be met by HVAC equipment. It is possible that by using a heat pump with an average COP of 3 that the heating requirement could be met with 12.5 GJ or 3472 kW-hr of electricity. Another alternative is to use a high efficiency natural gas furnace (condensing furnace at 90% efficiency), which would require 41.67 GJ or 394.9 therms. These options will be evaluated in the following sections of this chapter.

The other location of interest was Dallas, TX. This location is a warm/hot climate with approximately 3945 cooling degree days, measured with a base temperature of 10°C. The heating and cooling schedule along with monthly conditioning requirements are provided in Table 4.3.

Table 4.3: This table shows the heating and cooling months for the Dallas location. H - Heating, C - Cooling. Also, the monthly energy requirements to condition the home are shown. These values do not include HVAC inefficiencies. They represent the ideal amount of energy required to meet the building set point.

Month	Mode	Energy Req. [GJ]
Jan	H	3.61
Feb	H	2.66
Mar	C	0.34
Apr	C	0.82
May	C	2.49
Jun	C	4.44
Jul	C	6.47
Aug	C	6.37
Sep	C	4.48
Oct	C	1.3
Nov	H	0.73
Dec	H	3.18

The total conditioning requirement for Dallas is 36.78 GJ. The energy required for cooling contributes to 72.4% of the total energy required to condition the home.

4.1.1 Building Comfort Analysis

The other simulation method described in this thesis was temperature level control. A detailed 14 zone building (10 of which are conditioned) building model was developed (Chapter 4) and used to calculate building loads in Chicago, IL using temperature level control to determine the effects of an improperly tuned air delivery system. A single thermostat that controls the heating/cooling is located in the kitchen, which is a large open room that is 20 ft by 30 ft, including a dining area. When the thermostat indicates a need for heating or cooling, the heat pump is operated and conditioned air is delivered to each room/zone by ducts. The amount of flow deliver from each duct is determined by the tuning of the air delivery system.

Various comfort results are possible depending on the fraction of the conditioned air flow that is diverted to each room. For instance, sending equal amounts of flow to each zone will cause large zones to be under-heated while small zones will be over-heated during the heating season. Only the zone that includes the thermostat is conditioned properly, assuming that the heating and cooling equipment have sufficient capacity. In another extreme, a large fraction of the flow might be diverted to the zone with the thermostat. This situation causes the heat pump to run less, and reduces the heating provided to the other zones in the house. This scenario would consume less energy, as the heat pump is running and delivering nearly all of the energy to one zone, but most of the other zones in the house will not be comfortable. In a real application, the flow of conditioned air for each zone need to be balanced by positioning using splitters or other means. In order to determine the ideal values for the splitters (i.e., the ideal air distribution in the house), the previous ERC simulation results were used and the required energy to maintain each

room at a set temperature was recorded. Knowing the total amount of energy required to condition the home, the fractions were calculated for each room (by dividing the room requirement by the entire house requirement). These fractions are shown below in Table 4.4.

Table 4.4: Fractions for the splitters that determine the airflow delivered to each room for the Chicago, IL home.

Splitters	Kitchen	Living	Bed 1	D Bath	U Bath	Mast Bed	Bed 2	Hall	Mud	Basement
Year End Total	0.239	0.051	0.023	0.065	0.120	0.110	0.099	0.116	0.029	0.149
Hour 86.25	0.224	0.052	0.024	0.061	0.137	0.122	0.113	0.110	0.028	0.130
Hour 7714.88	0.154	0.012	0.007	0.103	0.167	0.123	0.064	0.177	0.059	0.134

It was found that the required splitter fractions for each room vary somewhat depending on the hour, due to internal or solar gains that change with time. An ideal conditioning system would need to have controls to determine the fraction of the flow should be delivered to each room, based on the varying solar generation and internal gains, but the likelihood of implementing a control scheme of this nature in a residential application is small.

To determine if the house is meeting zone comfort requirements, a tally was kept that records the number of time steps that the zone temperature drops below the thermostat set point. Table 4.5 and Table 4.6 summarize the number of hours that the room temperatures dropped below or rose above the thermostat set point for heating and cooling respectively, for three different cases corresponding to a 3 ton and 5 ton capacity system with the ideal distribution of flow identified in Table 4.4. Also shown in these tables are the results for a 3 ton capacity system in which all rooms are provided with an equal fraction (10%) of the conditioned air flow.

Table 4.5: This table shows the number of hours that the rooms dropped below the set point (during heating). The 3 and 5 ton simulations used the "Year End Total" splitter settings, while the Even 10% used an equal 10% division of the flow to each room. A 3 ton heat pump was used for that simulation. The house location is Chicago, IL.

Heating	Kitchen [hr]	Basement [hr]	Master Bed [hr]	Bed 1 [hr]	Bed 2 [hr]
3 Ton	0.9	1443.3	283.7	132.0	59.7
5 Ton	0.8	1669.8	345.9	191.7	64.2
Even 10%	257.1	1029.0	83.7	37.0	35.5

	Mud [hr]	Living [hr]	U Bath [hr]	D Bath [hr]	Hallway [hr]
3 Ton	143.6	9.2	516.1	9.2	451.7
5 Ton	180.9	2.8	592.1	3.2	530.5
Even 10%	0.0	1.4	25.4	0.0	89.8

Table 4.6: This table shows the number of hours that the room temperatures rose above the set point (during cooling). The 3 and 5 Ton simulations used the "Year End Total" splitter settings, while the Even 10% simulations used an equal 10% division of the flow to each room. A 3 Ton heat pump was used for that simulation as well.

Cooling	Kitchen [hr]	Basement [hr]	Master Bed [hr]	Bed 1 [hr]	Bed 2 [hr]
3 Ton	0.5	0.0	182.4	74.6	58.0
5 Ton	0.6	0.0	250.7	104.4	81.9
Even 10%	61.8	0.0	9.5	6.0	5.4

	Mud [hr]	Living [hr]	U Bath [hr]	D Bath [hr]	Hallway [hr]
3 Ton	0.0	0.1	63.6	0.2	4.0
5 Ton	0.0	0.1	118.5	0.2	6.2
Even 10%	0.0	0.0	5.0	0.0	3.9

In addition, the tally records the degree-hours (the number of hours multiplied by the number of degrees outside of the set point) for each zone in order to help quantify the magnitude that the temperature is below the set point (or above for cooling).

Table 4.7: Heating degree-hours calculated for each room. The 3 and 5 Ton simulations used the "Year End Total" splitter settings, while the Even 10% simulations used a equal 10% division of the flow to each room. A 3 Ton heat pump was used for that simulation as well. The house location is Chicago, IL.

Heating	Kitchen [C-hr]	Basement [C-hr]	Master Bed [C-hr]	Bed 1 [C-hr]	Bed 2 [C-hr]
3 Ton	0.5	2955.6	173.8	53.6	15.0
5 Ton	0.3	3488.8	258.0	94.9	17.9
Even 10%	546.9	1859.5	102.1	38.7	37.5

	Mud [C-hr]	Living [C-hr]	U Bath [C-hr]	D Bath [C-hr]	Hallway [C-hr]
3 Ton	64.7	2.3	508.1	2.8	449.1
5 Ton	88.1	0.8	676.1	0.6	632.2
Even 10%	0.0	0.5	14.0	0.0	70.4

Table 4.8: Cooling degree-hours calculated for each room. The 3 and 5 Ton simulations used the "Year End Total" splitter settings, while the Even 10% simulations used a equal 10% division of the flow to each room. A 3 Ton heat pump was used for that simulation as well. The house location is Chicago, IL.

Cooling	Kitchen [C-hr]	Basement [C-hr]	Master Bed [C-hr]	Bed 1 [C-hr]	Bed 2 [C-hr]
3 Ton	0.110	0.000	105.728	28.180	17.0
5 Ton	0.136	0.000	162.945	44.238	31.6
Even 10%	49.095	0.000	8.902	4.195	3.0

	Mud [C-hr]	Living [C-hr]	U Bath [C-hr]	D Bath [C-hr]	Hallway [C-hr]
3 Ton	0.0	0.0	14.3	0.0	1.6
5 Ton	0.0	0.0	38.4	0.0	1.7
Even 10%	0.0	0.0	3.0	0.0	1.5

These data are helpful because they allow for the quantification for how far off the set point the zone temperature is. Looking specifically at Bedroom 2 in Table 4.5 for the 3 ton heat pump capacity, the heating set point was not maintained during 59.7 hours during the year. The corresponding number of heating degree-hours (Table 4.7) that were not met by conditioning equipment for Bedroom 2 (using the 3 ton heat pump capacity) is 15 °C-hr. Many possibilities exist, but two examples can be examined. One possibility exists, while unlikely, that for 1 hour the temperature was below the set point by 14°C. Then, for the remaining the 58.7 hours, the temperature missed the set point by a total of 1°C, averaging out to 0.017°C below the set point for each of the remaining 58.7

hours. Again, this case is very unlikely. The most likely case is that the largest temperature drops occur when the outdoor temperature is the coldest and the internal gains are the smallest. Since it is not feasible to sort through all of the time steps, an average can be taken to determine the average ^{o}C above or below the set point for each room, seen in Table 4.9. This information gives insight on how comfortable each room is in terms of temperature. The basement tends to always be approximately 0.6°C too hot or cold, on average. This likely means that the temperature drops or rises several degrees from the set point when the outdoor temperature is cold or hot, respectively.

Table 4.9: Average temperature that set point is missed by per hour. These values are above the set point in the summer and below in the winter. These are yearly averaged values. The 3 and 5 Ton simulations used the "Year End Total" splitter settings, while the Even 10% simulations used a equal 10% division of the flow to each room. A 3 Ton heat pump was used for that simulation as well.

Averages	Kitchen [C]	Basement [C]	Master Bed [C]	Bed 1 [C]	Bed 2 [C]
3 Ton	0.4	1.0	0.6	0.4	0.3
5 Ton	0.3	1.0	0.7	0.5	0.3
Even 10%	1.5	0.9	1.1	0.9	0.8

	Mud [C]	Living [C]	U Bath [C]	D Bath [C]	Hallway [C]
3 Ton	0.2	0.2	0.6	0.3	0.7
5 Ton	0.2	0.2	0.7	0.1	0.7
Even 10%	0.0	0.2	0.6	0.0	0.6

The total amount of electricity consumed by each system is presented in Table 4.10. The first conclusion that can be drawn from these data is that over sizing the heat pump leads to larger energy consumption. In addition, over sizing can also lead to the heat pump running for a shorter amount of time, thus (counter-intuitively) reducing the zone comfort in the rooms that do not contain the thermostat. This result is seen by comparing the average temperature results (Table 4.9) of the 3 ton and 5 ton heat pumps. Also, while not shown in the above data, during summer months the heat pump also lowers the humidity in the zone. Humidity level is important to proper comfort, although it is

controlled indirectly in residential systems. If the heat pump is not running for a sufficiently long time, the humidity in all of the zones will increase causing possible discomfort, even if the temperature of zone is maintained close to the set point.

If the ducting system distributes an even amount of conditioned air to each zone, specified by the "even 10%" rows in the tables above, the amount of energy required to condition the building increases. This result is mainly based on the location of the thermostat. The thermostat is located in the kitchen, which is an open concept design including the dining area, with dimensions of 20 feet by 30 feet. This is one of the largest zones in the house and the heat pump struggles to condition this room to the required set point when it delivers only 10% of the total flow. This in turn causes the heat pump to run nearly continuously, over cooling and over heating the smaller rooms in the house. These results show the importance of having a duct system that is properly tuned.

Table 4.10: This data shows the energy consumed by the heat pump to provide heating and cooling for one year. The 3 and 5 Ton simulations used the "Year End Total" splitter settings, while the Even 10% simulations used a equal 10% division of the flow to each room. A 3 Ton heat pump was used for that simulation as well.

Electricity	Total [GJ]
3 Ton	21.34
5 Ton	22.19
Even 10%	32.28

4.2 Air-Source Heat Pump

This section will cover the results simulating the building heating and cooling needs using an air source heat pump. First, sizing of the heat pump will be addressed, which will be valid for any simulation location. Then simulations will be run for both the Chicago and Dallas locations are evaluated against the conventional system, on both

energy and economic savings bases. Lastly, a climate zone map will be presented to evaluate air-source heat pump in various climate types.

4.2.1 Air-Source Heat Pump Sizing

In order to successfully implement a heat pump for conditioning a home, it must be sized properly. This proper heat pump size is chosen by using building loads to determine the actual capacity required for condition the home. Contractors commonly oversize HVAC equipment to avoid potential occupant discomfort and customer dissatisfaction. However over-sizing is not a beneficial practice because as the equipment is oversized, it becomes less efficient, as seen in Figure 4.1 for Chicago, IL. When the available capacity of a heat pump is larger than the building load, the heat pump must cycle, which consumes more energy, reduces the ability to control humidity levels during the cooling season and also reduces the lifetime of the equipment.

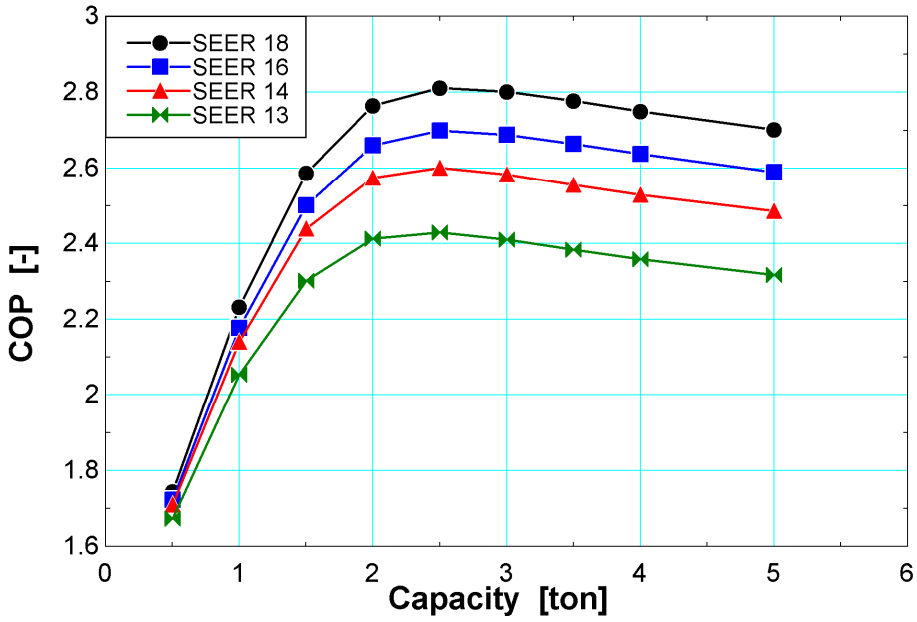

Figure 4.1: Heat pump performance vs. capacity when simulated in the Chicago, IL home.

To size the heat pump, various capacities are simulated with a building loads file (for any location). The results of interest are the fraction of the building load the heat pump meets. It is assumed that the heating system has unlimited auxiliary heating capacity, with the use of electric strip heaters. This assumption means that the heating system will always be able to meet the heating load. Even if the heat pump can only supply 5% of a large heating load, the auxiliary heaters will supply the remaining 95%. In this case, the size of the heat pump is solely determined by the cooling load. Table 4.11 presents the fraction of the cooling load met for Chicago, IL for a range of heat pump nominal cooling capacities. Both the total summer load and largest daily cooling load is shown. Rated cooling capacity is measured at 27°C dry bulb and 19°C wet bulb temperatures. Rated heating capacity is measured at 8°C dry bulb and 6°C wet bulb temperatures.

Table 4.11: Fraction of load met by the heat pump for Chicago, IL. Results include both total summer load and the summer day with the largest cooling load.

Chicago, IL	**Rated Capacity [ton]**					
	0.5	*1*	*1.5*	*2*	*2.5*	*3*
Frac. of Load Met On Worst Summer Day	0.59	0.89	1	1	1	1
Frac. of Total Summer Load Met	0.78	0.98	1	1	1	1

As the heat pump capacity is increased to 1.5 ton, the heat pump is able to meet the entire cooling load. A 1 ton may seem acceptable, as it meets 98% of the cooling load and 89% on the summer day with the largest cooling load. However, the cooling load data are for an average cooling season. If Chicago were to experience an abnormally hot summer, this fraction would drop further, potentially leading to occupant discomfort. Thus, for this Chicago home, the recommended heat pump capacity is 1.5 ton. Heat pump efficiency is not important in this choice because a SEER 18 rated model and SEER 13

rated model will both deliver the same capacity, the only difference being the energy consumption to do so.

For Dallas, the heat pump size must be larger, due to the larger cooling loads. Recall that in Chapter 2, it was determined that for the Dallas home the window type would be adjusted to reduce solar gains. Table 4.12 shows that the heat pump must have a 2 ton capacity to successfully condition the home during the cooling season. On the worst day, 94% of the cooling load is met.

Table 4.12: Fraction of load met by the heat pump for Dallas, TX. Results include both total summer load and the summer day with the largest cooling load.

Dallas, TX	**Rated Capacity [ton]**					
	0.5	*1*	*1.5*	*2*	*2.5*	*3*
Frac. of Load Met On Worst Summer Day	0.43	0.78	0.944	1	1	1
Frac. of Total Summer Load Met	0.63	0.91	0.99	1	1	1

The heat pump capacity chosen for a building affects both its energy use and economics. In cold climate locations such as Chicago, IL, increasing the heat pump capacity will reduce the amount of auxiliary heating (by increasing the load met by the heat pump). This is advantageous because auxiliary heating (electric resistance heating) has a COP of 1. The fraction of the heating load met for Chicago, IL is shown in Table 4.13.

Table 4.13: Fraction of the heating load met for Chicago, IL.

Chicago, IL	**Rated Capacity [ton]**								
	0.5	*1*	*1.5*	*2*	*2.5*	*3*	*3.5*	*4*	*5*
Fraction of heating load met	0.47	0.72	0.84	0.9	0.92	0.92	0.93	0.93	0.93

As the heat pump capacity is increased beyond the recommended minimum of 1.5 ton, the fraction of the heating load met by the heat pump increases. For the 2 ton capacity, the heat pump meets 6% more of the heating load than the 1.5 ton. An economic analysis

will determine if the extra capital cost of the large capacity is worth the 6% reduction in strip heating. A life-cycle economic analysis will be used for this, and the remainder of the results. This method looks at the capital costs and the present worth of fuel expenses over the life of the system. Equation (4.2) shows the P1, P2 method, or life cycle costs (Duffie and Beckman, 2006).

$$LCC = P_1 C_{fuel} L + P_2 C_{equip} \tag{4.2}$$

In this equation, C_{fuel} and C_{equip} represent the costs of electricity (0.14 $/kW-hr, assuming no seasonal adjustment) and equipment (HVAC or solar, including installation). L is the annual total electric energy required to run the heat pump. P_1 is equal to the present worth factor (PWF), which is based on the number of years of the analysis (16 years), the fuel inflation rate which will be varied, and the market discount rate (8%). Since this analysis assumes the unit was purchased without a loan and that no maintenance costs will occur over the lifetime, P_2 is equal to 1. The assumed lifetime for a heat pump is 16 years, which is the given equipment lifetime in the BEopt optimization software (BEopt, 2012).

For Chicago, simulations were run for 4 different heat pump seasonal efficiency ratings: SEER 13, 14, 16 and 18. The SEER 16 and 18 models utilized two stage compressor technology, allowing the compressor to operate at two different speeds (delivering two different capacities) improving the heat pump's load following abilities. The economic results of these simulations are seen in Table 4.14, for various capacities.

Table 4.14: This table presents the economic results ($) for various heat pump capacities and efficiencies for the Chicago, IL simulation case. The fuel inflation rate was set to 5%.

	Rated Capacity [ton]						
LCC [$], i_f=0.05	*0.5*	*1*	*1.5*	*2*	*2.5*	*3*	*3.5*
SEER 13/1 Stage	13647	11942	11497	11751	12382	13147	13939
SEER 14/1 Stage	13412	11598	**11123**	11385	12040	12839	13669
SEER 16/2 Stage	13429	11638	11186	11509	12229	13103	14013
SEER 18/2 Stage	13370	11590	11194	11593	12400	13364	14368

When the fuel inflation rate is set to 5%, the economic analysis shows that selecting the smallest available capacity is the best choice, in terms of economics. In addition, it is also found that selecting a model rated at a SEER of 14 is more economical than the higher efficiency models (SEER 16 and 18). In 2006, federal guidelines stated that a SEER 14 (or higher) unit qualifies for the EnergyStar rating, so this recommended SEER 14 would be considered an energy efficient model to most consumers (Consumer Energy Center, 2012). Another possibility is that electricity costs will inflate significantly in the future at a rate of 15%. If this were to happen, the recommended capacity would change, seen in Table 4.15.

Table 4.15: This table presents the economic results ($) for various heat pump capacities and efficiencies for the Chicago, IL simulation case. The fuel inflation rate was set to 15%.

	Rated Capacity [ton]						
LCC [$], i_f=0.15	*0.5*	*1*	*1.5*	*2*	*2.5*	*3*	*3.5*
SEER 13/1 Stage	27192	22980	21347	21144	21712	22553	23448
SEER 14/1 Stage	26660	22174	20427	20188	20755	21614	22537
SEER 16/2 Stage	26592	22049	20248	20030	20626	21535	22521
SEER 18/2 Stage	26368	21746	19957	**19791**	20461	21453	22527

With a higher inflation rate, the ability to save on yearly energy expenses becomes much more apparent, as the economic results point to choosing the 2 ton unit. Table 4.16 shows the annual electricity consumption for each heat pump.

Table 4.16: This table shows the energy consumption results for each heat pump efficiency and capacity in the Chicago, IL simulations.

	Rated Capacity [ton]						
Consumption [kW-hr]	*0.5*	*1*	*1.5*	*2*	*2.5*	*3*	*3.5*
SEER 13/1 Stage	7654	6238	5566	5308	5272	5315	5374
SEER 14/1 Stage	7486	5977	5258	4975	4925	4959	5011
SEER 16/2 Stage	7438	5884	5121	4815	4745	4765	4808
SEER 18/2 Stage	7345	5739	4952	4633	**4556**	4571	4610

The lowest energy consumption was provided by the 2.5 ton capacity SEER 18 heat pump. As the capacity increases beyond 2.5 ton, any energy savings from a reduction in auxiliary heating (seen in Table 4.13) are offset by the increase in energy consumption from cycling during the cooling months.

Table 4.17: Economic results ($) for the Dallas, TX simulations.

	Rated Capacity [ton]						
LCC [$], i_f=0.05	*0.5*	*1*	*1.5*	*2*	*2.5*	*3*	*3.5*
SEER 13/1 Stage	5625	6741	7672	8497	9324	10127	10907
SEER 14/1 Stage	5382	6416	7352	8212	9076	9918	10739
SEER 16/2 Stage	5262	6232	7157	**8091**	9032	9969	10892
SEER 18/2 Stage	5212	6217	7221	8246	9280	10311	11328

LCC [$], i_f=0.15	*0.50*	*1.00*	*1.50*	*2.00*	*2.50*	*3.00*	*3.50*
SEER 13/1 Stage	10782	12342	13522	14489	15457	16374	17247
SEER 14/1 Stage	10234	11574	12715	13699	14691	15638	16545
SEER 16/2 Stage	9886	10992	12007	13040	14086	15126	16136
SEER 18/2 Stage	9680	10755	11830	**12946**	14080	15208	16308

A similar trend is seen for the Dallas location. However, since Dallas does not experience the heavy reliance on strip heating due to small heating requirements, the economic optimum capacity is not affected by the fuel inflation rate. The economic analysis intuitively determines that a higher efficiency model should be chosen if the fuel inflation rate is high (15%), as seen in Table 4.17

4.2.2 Air-Source Heat Pump vs. Conventional System

The primary purpose of this research was to compare the heat pump system to a conventional system, on both an energy and cost savings basis. The previous section outlined optimally sizing the heat pump on a comfort and economic basis. Now, with a properly sized heat pump, the heat pump heating and cooling system can be compared to the conventional system, consisting of a condensing natural gas furnace (90% efficiency) and central air system (SEER 16, single stage compressor). The conventional system has been sized in the same manner as the heat pump systems, by using the building loads. The results of comparing the heat pump to the conventional system for the Chicago, IL house are seen below in Figure 4.2, where the fuel inflation rate is 5% for both natural gas and electricity.

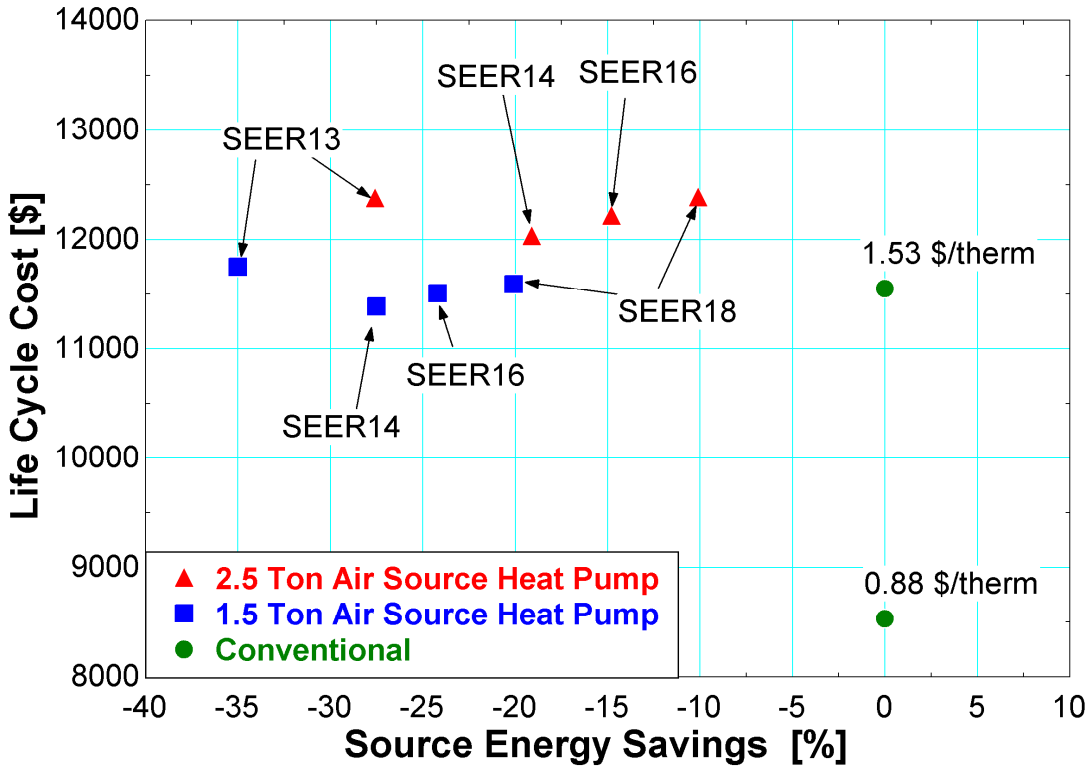

Figure 4.2: Life cycle cost vs. source energy savings for the heat pump systems and conventional system in Chicago. The conventional system is the baseline and represents 0% energy savings.

Energy savings are evaluated on a source energy basis, in which, Figure 4.2 shows that the heat pump systems consume at least 10% more source energy than the conventional system. Source energy considers that in addition to the energy used on site, there is an amount of energy required to deliver usable energy to the site. This research uses a site-source ratio (converting site energy to source energy) of 3.34 for electricity and 1.047 for natural gas (EnergyStar, 2011).

Another way to look at the source vs. site energy basis is to consider the heating loads. For example, consider a case where the electricity is produced at a natural gas fired power plant (operating with an overall efficiency of 33%). The total amount of electricity consumed for heating by the 2.5 ton SEER 18 heat pump system in Chicago was 3992.4 kW-hr (14.37 GJ). For the natural gas furnace, the amount of energy consumed to heat the home was 384.34 therms (40.37 GJ). Since the electricity is assumed to be produced by burning natural gas at 33% efficiency, it is possible to determine how much natural gas was consumed to produce the 3992.4 kW-hr (14.37 GJ) of electricity that ran the heat pump. For this situation, the natural gas required to create 3992.4 kW-hr of electricity is 43.55 GJ (412.8 therms), more than was required to use the natural gas furnace. A possibility also exists that the electricity was generated by a renewable power plant, which would yield a site-source ratio close to 1, making the heat pump a superior option for source energy savings (compared to the natural gas furnace). Figure 4.3 shows the results if the electricity for both the heat pump and conventional system were produced at a renewable energy power plant. A conservative site-source ratio of 1.2 is used to account for distribution and any other unforeseen factors.

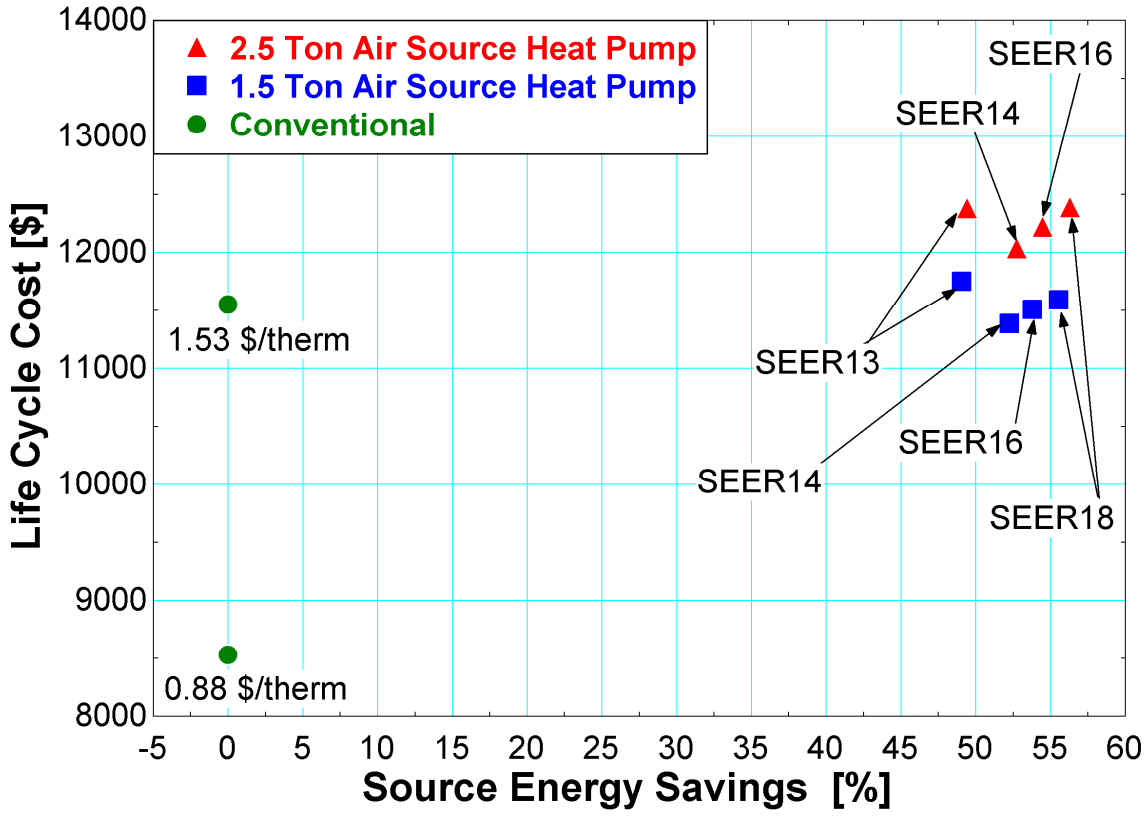

Figure 4.3: Life cycle cost vs. source energy savings for both the heat pump systems and conventional system in Chicago. The conventional system is considered the baseline and represents 0% energy savings. The fuel inflation rate for electricity and natural gas is 5%. This case represents a site-source ratio of 1.2 for electricity (off-site renewable electricity generation).

Figure 4.2 shows that the heat pump systems have significantly larger life cycle costs than the conventional system. This is primarily because current natural gas prices are inexpensive, at 0.70 to 0.90 $/therm. If natural gas were to double in price (1.53 $/therm data point) while electricity prices remain unchanged, the heat pump system would be economically competitive. Figure 4.3 shows that even off-site renewable generation of electricity would not change the life cycle costs outcome, unless electricity generation were to become less expensive.

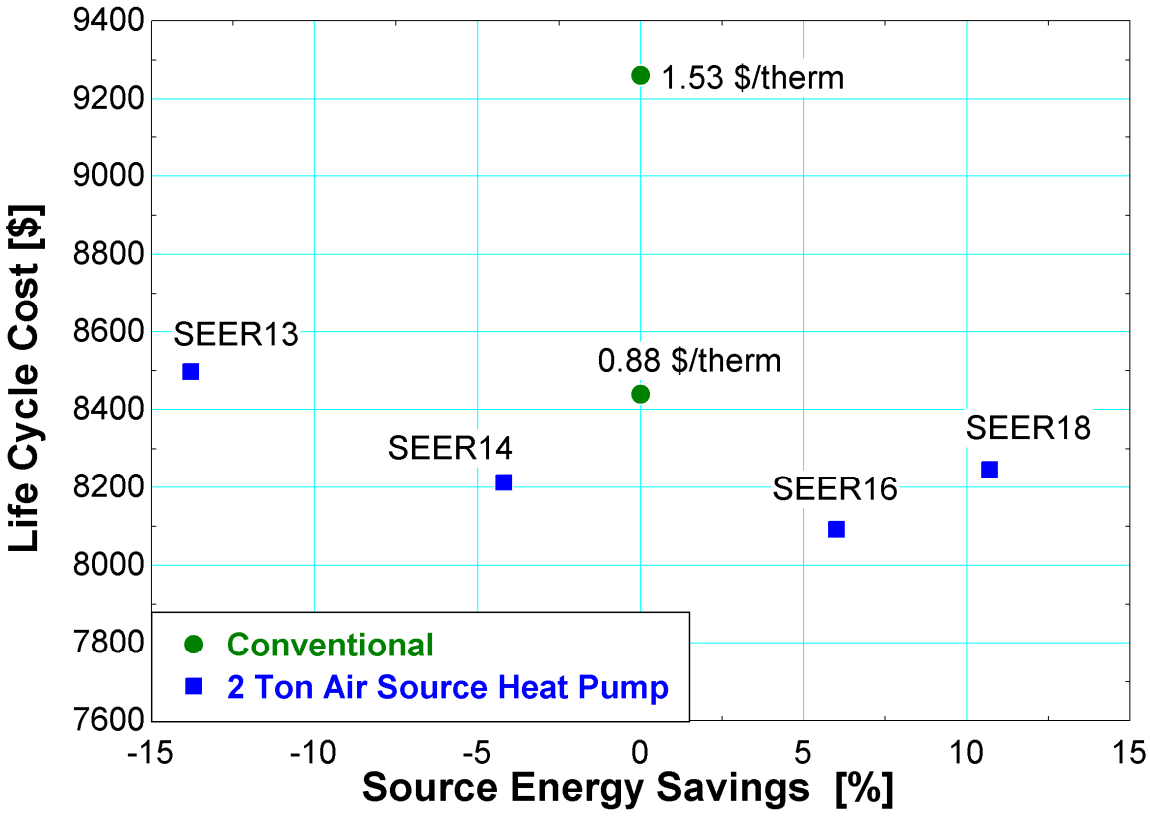

Figure 4.4: Life cycle cost vs. source energy savings for both the heat pump systems and conventional system located in Dallas, TX. The conventional system is considered the baseline and represents 0% energy savings. The fuel inflation rate for electricity and natural gas is 5%.

Simulation results for the house located in Dallas, TX are shown in Figure 4.4 for a fuel inflation rate of 5%. These results support the conclusion that heat pumps are more advantageous in warmer climates. The heat pump saves both source energy and has lower life cycle costs than the conventional system in the Dallas climate. Another added benefit is that the heat pump is a single system, where as the conventional system requires and air conditioner (a heat pump that only provides cooling) and a furnace to be installed.

4.2.3 Air Source Heat Pump Climate Zone Map

The performance of the air-source heat pump was determined in various climate zones. Representative cities for each climate zone in the United States were selected and are found in Table 4.18, along with the typical heating or cooling degree days associated with that climate zone.

Table 4.18: Climate zones and representative cities that are used to create the heat pump climate zone map.

Zone	Climate Zone	Thermal Criteria	Representative City
1A	Very Hot-Humid	5000>CDD10°C	Miami, FL
1B	Very Hot-Dry	5000>CDD10°C	-
2A	Hot-Humid	3500<CDD10°C<5000	Houston, TX
2B	Hot-Dry	3500<CDD10°C<5000	Phoenix, AZ
3A	Warm-Humid	2500<CDD10°C<3500	Memphis, TN
3B	Warm-Dry	2500<CDD10°C<3500	El Paso, TX
3C	Warm-Marine	HDD18°C<2000	San Francisco, CA
4A	Mixed-Humid	CDD10°C<2500 AND HDD18°<3000	Baltimore, MD
4B	Mixed-Dry	CDD10°C<2500 AND HDD18°<3000	Albuquerque, NM
4C	Mixed-Marine	2000<HDD18°<3000	Salem, OR
5A	Cool-Humid	3000<HDD18°<4000	Chicago, IL
5B	Cool-Dry	3000<HDD18°<4000	Boise, ID
5C	Cool-Marine	3000<HDD18°<4000	-
6A	Cold-Humid	4000<HDD18°<5000	Burlington, VT
6B	Cold-Dry	4000<HDD18°<5000	Helena, MT
7	Very Cold	5000<HDD18°<7000	Duluth, MN

Building simulations were run for each city so that building load files could be created for each climate. Climate zones 5-7 utilized high solar heat gain coefficient (SHGC) windows to take advantage of solar gains. Climate zones 1-4 reduced solar gains by using low SHGC windows, as described in Chapter 2. With building loads files, both the air-source heat pump and conventional systems could be simulated. Sizing of the heat pump was performed by first determining the minimum capacity that could meet the cooling load and then by analyzing the annual energy consumption, to determine if choosing a larger heat pump capacity could reduce the energy consumption. The heat

pumps chosen for each location represent the highest source energy savings, not necessarily the lowest life cycle cost. The economics are kept constant for each location, with an electricity cost of 0.14 $/kW-hr and natural gas cost of 0.88 $/therm. The air source heat pump climate map is presented in Figure 4.5, for a fuel inflation rate of 15% for both electricity and natural gas.

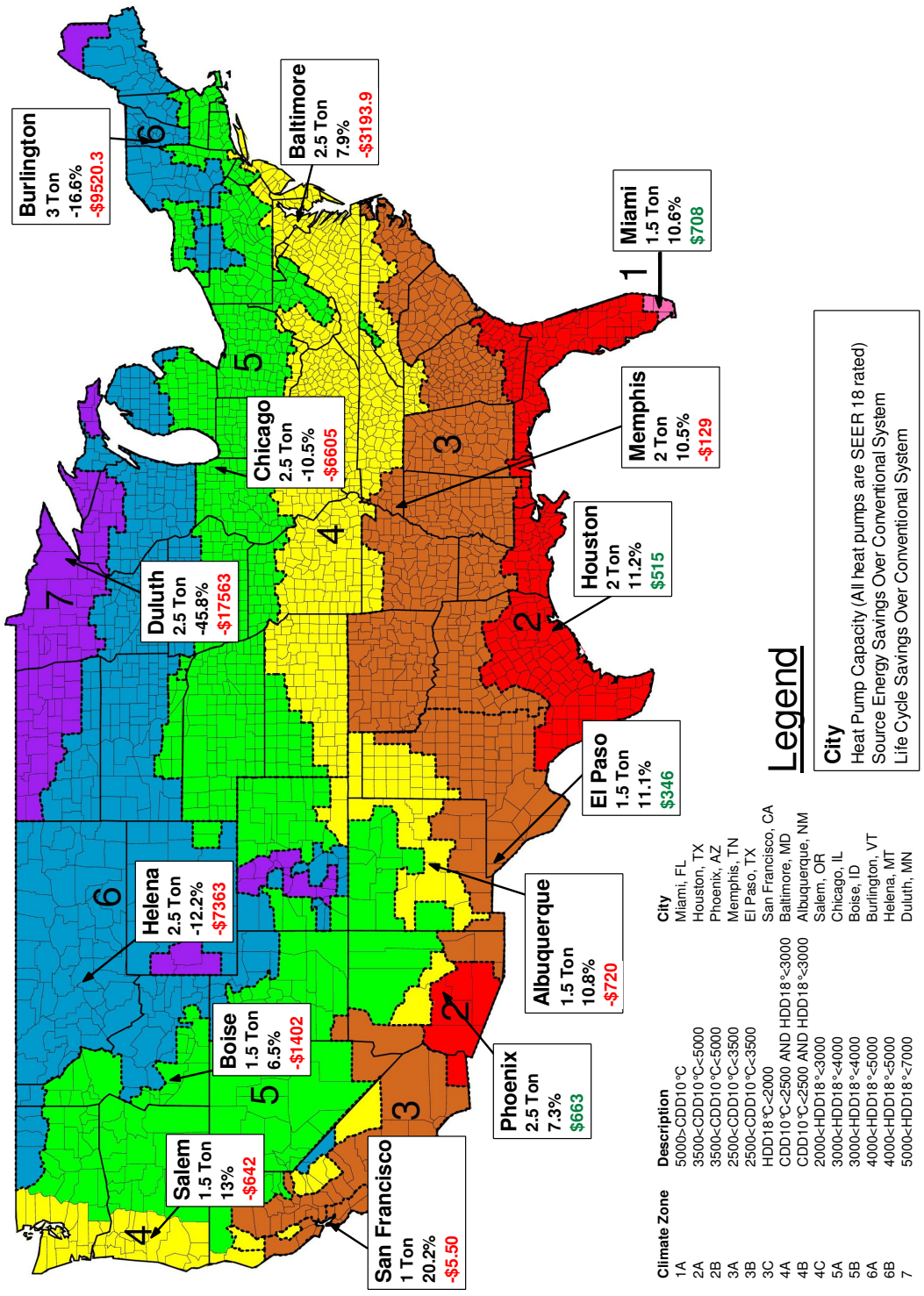

Figure 4.5: Air source heat pump climate zone map. The fuel inflation rate for electricity and natural gas is 15%. Heat pump sizing is based on largest source energy savings. (IECC, 2004)

Each box presents a location name, heat pump capacity that yields the largest source energy savings, source energy savings vs. the conventional system, and life cycle savings over the conventional system. If the source energy savings percentage is negative, such as for Chicago, the heat pump system is consuming more source energy than the conventional system. Likewise, if the life cycle savings are negative and red in color, the heat pump system costs more over the life of the equipment than the conventional system.

It is found that the air-source heat pump shows source energy savings in nearly every location except for heating dominated climates such as Burlington, Vermont, Chicago, Illinois or Duluth, Minnesota. The heat pump system also yields life cycle savings or breaks even with the conventional system in most southern locations and Pacific coast regions.

One conclusion that was made in the previous section that analyzed the results of Chicago, IL and Dallas, TX was that when natural gas is inexpensive it is difficult to justify consuming electricity (on an economic basis) for heating. If the economic outlook was to change, and natural gas was assumed to inflate at 15% while electricity inflated at 5%, a different economic outlook is seen in the heat pump climate zone map, Figure 4.6.

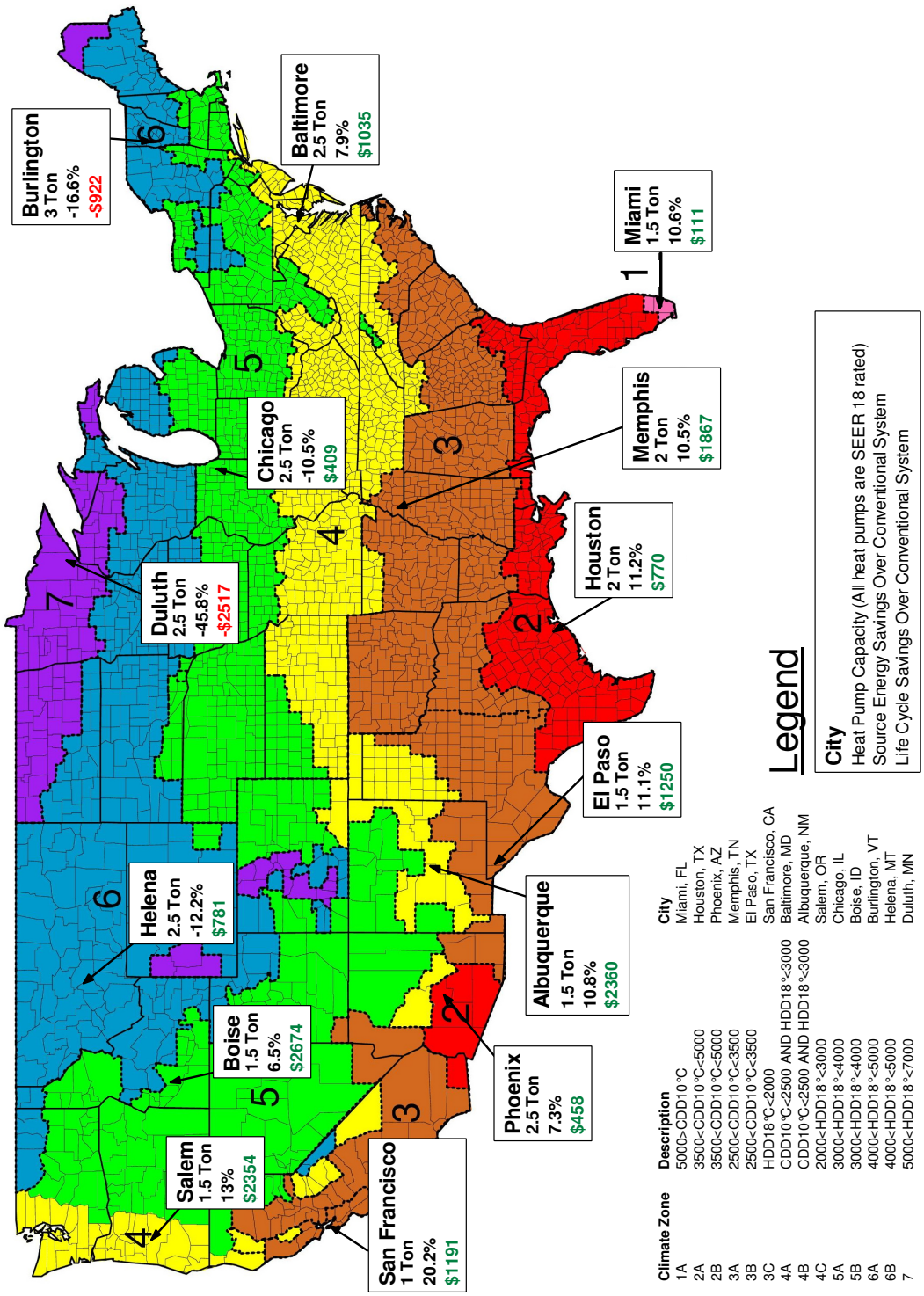

Figure 4.6: Air source heat pump climate zone map. The fuel inflation rate for natural gas is 15% while the rate for electricity is 5%. Heat pumps have a much better economic outlook with these fuel projections. (IECC, 2004)

With this economic forecast, a different outlook is seen for the economics of using a heat pump. In nearly every location (again, except for heating dominated climates such as Duluth, MN or Burlington, VT) the heat pump system yielded life cycle savings of $400 to $2360 over the conventional system. One problem with this analysis is that it assumes that a large inflation in the price of natural gas will have no effect on electricity. Currently, with new extraction advancements and availability, natural gas is becoming a popular power generation source. In addition, the current stigmatization of coal power generation has also caused natural gas power generation to gain popularity. If this trend continues, any inflation of natural gas prices would directly lead to the inflation of electricity prices, making the economic forecast in Figure 4.6 unrealistic.

4.2.4 Air-Source Heat Pump Performance

A reoccurring trend seen in the air source heat pump results is the poor energy and economic savings in cold climate cases when compared to the conventional system. A way to investigate the causes of poor performance is to look at the monthly COP values. The monthly COP can be calculated by using equation (4.3).

$$COP_{monthly} = \frac{Q_{monthly}}{W_{monthly}} \tag{4.3}$$

The monthly COP is simply the conditioning energy delivered by the heat pump, $Q_{monthly}$, divided by the energy required to operate the heat pump for the course of the month, $W_{monthly}$. Since energy rate control simulations are used and the heat pump always meets the conditioning requirement, $Q_{monthly}$ is also equal to the building conditioning

requirement for a specific month. The monthly COPs for the Chicago and Dallas simulations are shown in Figure 4.7.

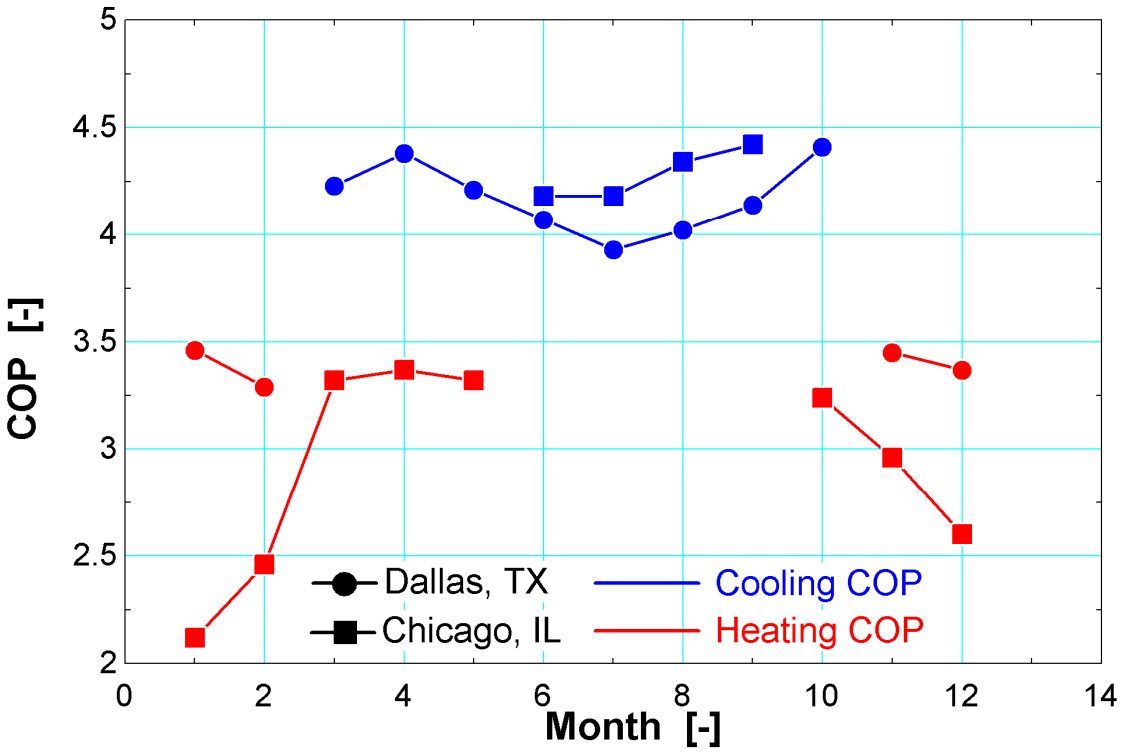

Figure 4.7: Monthly COP for the Chicago and Dallas simulations. The Dallas simulation used a 2 ton SEER 18 heat pump while the Chicago location used a 2.5 ton SEER 18 heat pump. Dallas results are represented with a circle while the Chicago results are signified with a square. Cooling COP results are blue in color while heating COP results are red in color.

The COP for the Chicago home is lower than the Dallas location primarily because of the cold operating conditions the heat pump is required to operate in. This figure presents an opportunity to investigate the theoretical performance of the heat pump. For example, if the performance of the heat pump is increased by 10% or 20%, will this cause the heat pump to save source energy over the Chicago conventional system? To accomplish this, the monthly COP, $COP_{monthly}$, is increased by 10% or 20%. Since the energy delivered to the building must be equal to the building conditioning requirement, it is possible to use equation (4.3) to calculate the amount of energy required to operate the heat pump when

the monthly COP increased by 10% or 20%. These results are then plotted against the conventional system (and the non-enhanced heat pump system) for Chicago, IL; Figure 4.8.

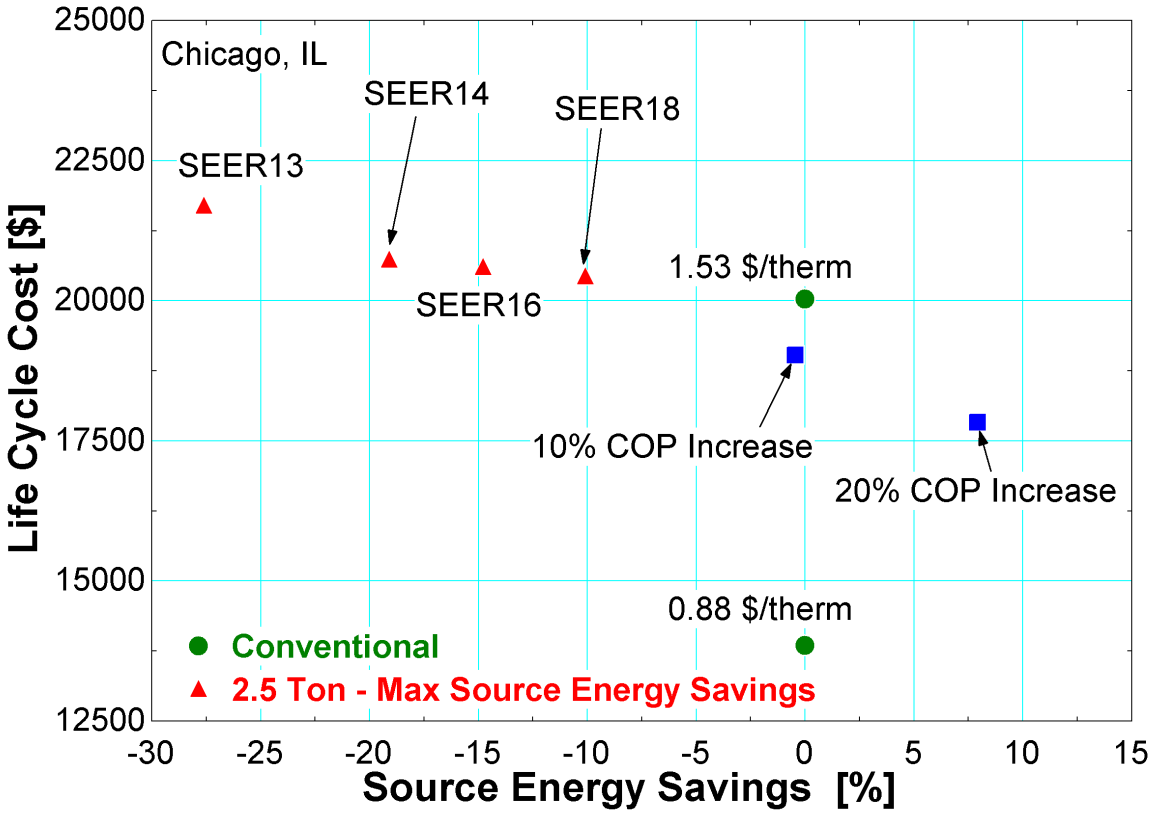

Figure 4.8: This figure shows the performance of the 2.5 Ton SEER 18 heat pump if the performance were increased by 10% and 20% for the Chicago location. The fuel inflation rate used for the economic analysis was 15%.

If the 2.5 Ton SEER 18 heat pump performance could theoretically be improved by 10% the air-source heat pump system could match the source energy consumption of the conventional system for the home located in Chicago, IL. If the performance were further increased to 20%, the heat pump system could save 7% source energy over the conventional system. However, in both cases, with equal fuel inflation rates for natural

gas and electricity, the heat pump would not present economic savings over the conventional system at the current market prices of natural gas (0.88 $/therm).

Unfortunately, it is not possible to easily or economically increase the heat pump performance by 10% or 20%. One alternative to using an air source heat pump is to use a liquid source heat pump that interfaces with the ground as a heat source or sink. This alternative eliminates the large range of temperatures that the air-source heat pump is required to operate in, thus increasing its performance. These results will be covered in the next section.

4.3 Geothermal Heat Pump System

The geothermal heat pump system discussed in Section 3.3 was simulated for the Chicago, IL location to determine the energy savings by improving the cold weather performance of the heat pump. Three different capacities of a ClimateMaster EER 20 heat pump were used: a 1.5, 2 and 2.5 ton, as these were the primary capacities of interest for the air-source system. The soil was assumed to be sandy, with a thermal conductivity of 1.3 W/m-K, which is typical for heavy to light sand with 5 to 15% water content (ASHRAE, 2007). The soil conditions affect the ability for the heat pump system to transfer heat to and from the ground during operation. Soil conditions may also adjust the depth of the borehole; if the soil conductivity is low a larger heat transfer area (borehole) may be required. Figure 4.9 compares the energy savings and economic expenses of the air-source and geothermal heat pump systems (conventional system as the baseline for energy savings).

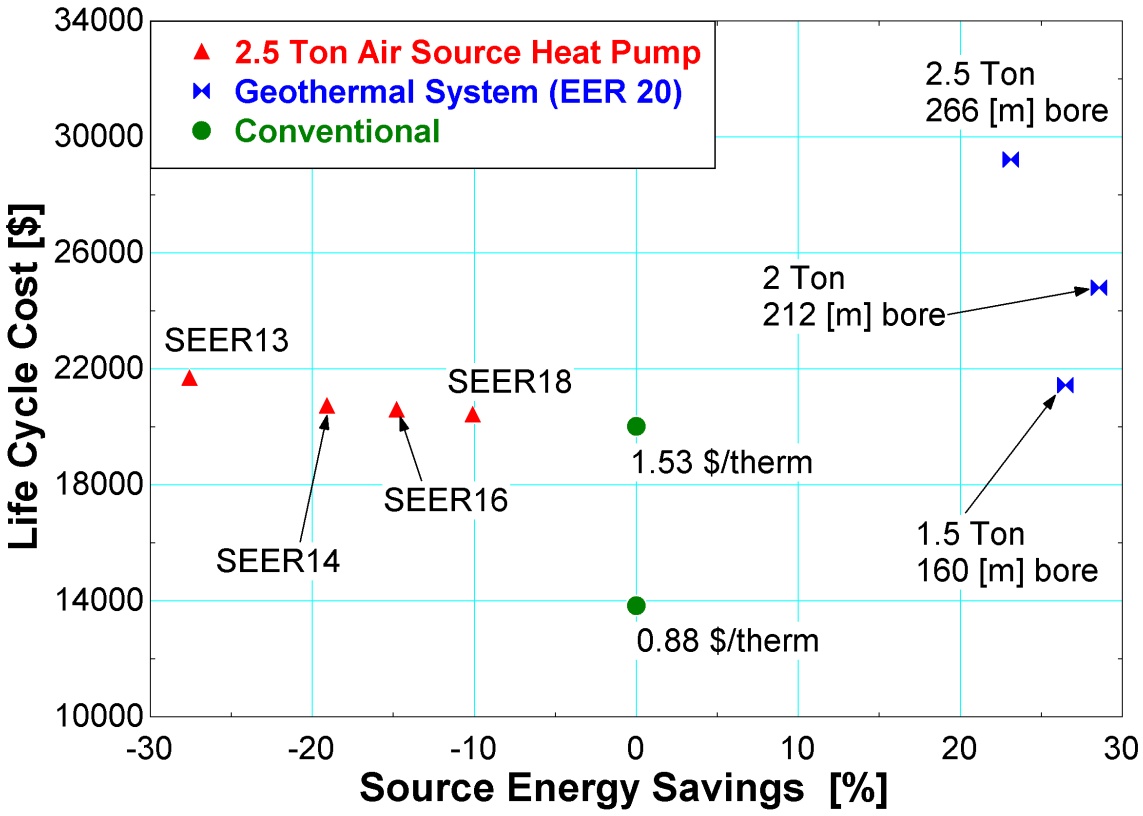

Figure 4.9: Life cycle cost vs. source energy savings for the geothermal heat pump systems and conventional system. The conventional system is considered the baseline and represents 0% energy savings. The fuel inflation rate for electricity and natural gas is 15%.

By using a geothermal heat pump system, source energy savings of up to 28% are possible over the conventional system. For the geothermal system, the 2 ton heat pump capacity is the optimum for source energy savings, although the advantage over the 1.5 and 2.5 ton systems is small. This system balances the effects of auxiliary heating and cycling. The cycling penalty affects the 2.5 ton heat pump causing it to consume more source energy that both the 1.5 and 2 ton systems.

The geothermal heat pump offers an ability to save source energy over the conventional system, but at significantly higher life life-cycle costs, which are around $8,000 over 16 years for the 1.5 ton system. If the economic return of a system is unimportant this

system is recommended for any cold climate location. For warm climates, the returns will be less significant, as the air-source heat pump operates efficiently during hot weather conditions, as seen from the monthly COP plots. The performance, both in terms of economic and energy savings, are most affected by cold climate conditions.

4.4 Photovoltaic System

A PV array from Section 3.4 was added to the house to determine the effect PV would have on costs and energy savings. Simulations used the 2.5 ton heat pump as it displays the largest source energy savings. The capital costs of the PV array are determined by 3 different ranges; 4, 6 and 8 $/W$_P$. This cost includes the inverter and all other installation related costs. By breaking down almost any capital and installation cost (including incentives) to a $/W$_P$ value, most cases should fall somewhere within (or close to) the provided range (4, 6, 8 $/W$_P$).

Figure 4.10 shows the PV results when used in conjunction with the 2.5 ton SEER 18 heat pump in the Chicago location. The PV array is mounted on the south facing roof at 26.5°. The life cycle costs indicated on this plot include both the PV array and heat pump capital cost. Moving towards the right from the SEER 18 with no PV array data point increases the PV array size. Two array sizes are marked with square data points and dashed vertical lines for reference; a 1.42 and 2.84 kW array.

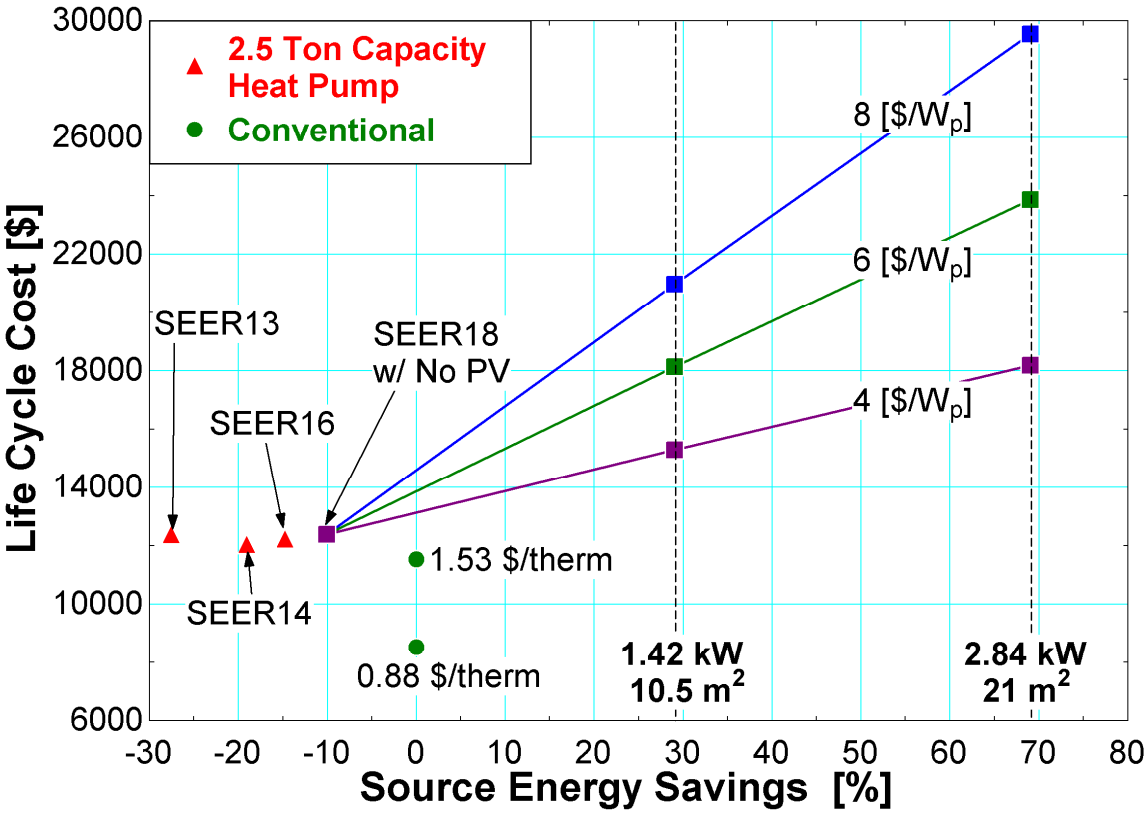

Figure 4.10: Simulation results when PV is used in conjunction with the 2.5 ton SEER 18 air-source heat pump system for Chicago, IL. The fuel inflation rate is 5%.

For example, the cost to achieve 50% source energy savings over the conventional system (not whole house energy savings) at an installed cost of 4 $/W_P$ is the intersection of the purple 4 $/W_P$ curve and the 50% source energy savings vertical gridline. This point would correspond to an array size near 2.13 kW (roughly between the 1.42 and 2.84 kW array sizes) and a life cycle cost of approximately $17,000. If a 6 $/W_P$ installed cost were used, the array size would not change, however the life cycle costs would increase to estimated to be $21,000. The PV driven air-source heat pump systems exhibit significantly higher life-cycle costs than the conventional system for Chicago, IL.

The Dallas results are similar, shown in Figure 4.11. One change is that the heat pump system was already provided energy and economic savings.

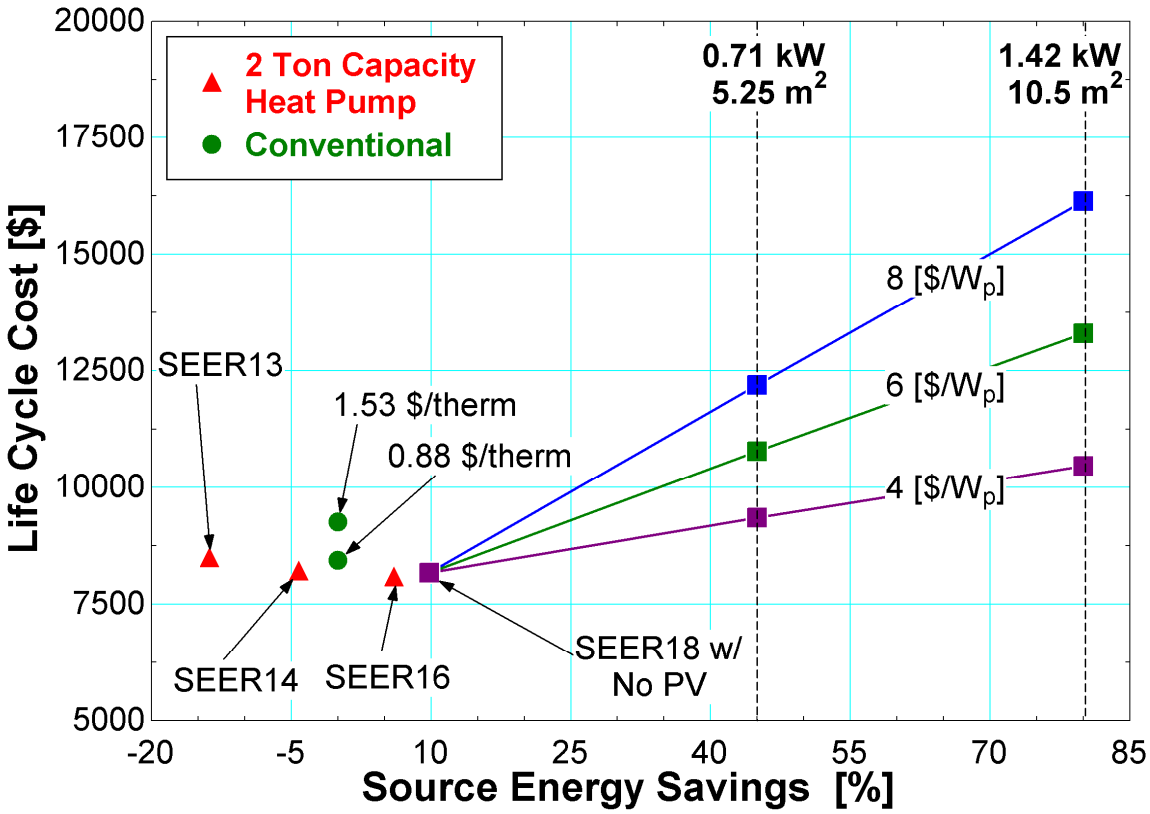

Figure 4.11: Simulation results when PV is used in conjunction with the 2 ton SEER 18 air-source heat pump system for Dallas, TX. The fuel inflation rate is 5%.

One interesting result for the Dallas location is that if natural gas were to be twice the current price (~1.53 $/therm), the heat pump system plus a 0.71 kW array could be purchased (at 4 $/$W_P$) for the same life cycle cost as the conventional system. This heat pump and solar system would provide source energy savings of approximately 45% over the conventional system.

In conclusion, both locations show that, with current natural gas prices, PV does not change the economic outlook. However, as with the geothermal heat pump system, if

economic savings is not required, a PV array provides an unlimited amount of source energy savings, depending on the array size and ability to resell excess electricity.

4.5 Solar Thermal Heating System

A nodal analysis was preformed on the thermal storage tank, validating the benefit of having a stratified tank. A nodal analysis increases the number of temperature nodes from 1 (representing a fully mixed tank) to more than 1, which models the stratification effect in the tank. The effect of stratification on performance can be studied with a tank that is modeled with more than one node. Then the solar thermal system was used in parallel with the air-source heat pump system, reducing the building load whenever possible to reduce the amount of times the heat pump must operate.

The design of the thermal system was carried out according to Duffie and Beckman (2006). There are also two examples of experimental solar thermal systems. The parameters chosen for the solar system are summarized in Table 4.19. System costs range from \$1000-1500 per m^2 according to Full Spectrum Solar, a solar system installer located in Madison, WI (DeRocher, 2012). These costs do not include incentives and are for retrofit systems. When solar thermal systems are installed during the construction of a new home, it is likely that the system cost will decrease, since many of the carpenters, plumbers and electricians are already on site. To account for both incentives and new constructions systems a lower bound of \$500/m^2 system cost will be included as well.

Table 4.19: This table presents the solar thermal design parameters.

Parameter	Value
Collector Flow Rate	0.015 [kg/m^2-s]
Storage Capacity	75 [L/m^2]
System Cost	1000-1500 [\$/m^2]

4.5.1 Nodal Analysis of Thermal Tank

With the Type 4 storage tank, the number of nodes can be adjusted from 1 to 100. With a single node tank, the model assumes that the tank is fully mixed. A stratified tank (multi-node) models the temperature distribution within the tank with the hottest fluid located at the top node. Stratification is advantageous for solar thermal because the collector inlet draws from the bottom node of the tank and thus will be the same temperature (neglecting any losses). With a stratified tank, the bottom node of the tank will be a colder temperature than with the mixed tank (while the top node will be hotter than the mixed tank). The useful gain of the collector is defined by equation (4.4) (Duffie and Beckman, 2006).

$$Q_u = A_c \left[F_R \left(\tau\alpha\right)_n I_T - F_R U_L \left(T_{inlet} - T_{amb}\right) - F_R U_{L/T} \left(T_{inlet} - T_{amb}\right)^2 \right] \qquad (4.4)$$

In this equation and in Figure 4.12, it is seen that reducing the inlet temperature, T_{inlet}, will increase the useful energy gain from the collector. Also represented by equation (4.4) is the collector area (A_c), the heat removal efficiency factor (F_R), the product of the cover transmittance and absorber absorptance at normal incidence ($\left(\tau\alpha\right)_n$), the thermal loss coefficient (U_L), and the thermal loss coefficient dependency on temperature ($U_{L/T}$).

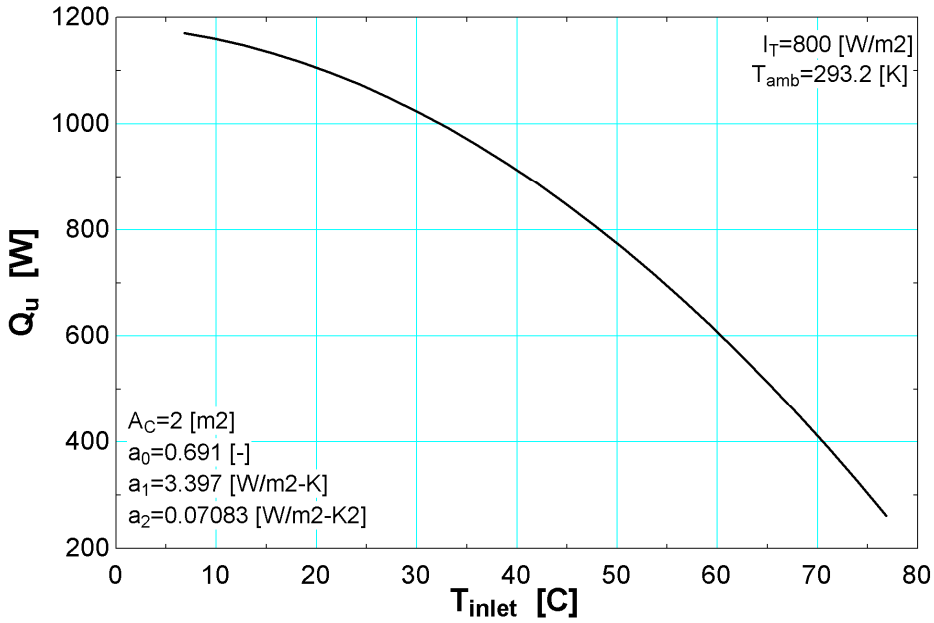

Figure 4.12: Useful gain from the collector vs. inlet temperature.

By using a stratified tank, more useful energy gain from the collector should be seen as colder inlet temperatures will be recorded at the collector inlet than if a mixed tank were used. Simulations were run with various number of tank nodes. The solar thermal system parameters are found in Table 4.20.

Table 4.20: Solar thermal system properties for the nodal analysis.

Parameter	System		
Collectors [-]	2	5	10
Area [m^2]	8.8	22	44
Tank Volume [m^3]	0.66	1.65	3.3
Radius [m]	0.3688	0.5005	0.6306
Height [m]	1.545	2.097	2.641
Node Height [m]	0.06436	0.08736	0.1101
Flow Rate [kg/hr]	475.2	1188	2376

The height of the nodes is determined by dividing the tank height by the number of nodes. This is shown in Table 4.21. Note that a single node tank represents a fully mixed tank.

Table 4.21: This table shows the height of the nodes for each analysis. As the number of nodes increases, the height of each node decreases. A tank with one node represents a fully mixed tank.

Number of Nodes	Node Height [m] (2 Collector)	Node Height [m] (5 Collector)	Node Height [m] (10 Collector)
1	1.5	2.1	2.6
3	0.5	0.7	0.9
6	0.3	0.3	0.4
12	0.13	0.17	0.22
24	0.06	0.09	0.11
48	0.03	0.04	0.06
100	0.015	0.021	0.026

The useful energy gain from the collector will increase as the number of nodes increases in an asymptotic manner. Figure 4.13 shows this trend for the month of February. In this figure, the useful energy gain is normalized (equation (4.5)) to allow for a direct comparison between the three different thermal system sizes. For each system, it is assumed that with 100 nodes, the tank model simulation results have reached the useful energy gain limit. Thus, this would represent 1. For cases with nodes less than one, the useful energy gain is divided by the useful energy gain from the 100 node simulation.

$$Q_{normalized} = \frac{Q_{u,n\ nodes}}{Q_{u,100\ nodes}} \tag{4.5}$$

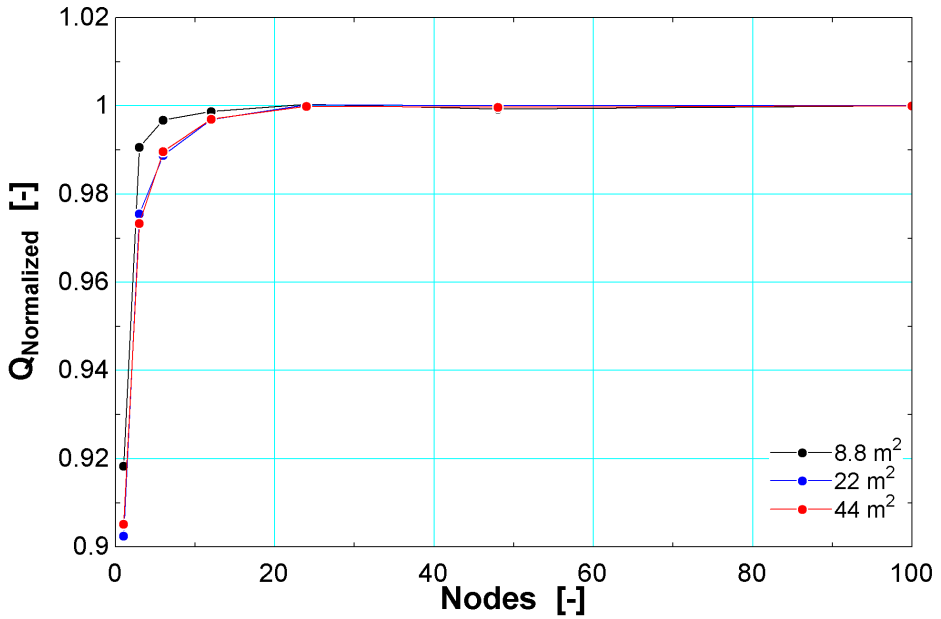

Figure 4.13: This figure shows how the useful energy increases when the tank is stratified for each thermal system. After approximately 20 nodes, increasing the number of nodes does not change the amount of useful energy gain because the tank is fully stratified.

In addition to the useful energy gain, the efficiency and fraction of the heating load met for the Chicago location can be plotted as seen in Figure 4.14 and Figure 4.15.

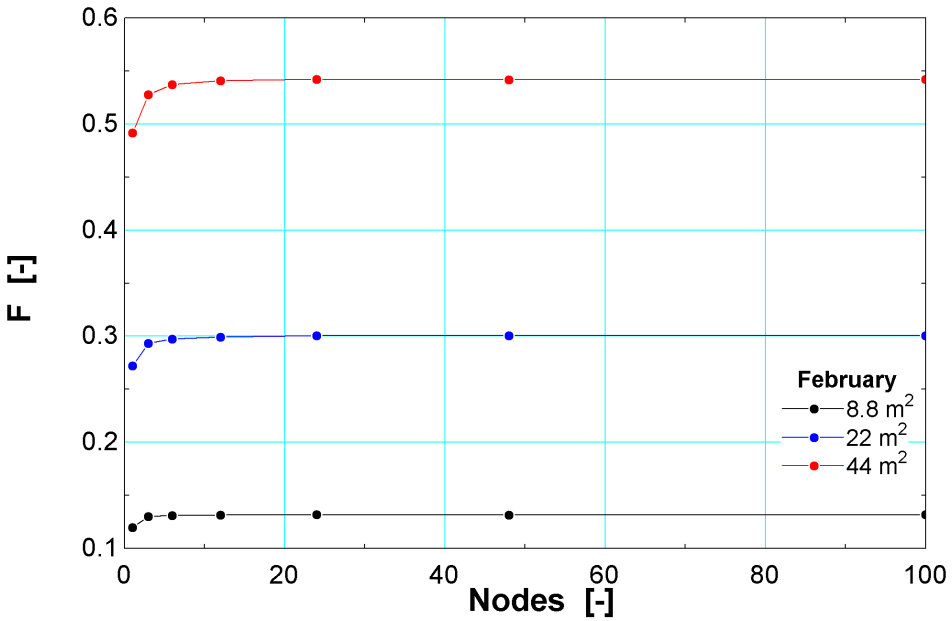

Figure 4.14: This figure shows the fraction of the load met vs. the number of tank nodes. Increasing the nodes from 1 (fully mixed) increases the amount of useable energy.

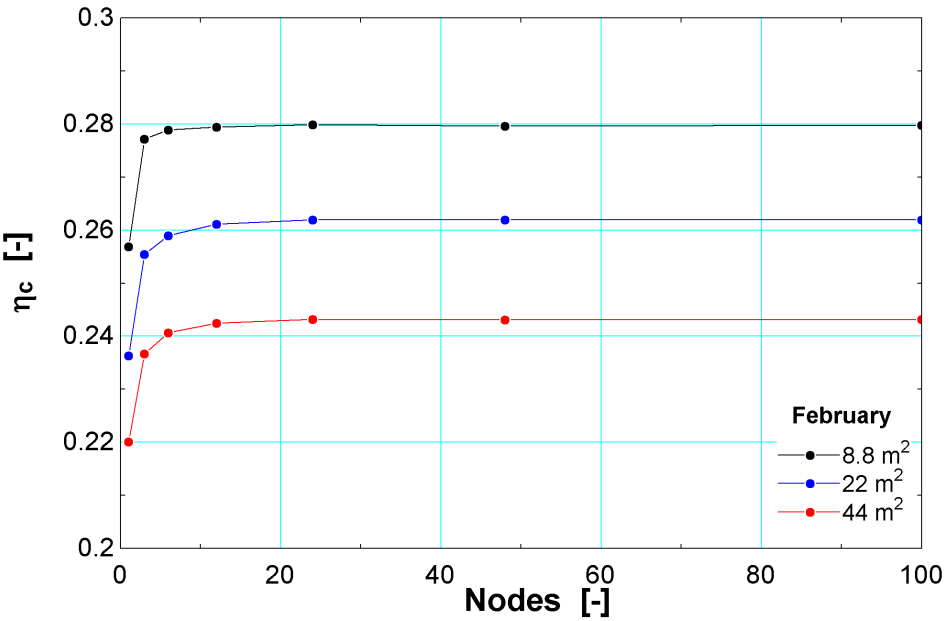

Figure 4.15: This figure shows the collector efficiency vs. the number of nodes. As the number of nodes is increased beyond 1 (full mixed), cooler temperatures are recorded at the collector inlet, yielding higher efficiency.

The conclusion of the nodal analysis is that a stratified tank is advantageous, producing higher collector efficiencies and greater useful energy gains, which can subsequently be used to reduce the building load. Most thermal systems today are stratified as a result.

4.5.2 Solar Thermal System Simulations

Three different size solar thermal systems were simulated on the house. These systems were summarized in Table 4.20. A domestic hot water load is not simulated, so this system is not used during cooling months. Currently, the control strategy solely reduces the building heating load, and the heat pump operates whenever the solar thermal system cannot meet the building load.

The first solar thermal results to consider are the fraction of the heating load met and the efficiency of the collectors. The collector efficiency is the ratio of the useful energy gain over the radiation on the collector surface. Figure 4.16 below shows the monthly

collector efficiency for each system. Since the system is not used in the summer months, the efficiency is set to zero. Also, during warmer heating months (October and May), the efficiencies are slightly skewed since the tank temperature is very hot due to a small building load requirement. The fraction of the load met increases with system size as expected as seen in Figure 4.17. This fraction of the load met includes the gains from tank losses.

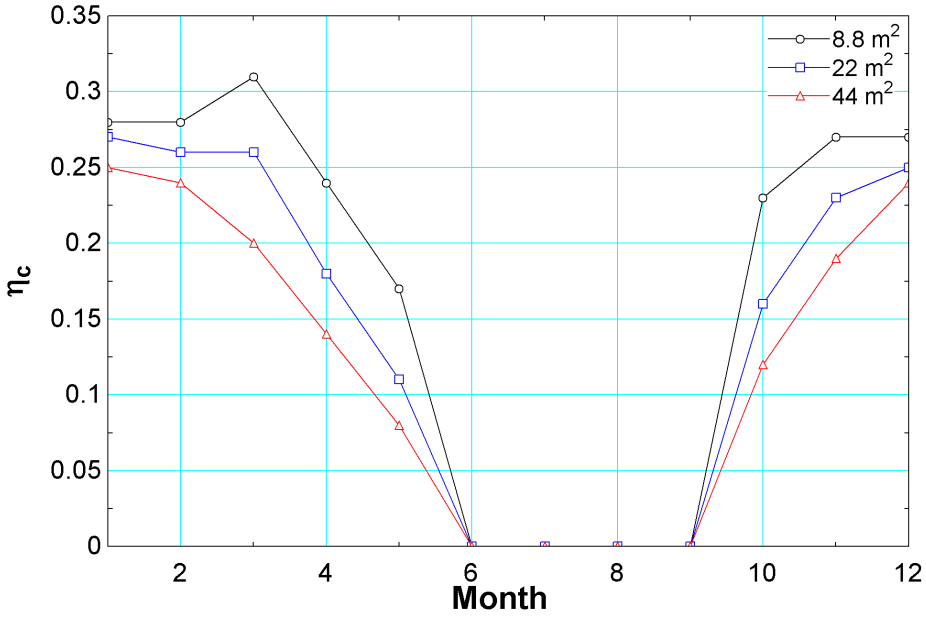

Figure 4.16: Monthly collector efficiency for each thermal system. Note that the system is not in use during the cooling months.

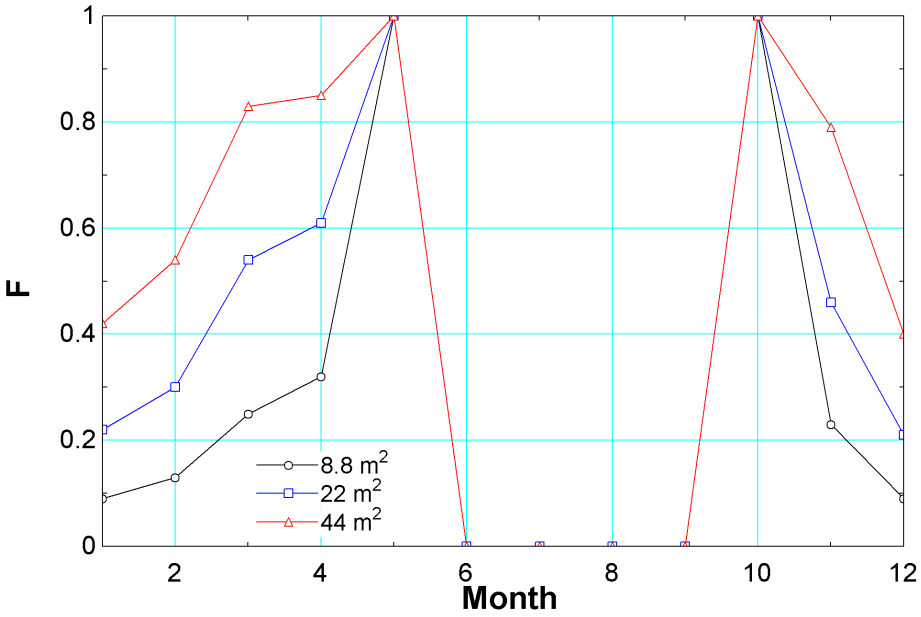

Figure 4.17: Fraction of the heating load met by the solar thermal system. Note that the solar thermal system is not in use during the cooling months.

Figure 4.18 shows the life cycle costs compared to the conventional system and the heat pump and PV system for Chicago, IL.

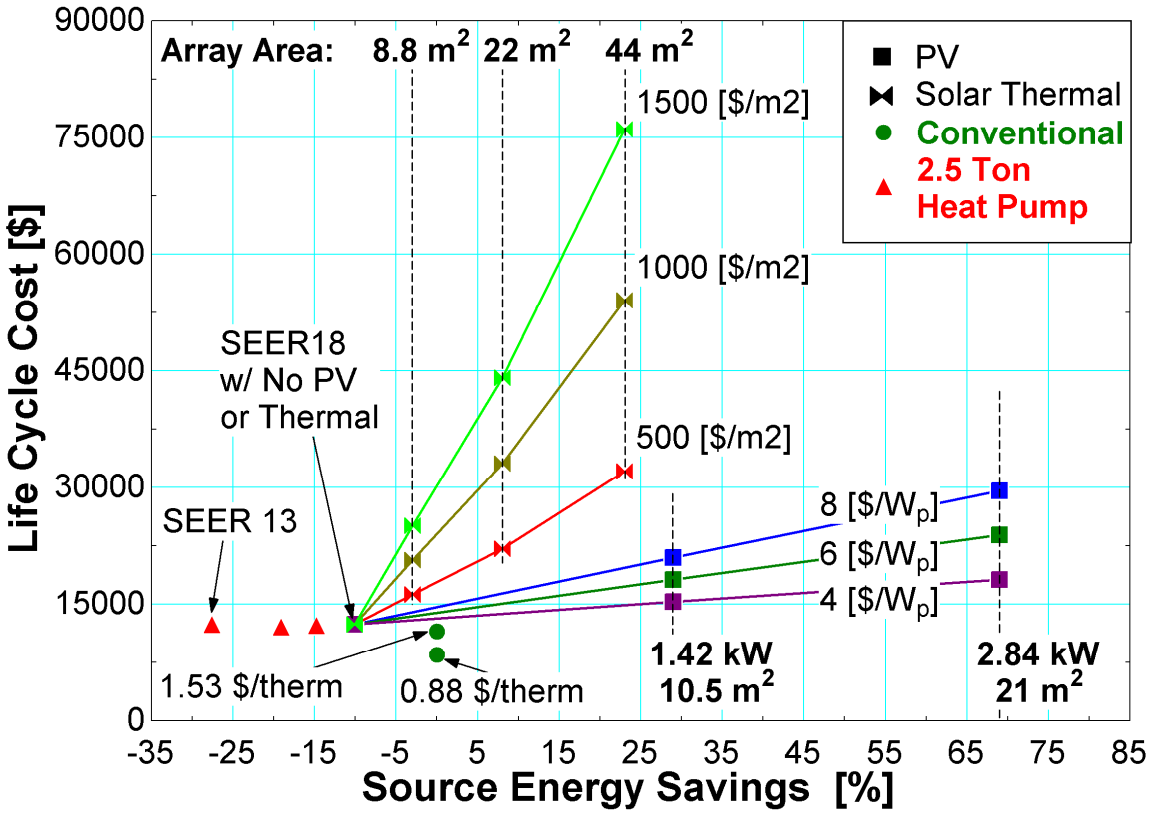

Figure 4.18: Solar thermal life cycle costs vs. the conventional system and PV system for Chicago, IL. The fuel inflation rate is 5%. The solar thermal system is not used during the summer while the PV system is.

This result offers an easy way to compare the PV and solar thermal performance, both on an energy and economic savings basis. The source energy savings (over the conventional system only) are much larger for the PV systems, at a lower life cycle costs. While it is noted that the PV system works year round to provide electricity and the solar thermal is not in use during the summer, the end result does not change significantly even if the PV system is turned off in the summer, shown in Figure 4.19. In addition, the PV system is roof mounted with a slope of 26.5°, which is not ideal for winter only use, whereas the solar thermal collectors are optimized for winter use with a rack mounted slope of 60°. Comparing the PV and solar thermal results, it is clear that PV offers more source energy savings over the conventional system at lower life cycle costs when compared to the solar

thermal system. This is likely why solar thermal systems are more common for supplementing domestic hot water heating.

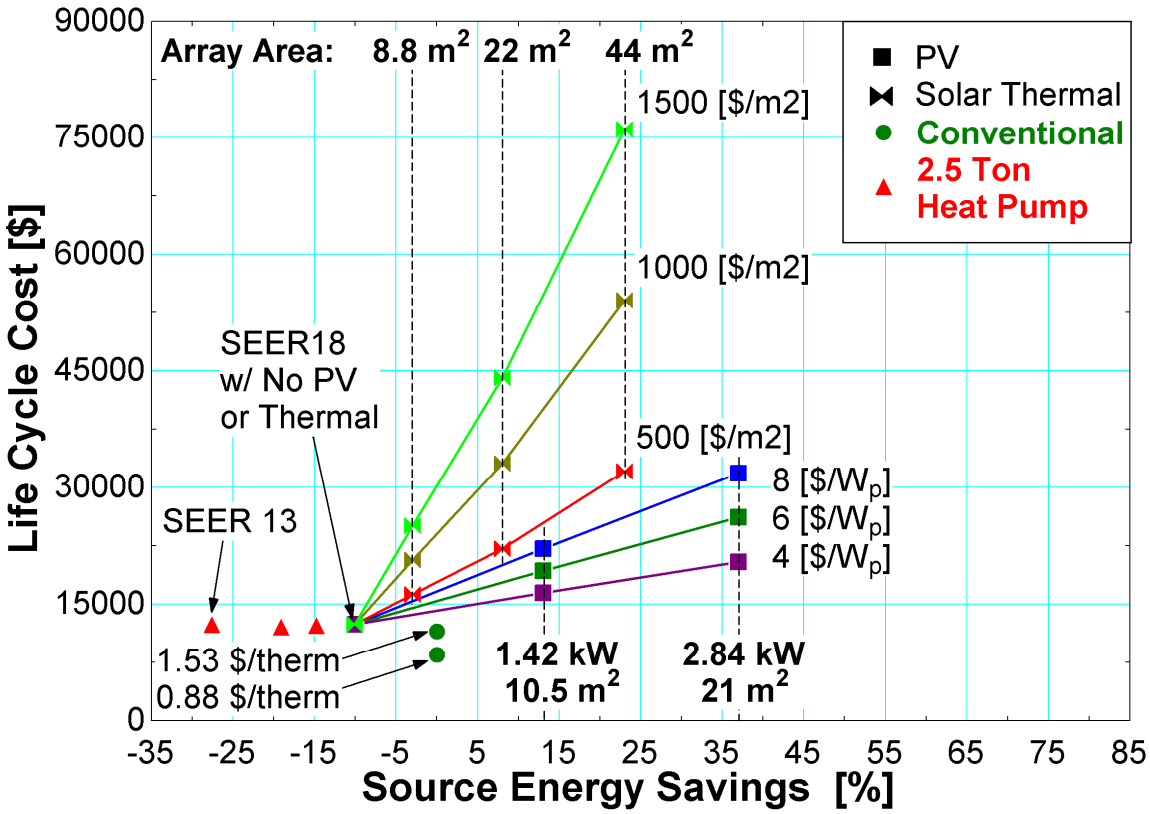

Figure 4.19: Simulation results for Chicago, IL when the PV system is only allowed to operate during the months that the solar thermal system operates. This creates a fair comparison.

5. Conclusions and Recommendations

5.1 Conclusions

A model of a thermally efficient building was developed in TRNSYS. The model indicated that energy consumption would be reduced by 38% (through improvements in insulation and windows) compared to the baseline Building America building (BAHSP, 2010). Combining the reduced energy consumption results with the heat pump/conventional system simulations reflect on the importance of having a thermally efficient building envelope prior to continuing with the implementation of high performance conditioning equipment. The thermally efficient building located in Chicago, IL required 46.11 GJ of energy to maintain the building at its temperature set point (this is ideal energy, not including HVAC inefficiencies) whereas the baseline house required 63 GJ. If both systems used a heat pump with an annual average COP of 3, the amount of required electricity would be 5892 kW-hr for the baseline home and 4269 kW-hr for the efficient home.

Models of several different HVAC options were developed to meet the calculated building loads. The first was an air-source heat pump. When sizing the heat pump in the Chicago location, with a fuel inflation rate of 5%, it was found that a SEER 14, 1.5 ton heat pump system is the most economical alternative. However, when the fuel inflation rate is increased to 15%, the economic optimum heat pump capacity increased to 2 ton with a higher efficiency of SEER 18. This result is explained by the increased electricity expense when the fuel inflation rate is increased. When this occurs, the analysis determines that saving energy from a capacity increase (reducing auxiliary heating) and efficiency increase offsets the increased capital cost of the larger capacity more efficient

system. In Dallas, an economic analysis concluded that a SEER 16, 2 ton system is most economical (heat pump system) when the fuel inflation rate was 5%. If the fuel inflation rate increased to 15%, the analysis determined a SEER 18, 2 ton system to have the lowest life cycle cost. Over-sizing a heat pump or air conditioner is detrimental to the performance of the system because of increased cycling losses and in extreme cases, a decrease in occupant comfort from an inability to control humidity levels. In addition, the compressor cycling due to excess capacity with a one-speed compressor leads to reduced performance and equipment lifetime. Unfortunately, for many installations in the consumer market, systems are often oversized.

When the air-source system is compared to the conventional system, consisting of a high efficiency natural gas furnace and SEER 16 air conditioning system, the results find that the heat pump system consumes more source energy and has higher life cycle costs. A 2.5 ton SEER 18 heat pump system displayed the lowest annual energy consumption for Chicago, IL; however, when compared to the conventional system, it consumed 10% more source energy. This system had life cycle costs that were roughly $4,000 higher than the conventional system. The lowest life cycle cost heat pump system (for a 5% fuel inflation rate) was the SEER 14, 1.5 ton system. This system had life cycle costs that were $3,000 higher than the conventional system, but this system consumed 27% more source energy than the conventional system. For a cooling dominated location, the heat pump outperforms the conventional system. In Dallas, the SEER 18, 2 ton heat pump saved 11% more source energy and $200 in life cycle cost. The lowest life cycle cost system, a SEER 16, 2 ton heat pump saved 6% source energy and $350 in life cycle cost.

When the air-source heat pump system is simulated around the United States in various climate zones, a clear trend exists. In cold climates, a natural gas furnace is by far the most economical choice for space conditioning (with the current natural gas prices of approximately 0.88 $/therm). If natural gas were to double in cost, the heat pump would be economically competitive, however, it these systems would still consume more source energy than the conventional system. In temperate to hot climates, the heat pump is an energy and cost saving solution for space conditioning when compared to the conventional system.

A geothermal system was simulated for the Chicago, IL home. Using the ground as a sink or source provided much higher system performance compared to the air-source system. Unfortunately, geothermal systems have much higher life cycle costs due to the expense of having the bore field installed. For Chicago, source energy savings of up to 28% over the conventional system were found at a life cycle increase of at least $8,000 over the conventional system.

Hybrid solar energy - heat pump systems were also evaluated. The first system was a roof mounted PV array. This system assumed that excess electricity could be resold to the utility at the purchase price of (0.14 $/kW-hr). A simple PV model was used (Chapter 1), which allowed for the array size and output to be scaled (doubling the array size would double the output). Results from this analysis found that a 2.84 kW rated PV array paired with the air-source system could create source energy savings over the conventional system of nearly 70% in Chicago, IL. However, this system increased the life cycle costs even further over the conventional system, from $4,000 without a PV array, to $18,000 with the 2.84 kW array (at an installed cost of 4 $/$W_P$). In Dallas, TX

the PV array yields large source energy savings, up to 80% with a 1.42 kW array. Unlike the Chicago location, these large source energy savings come with life cycle costs that are only slightly over the conventional system (approximately $2,500 more). PV is currently inexpensive and is very effective in reducing source energy consumption, if the homeowner is willing to pay the initial upfront cost.

The second solar energy system was a solar thermal heating system. This system consisted of a storage tank, water to air heat exchanger and flat plate solar collector. The control scheme used provided thermal energy to reduce the building load. The heat pump was used to meet the building load when the solar thermal system did not have the required capacity. The results from these simulations (Chicago, IL only) showed that the solar thermal system not only has higher life cycle costs, but also saves less source energy than the PV and heat pump system. This is because the PV array has much lower installation costs. The PV system is also advantageous because it requires much less equipment (i.e., no storage tanks, pumps, plumbing for fluid).

5.2 Recommendations

This research raises questions about the current move towards net-zero buildings. While reducing the energy consumption of the residential sector to zero would be a beneficial goal, it may be an economically unrealistic one. The results from this research have shown that a clear economic path to net-zero through means of readily available equipment and construction methods is not a possibility. The current consumer market is not prepared for the large upfront cost of a net-zero home. In many cases where an economic return is predicted, the duration of the analysis required to achieve such a return can approach 20 or 30 years, which is a risk that most new home owners will not

take as most consumers will not typically own the same home for that long. In addition, there has always been a focus of the net-zero research motivated by the anticipation that there will be a large increase in fuel expenses in the future, making net-zero energy consumption a valuable strategy. This argument has been present since the 1980's but such a drastic increase in energy prices has never occurred; reviewing the historic energy prices data reveals no such dramatic increase of energy expenses. This does not imply that the results and benefits of the net-zero research are not worthwhile. However, several main research topics arise.

First, net-zero research has shown the importance of having an efficient thermal envelope. While net-zero energy designs (featuring double stud walls, tight infiltration, etc) are the best option available and are required to achieve a net-zero home, they should not be the focus for the current building market. With significant capital costs, the majority of consumers will not be willing to invest in a home that they may not reside in long enough to see an economic return. However, the push towards "low energy" buildings is a possibility through higher building standards (higher standards for insulation, windows, etc).

One example of the difficulty in employing high building standards is Ty Newell's net-zero home in Champaign, IL, (Newell, 2010). An interesting note was the caution that was taken in choosing a contractor who would be willing to following specific directions when constructing the thermal envelope. Care was taken to not drill holes (for wiring, etc) through the thermal envelope unless permission from the homeowner, Newell, was explicitly given. Again relating to higher building standards, "lower energy" buildings are a reality through better construction methods that increase building "tightness".

When a new home is built, it is rare that the infiltration is known until a test is performed. Construction methods should be improved so that new houses are easily reproducible with tight infiltration.

The second topic relates to the HVAC equipment. This research shows that over-sizing a heat pump is detrimental to its performance and results in more energy consumption. It would be interesting to examine the effects of HVAC the equipment not working properly through poor maintenance or design can be (faulty seals, ice build up on outdoor heat exchangers, etc). More research could be done to determine the actual effect of over-sized and improperly operated HVAC equipment. What percent of the population has oversized equipment or equipment that is not operating correctly? What is the possibly energy reduction that would arise if the entire population had properly sized and functioning HVAC equipment? The development of methods to easily and properly size equipment could lead to large energy savings.

One solution to over-sized heat pumps is to use a variable speed heat pump system, which has a variable drive compressor motor that allows the heat pump system to load follow more accurately than the tradition single or two stage heat pump systems. A variable speed system can experience an even larger reduction cycling and auxiliary heating than the two stage heat pumps. Another recommended research topic involves using series heat pump system, where solar energy can create more favorable operating condition for the heat pump. For example, the heat pump source in the heating mode may be a thermal storage medium that utilizes solar energy.

Net-zero research focuses on a very small segment of the population in hopes of having an idea “take-off”, but it may be more beneficial to effect the entire building population by creating higher standards and practices for building construction and HVAC installations. In the future, net-zero buildings could simply come through vastly improved standard building practices and the addition of inexpensive PV systems.

References

AHRI, 2011, *Seasonal Energy Efficiency Ratio*, http://www.ahrinet.org/seasonal+energy+efficiency+ratio.aspx

ASHRAE, 2007, *Geothermal Energy*, ASHRAE Handbook: HVAC Applications, Chapter 32

BEopt, 2012, Ver. 1.3, National Renewable Energy Laboratory

Bergey, D., Ueno, K., 2011, *New England Net Zero Production Houses*, Building Science Press, http://www.buildingscience.com/documents/reports/rr-1103-new-england-net-zero-production-houses

BAHSP, Hendron, R., Engebrecht, C., 2010, *Building America House Simulation Protocol*, U.S. Department of Energy

Christensen, C., et al., 2008, *The NREL/Habitat for Humanity Zero Energy Home: A Cold Climate Case Study for Affordable Zero Energy Homes*, http://www.nrel.gov/docs/fy08osti/43188.pdf

Consumer Energy Center, 2012, *Central HVAC*, California Energy Commission, http://www.consumerenergycenter.org/home/heating_cooling/heating_cooling.html

Crawley, D., Pless, S., Torcellini, P., 2009, Getting to Net Zero, *ASHRAE Journal*, Volume 51, Issue 9, Pages 18-25

DegreeDays, 2012, Degree Days – Custom Degree Day Data, http://www.degreedays.net/

DeRocher, M., 2012, Full Spectrum Solar, Madison, WI, Email Communication

DOE-2.2, 2009, Ver. 47d, Lawrence Berkley National Laboratory, James J. Hirsch & Associates

Duffie, J.A., Beckman, W.A., 2006. *Solar Engineering of Thermal Processes*, third ed. John Wiley & Sons Inc., New York

EWC, 2012, *Efficient Windows Collaborative*, University of Minnesota, Lawrence Berkley National Laboratory, Alliance to Save Energy, http://www.efficientwindows.org/

EnergyPlus, 2010, Ver. 6.0, Department of Energy

EnergyStar, 2011, EnergyStar Performance Ratings Methodology for Incorporating Source Energy Use, http://www.energystar.gov/ia/business/evaluate_performance/site_source.pdf

Goodman, 2011, SEER 18 Split System Heat Pump Product Specifications, http://www.goodmanmfg.com/Portals/0/pdf/SS/SS-DSZC18.pdf

Google Sketchup 8, 2011, Ver. 8, Google

Hellström, G., 1989, *Duct Ground Heat Storage Model (Manual for Computer Code)*, Deptarment of Mathematical Physics, University of Lund

Henderson, H.I., Huang, Y.J. and Parker, D., 1999, *Residential Equipment Part-Load Curves for use in DOE-2*, Lawrence Berkley National Laboratory

Hong, T., et al., 2008, *Comparisons of HVAC Simulations between EnergyPlus and DOE-2.2 for Data Centers*, Berkley National Laboratory

IECC, 2004, Climate Zones Map (By County), Supplement to the 2004 IECC, http://resourcecenter.pnl.gov/cocoon/morf/ResourceCenter/dbimages/full/973.jpg

Kansas City Power & Light, 2012, *Ground Loop Heat Exchangers*, http://www.kcpl.com/efficiency/hee_geohp2.html

Kusuda, T., Achenbach, P., 1965, "Earth Temperature and Thermal Diffusivity at Selected Stations in the United States, *ASHRAE Transactions*, Volume 71, Part 1, Pages 61-75

Klein, S.A. and Nellis, G., 2011, *Thermodynamics*, Cambridge University Press.

Myers, K.S., 2012, *Assessment of High Penetration Photovoltaics in Wisconsin*, University of Wisconsin-Madison Master's Thesis

National Weather Service, 2012, NOAA, http://www.weather.gov/

NIST, 2011, *Measuring Performance of Net-Zero Energy Homes Project*, http://www.nist.gov/el/building_environment/heattrans/mpnz.cfm

North Dakota State University, 2012, *Archived Deep Soil Temperatures at select NDAWN stations*, http://www.ndsu.edu/ndsco/soil/index.html

NREL, 2011, System Advisor Model, Ver. 2011.6.30, https://sam.nrel.gov/

O'Brien, W, et al., 2010, *A Study of Design Tools and Processes Through a Near Net-Zero Energy House Redesign*, EuroSun 2010 International Conference Paper

SRCC, 2012, Solar Rating & Certification Corporation, http://www.solar-rating.org/

TESS, 2009, Type 922 Air-Source Heat Pump TRNSYS Model

TESS, 2010, Type 919 Liqiud-Source Heat Pump TRNSYS Model

TESS, 2010, Type 557a Vertical U-Tube Ground Heat Exchanger TRNSYS Model

TRNSYS, 2010, A Transient Simulation Program, Ver. 17.01.0019, Solar Energy Laboratory, University of Wisconsin – Madison

U.S. Department of Energy, 2012, *2011 Buildings Energy Data Book*, http://buildingsdatabook.eren.doe.gov/

U.S. Energy Information Administration, 2011, *Annual Energy Review 2010*, http://www.eia.gov/totalenergy/data/annual/pdf/aer.pdf

Appendix A

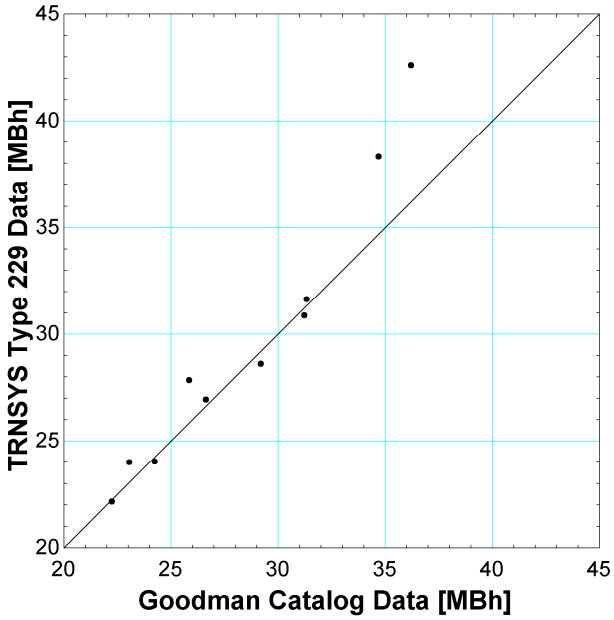

Figure A.1: A comparison of total cooling capacity results for a 3 Ton SEER 18 heat pump. Each point represents a different operating condition. The TRNSYS data used the original Type 229 normalized data files and are compared to Goodman Performance data. Points falling on the 45° indicate for that specific operating condition that TRNSYS is agreement with the Goodman data.

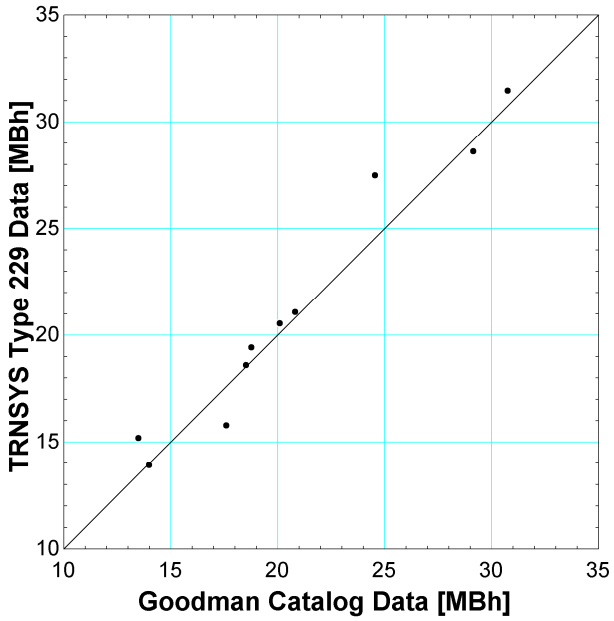

Figure A.2: A comparison of sensible cooling capacity results for a 3 Ton SEER 18 heat pump. Each point represents a different operating condition. The TRNSYS data used the original Type 229 normalized data files and are compared to Goodman Performance data. Points falling on the 45° indicate for that specific operating condition that TRNSYS is agreement with the Goodman data.

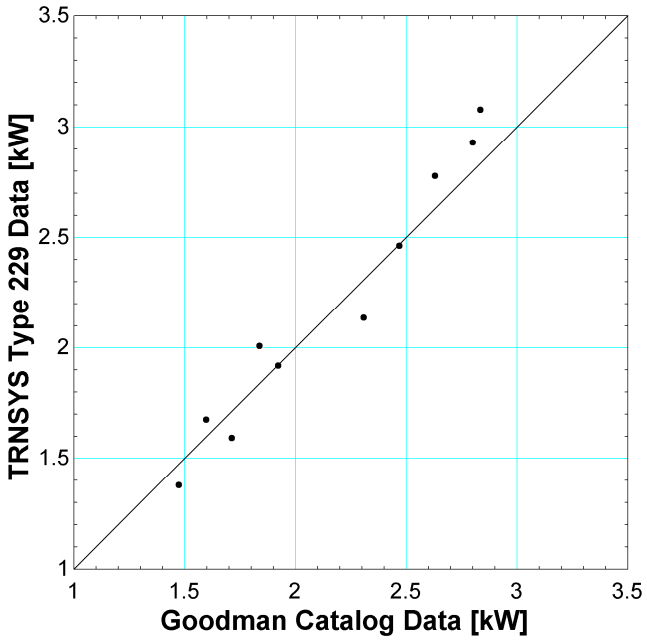

Figure A.3: A comparison of power consumption results for a 3 Ton SEER 18 heat pump. Each point represents a different operating condition. The TRNSYS data used the original Type 229 normalized data files and are compared to Goodman Performance data. Points falling on the 45° indicate for that specific operating condition that TRNSYS is agreement with the Goodman data.

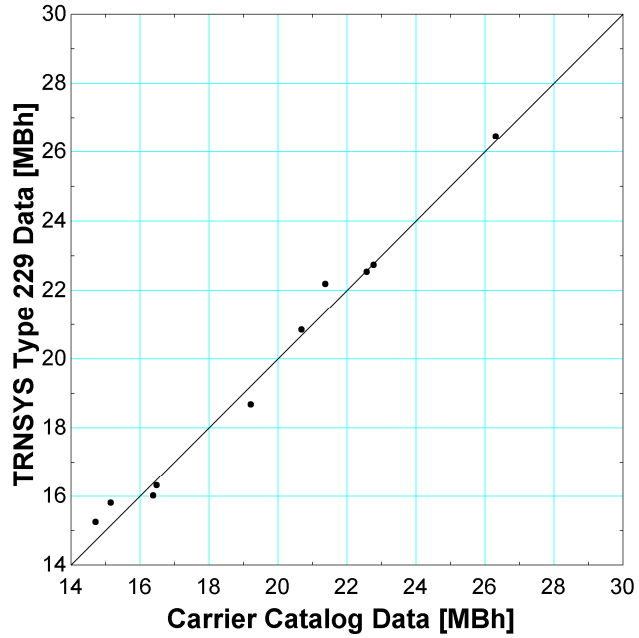

Figure A.4: A comparison of total cooling capacity results for a 2 Ton SEER 16.5 heat pump. Each point represents a different operating condition. The TRNSYS data used the original Type 229 normalized data files and are compared to Carrier Performance data. Points falling on the 45° indicate for that specific operating condition that TRNSYS is agreement with the Carrier data.

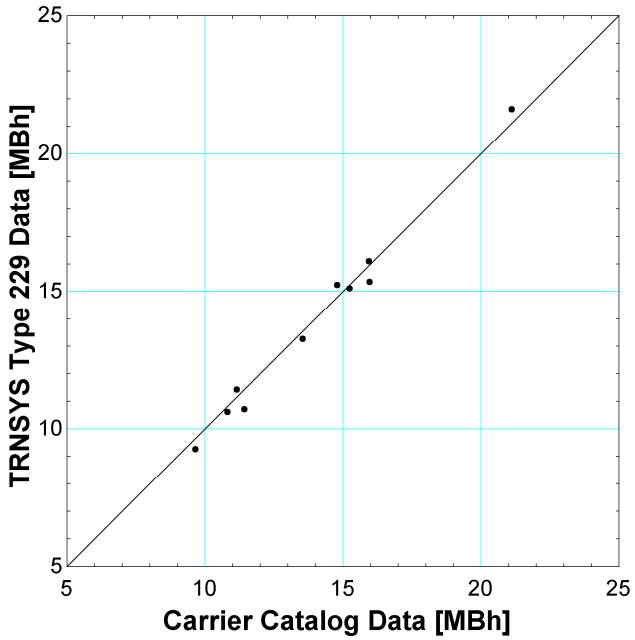

Figure A.5: A comparison of sensible cooling capacity results for a 2 Ton SEER 16.5 heat pump. Each point represents a different operating condition. The TRNSYS data used the original Type 229 normalized data files and are compared to Carrier Performance data. Points falling on the 45° indicate for that specific operating condition that TRNSYS is agreement with the Carrier data.

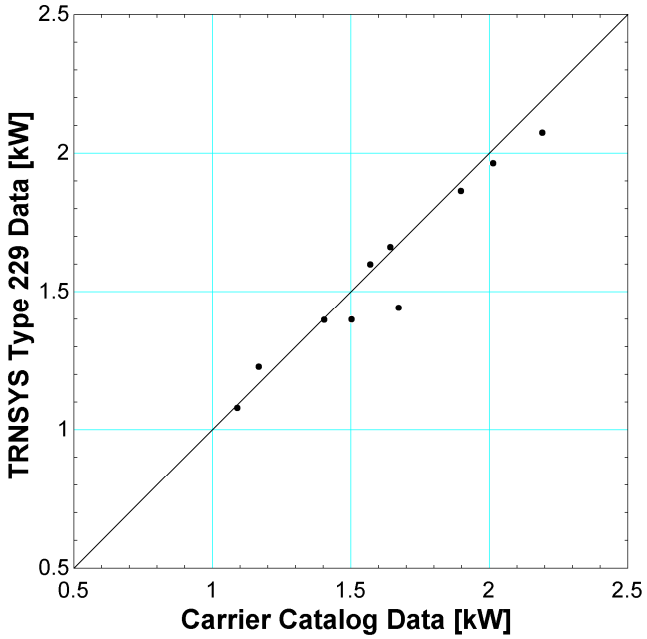

Figure A.6: A comparison of power consumption results for a 2 Ton SEER 16.5 heat pump. Each point represents a different operating condition. The TRNSYS data used the original Type 229 normalized data files and are compared to Carrier Performance data. Points falling on the 45° indicate for that specific operating condition that TRNSYS is agreement with the Carrier data.

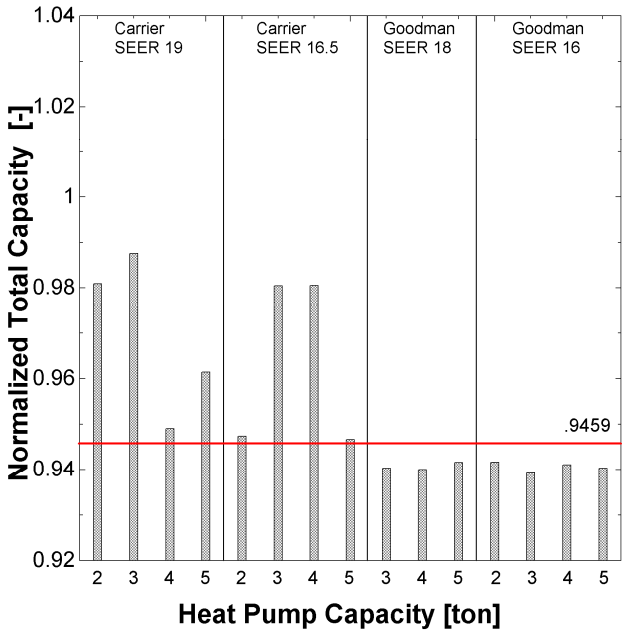

Figure A.7: Comparing normalized values for total cooling capacity. Operating conditions: IDB - 26.67, ODB - 46.1, IWB - 21.67. The red line signifies the normalized value used in the Type 229 data file at this operating condition. The bars indicate the normalized value from the manufacturer's data (Goodman or Carrier). It is difficult to normalize to one value at a given operating condition.

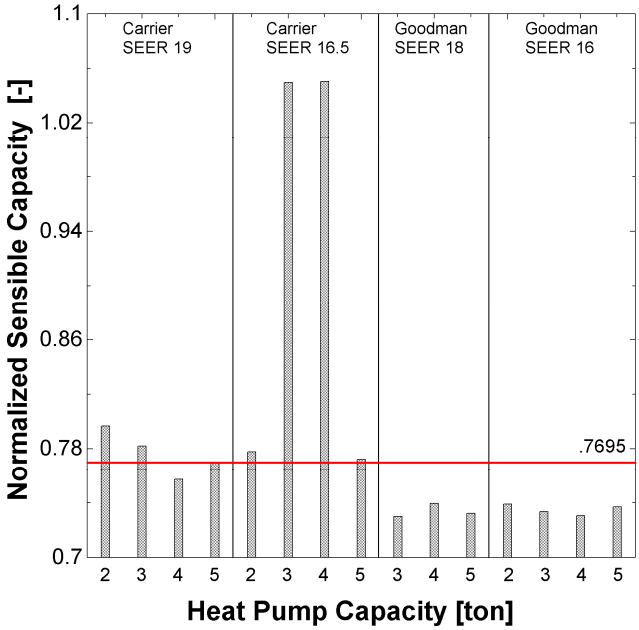

Figure A.8: Comparing normalized values for sensible cooling capacity. Operating conditions: IDB - 26.67, ODB - 46.1, IWB - 21.67. The red line signifies the normalized value used in the Type 229 data file at this operating condition. The bars indicate the normalized value from the manufacturer's data (Goodman or Carrier). The Carrier SEER 16.5 model data displayed high latent cooling capacity. It difficult to normalize to one value at a given operating condition.

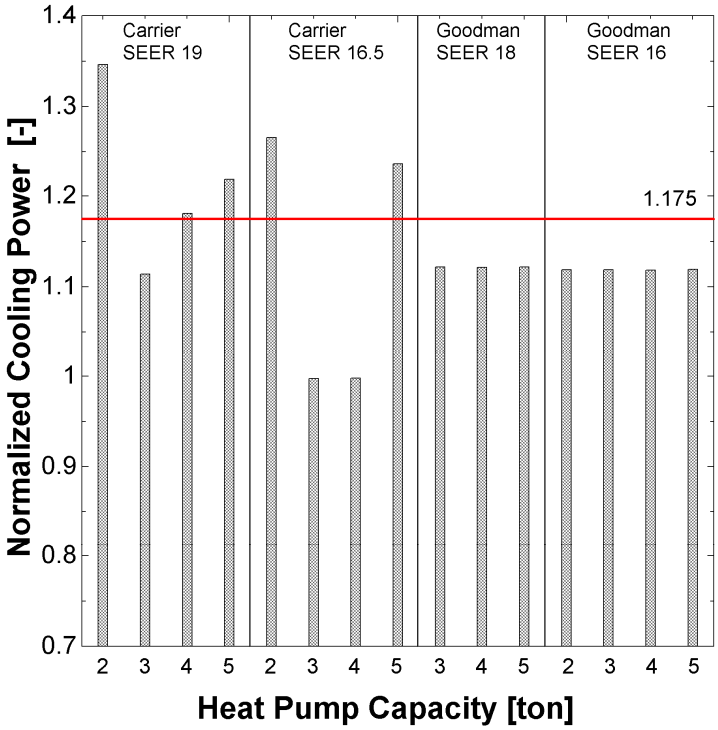

Figure A.9: Comparing normalized values for cooling power consumption. Operating conditions: IDB - 26.67, ODB - 46.1, IWB - 21.67. The red line signifies the normalized value used in the Type 229 data file at this operating condition. The bars indicate the normalized value from the manufacturer's data (Goodman or Carrier). It is seen that it is difficult to normalize to one value at a given operating condition.

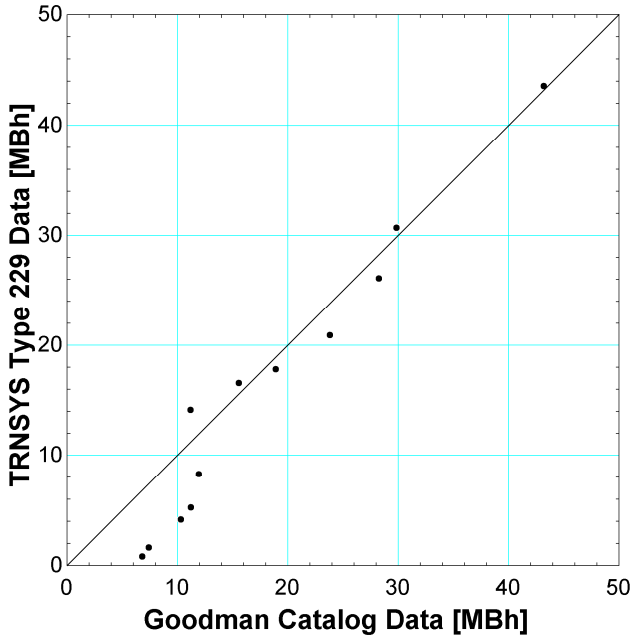

Figure A.10: A comparison of total heating capacity results for a 3 Ton SEER 18 heat pump. Each point represents a different operating condition. The TRNSYS data used the original Type 229 normalized data files and are compared to Goodman Performance data. Points falling on the 45° indicate for that specific operating condition that TRNSYS is agreement with the Goodman data.

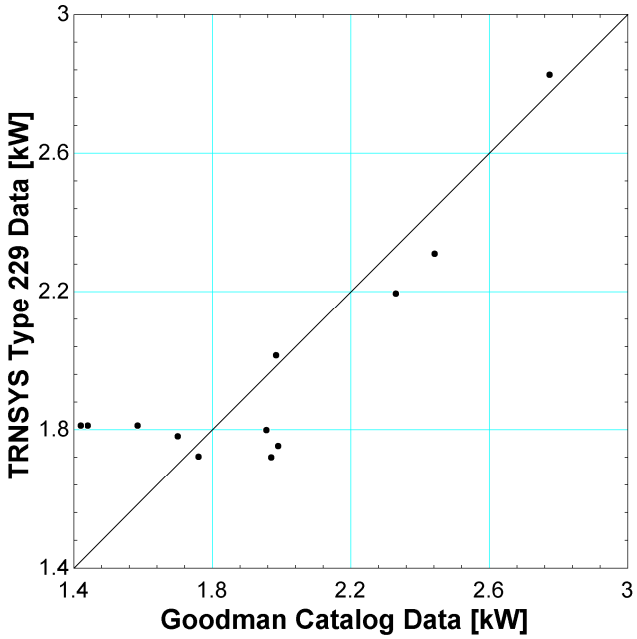

Figure A.11: A comparison of heating power consumption results for a 3 Ton SEER 18 heat pump. Each point represents a different operating condition. The TRNSYS data used the original Type 229 normalized data files and are compared to Goodman Performance data. Points falling on the 45° indicate for that specific operating condition that TRNSYS is agreement with the Goodman data. This original Type 229 data file over predicted the power consumption, as seen at 1.8 kW.

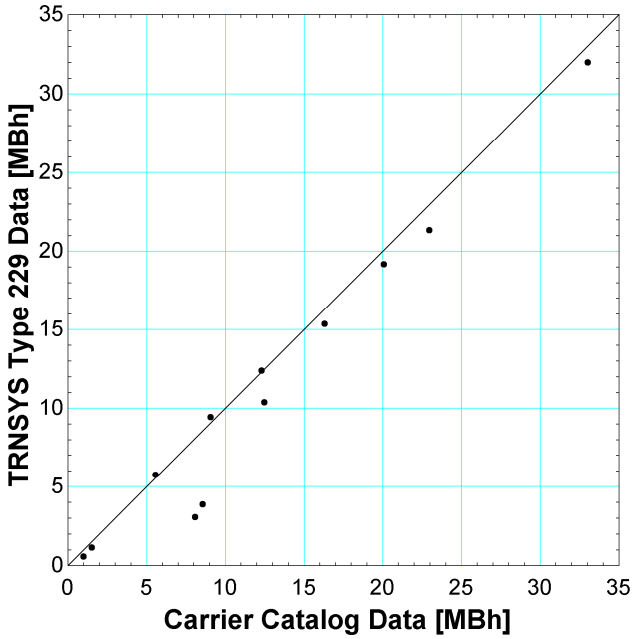

Figure A.12: A comparison of total heating capacity results for a 2 Ton SEER 16.5 heat pump. Each point represents a different operating condition. The TRNSYS data used the original Type 229 normalized data files and are compared to Carrier Performance data. Points falling on the 45° indicate for that specific operating condition that TRNSYS is agreement with the Carrier data.

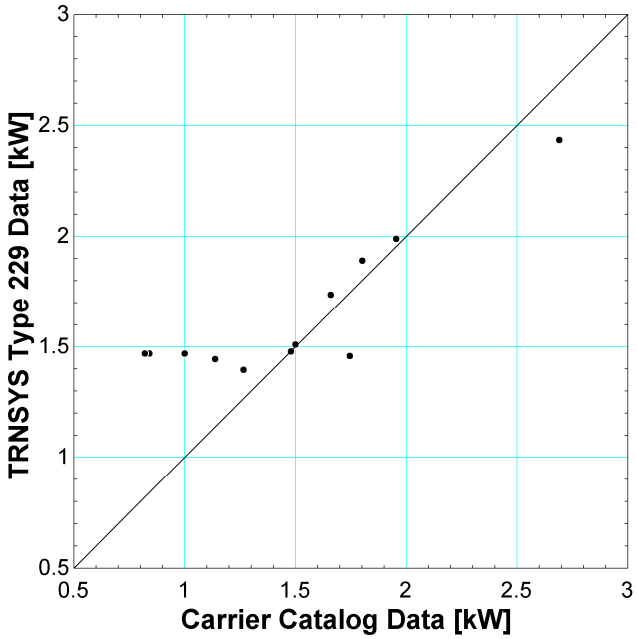

Figure A.13: A comparison of heating power consumption results for a 2 Ton SEER 16.5 heat pump. Each point represents a different operating condition. The TRNSYS data used the original Type 229 normalized data files and are compared to Carrier Performance data. Points falling on the 45° indicate for that specific operating condition that TRNSYS is agreement with the Carrier data. This original Type 229 data file over predicted the power consumption, as seen at 1.5 kW.

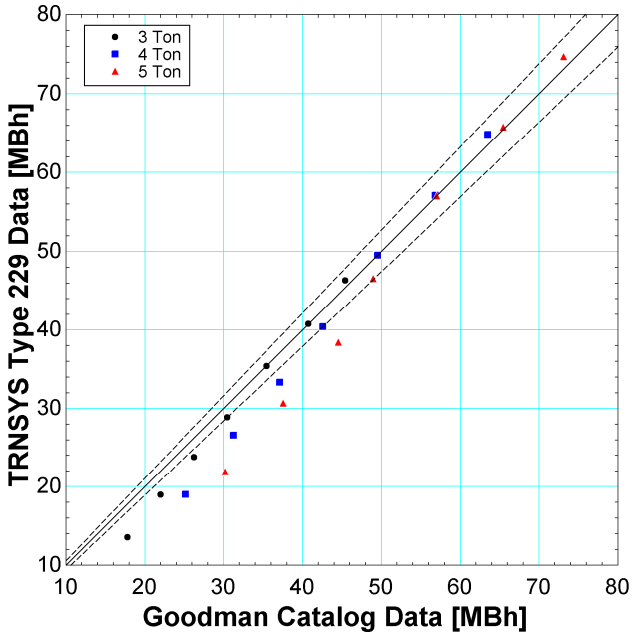

Figure A.14: Heating capacity results using original Type 229 data file for the SEER 18 heat pump. Each point represents a specific operating condition specified by the indoor and outdoor drybulb temperatures. The dashed lines represent a percent error of 5%.

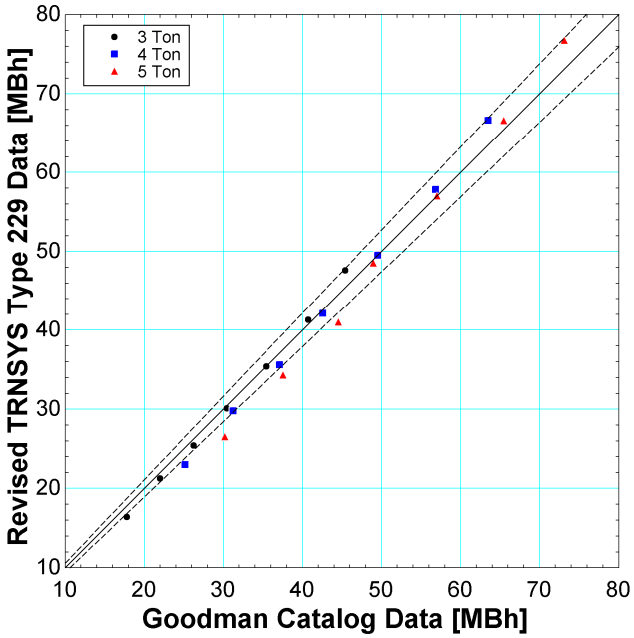

Figure A.15: Capacity results using revised Type 229 data file for the SEER 18 heat pump. Each point represents a specific operating condition specified by the indoor and outdoor drybulb temperatures. The dashed lines represent a percent error of 5%. By using this revised file, nearly all of the data points fall within the 5% error lines, a significant improvement over the original data file.

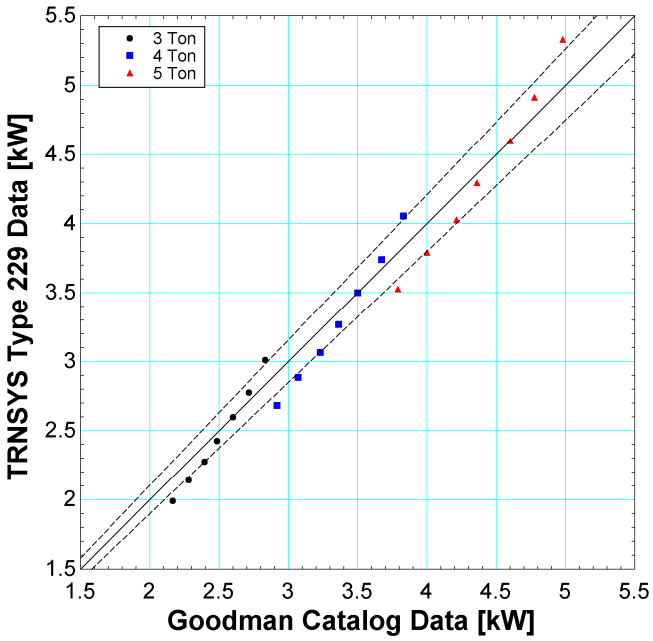

Figure A.16: Heating power consumption results using original Type 229 data file for the SEER 18 heat pump. Each point represents a specific operating condition specified by the indoor and outdoor drybulb temperatures. The dashed lines represent a 5% error.

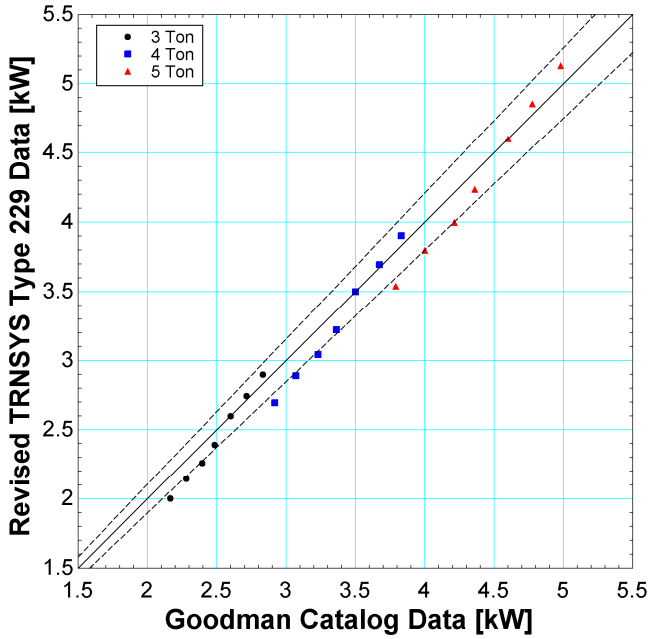

Figure A.17: Heating power consumption results using revised Type 229 data file for the SEER 18 heat pump. Each point represents a specific operating condition specified by the indoor and outdoor drybulb temperatures. The dashed lines represent a 5% error.

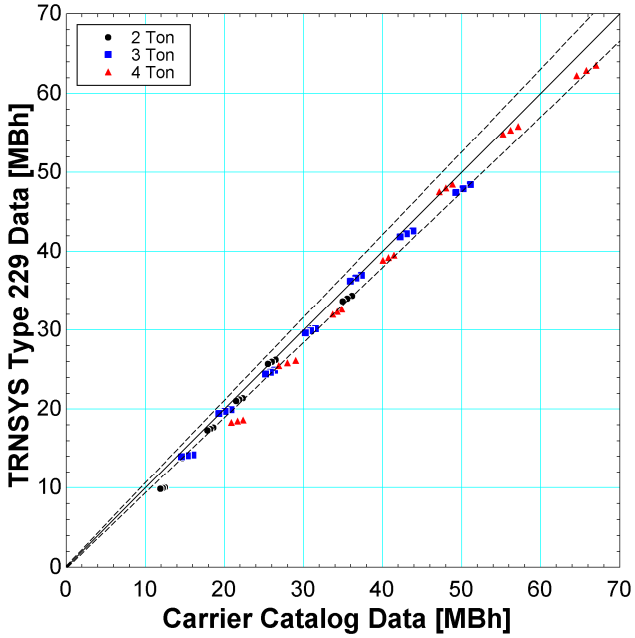

Figure A.18: Heating capacity results using the original Type 229 data file for the SEER 16.5 heat pump. Each point represents a specific operating condition specified by the indoor and outdoor drybulb temperatures. The dashed lines represent a percent error of 5%.

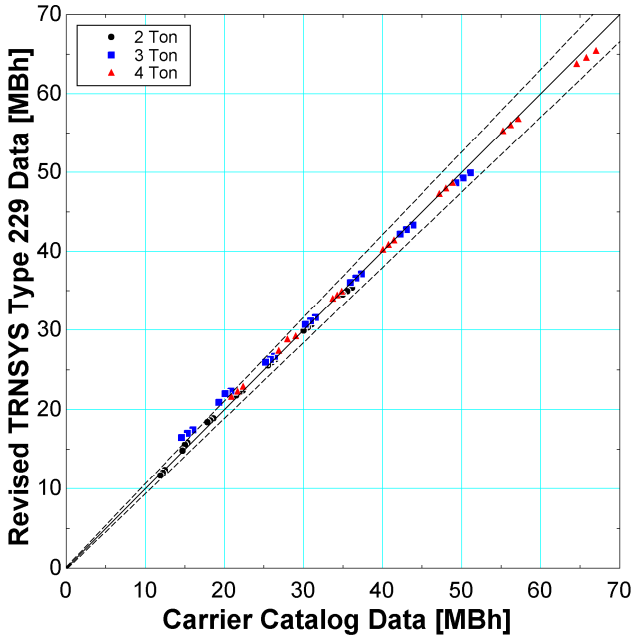

Figure A.19: Capacity results using revised Type 229 data file for the SEER 16.5 heat pump. Each point represents a specific operating condition specified by the indoor and outdoor drybulb temperatures. The dashed lines represent a 5% error. When compared to the original Type 229 data file, all the points fall within the 5% error lines.

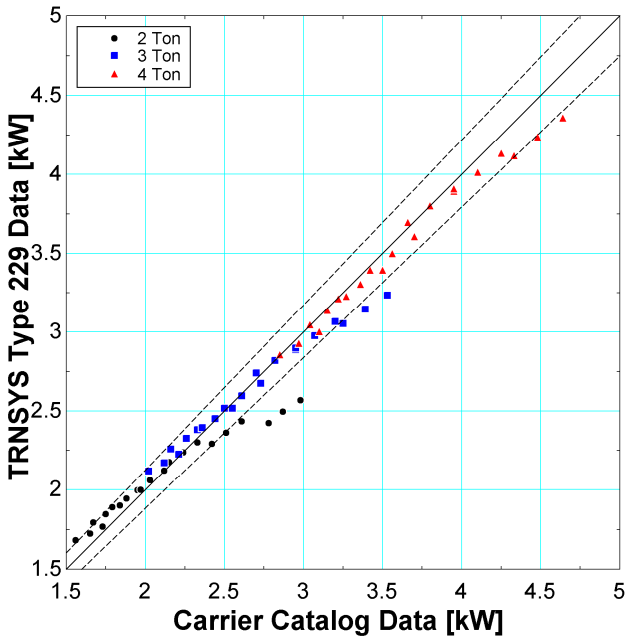

Figure A.20: Heating power consumption results using original Type 229 data file for the SEER 16.5 heat pump. Each point represents a specific operating condition specified by the indoor and outdoor drybulb temperatures. The dashed lines represent a 5% error.

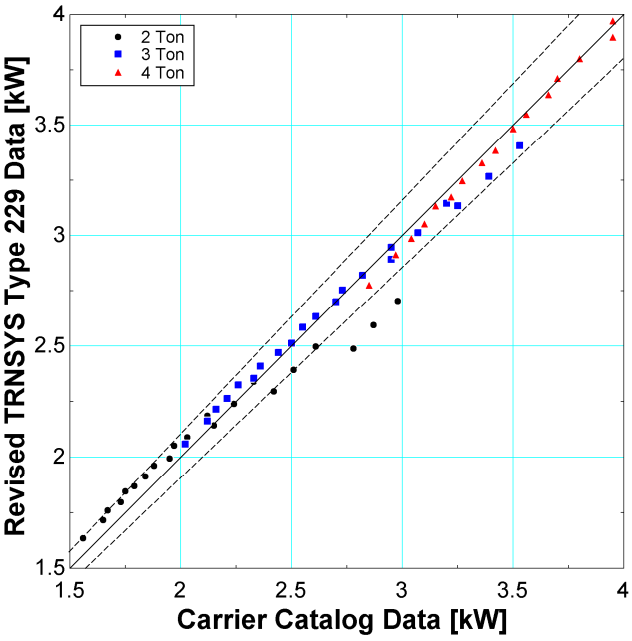

Figure A.21: Heating power consumption results using revised Type 229 data file for the SEER 16.5 heat pump. Each point represents a specific operating condition specified by the indoor and outdoor drybulb temperatures. The dashed lines represent a 5% error. This data agrees with the Carrier data as a majority of the points fall on the 45° diagonal line.

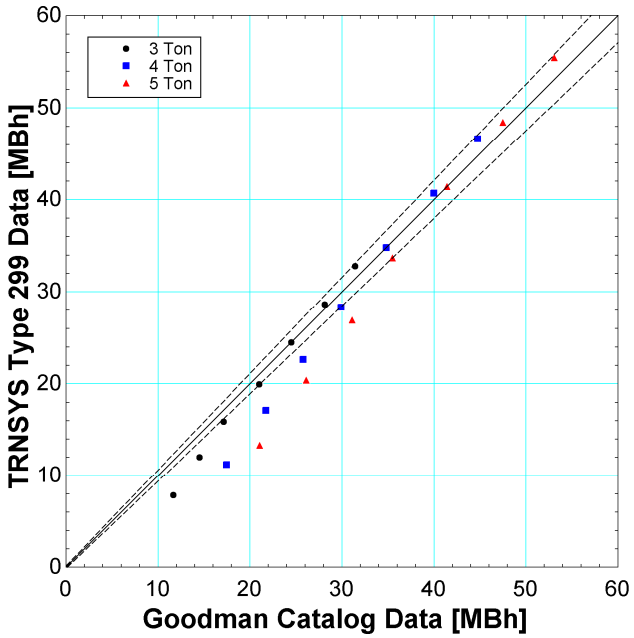

Figure A.22: Heating capacity results using original Type 229 data file for the SEER 18 heat pump. Each point represents a specific operating condition specified by the indoor and outdoor drybulb temperatures. The dashed lines represent a 5% error.

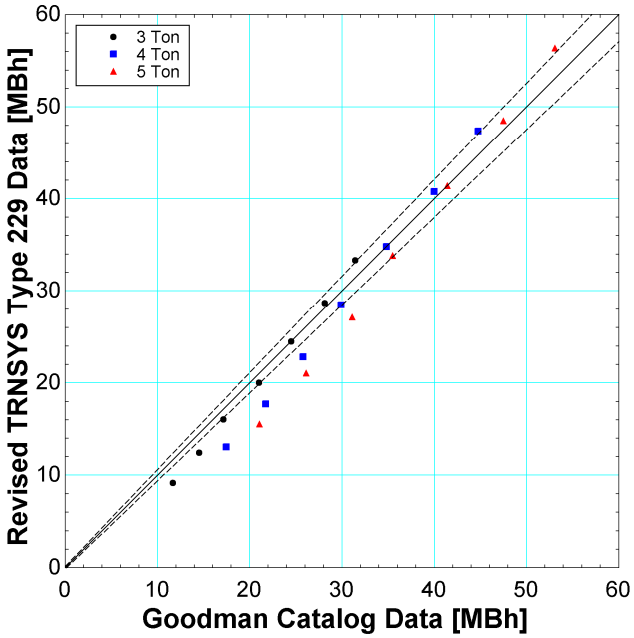

Figure A.23: Heating capacity results using revised Type 229 normalized data file for the SEER 18 heat pump. Each point represents a specific operating condition specified by the indoor and outdoor drybulb temperatures. The dashed lines represent a 5% error.

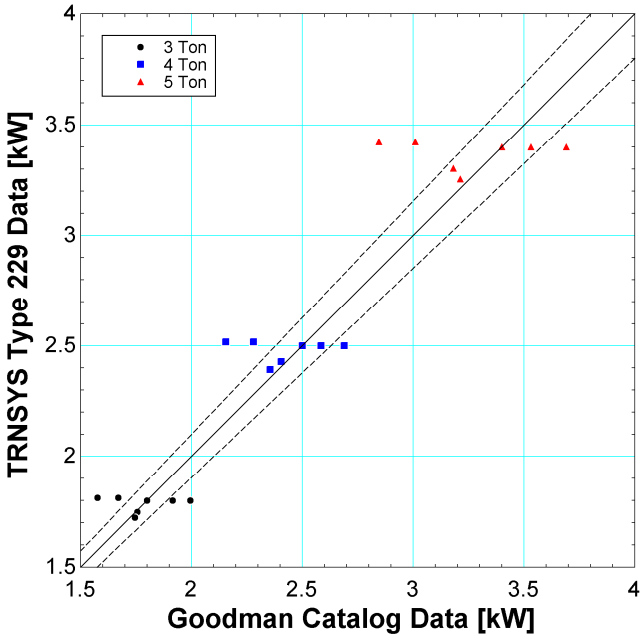

Figure A.24: Heating power consumption results using the original Type 229 data file for the SEER 18 heat pump. Each point represents a specific operating condition specified by the indoor and outdoor drybulb temperatures. The dashed lines represent a 5% error. This data file exhibited a poor ability to reproduce the manufacturer's data.

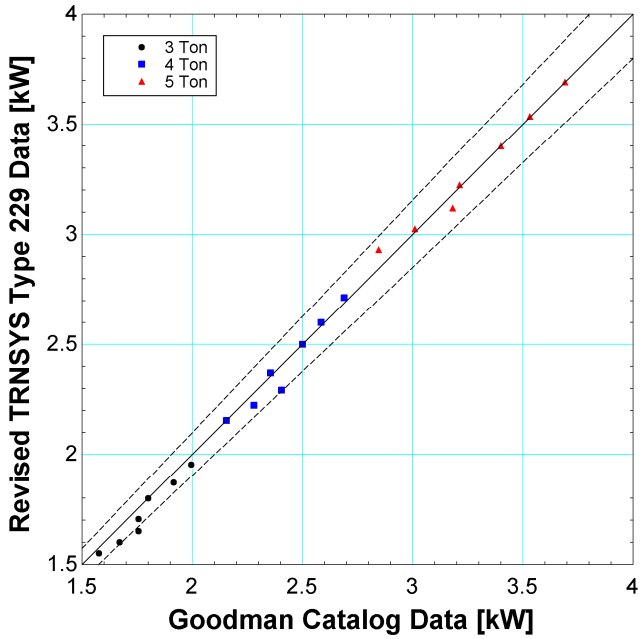

Figure A.25: Heating power consumption results using revised Type 229 normalized data file for the SEER 18 heat pump. Each point represents a specific operating condition specified by the indoor and outdoor drybulb temperatures. The dashed lines represent a 5% error. These results show a much better ability to reproduce the manufacturer's data.

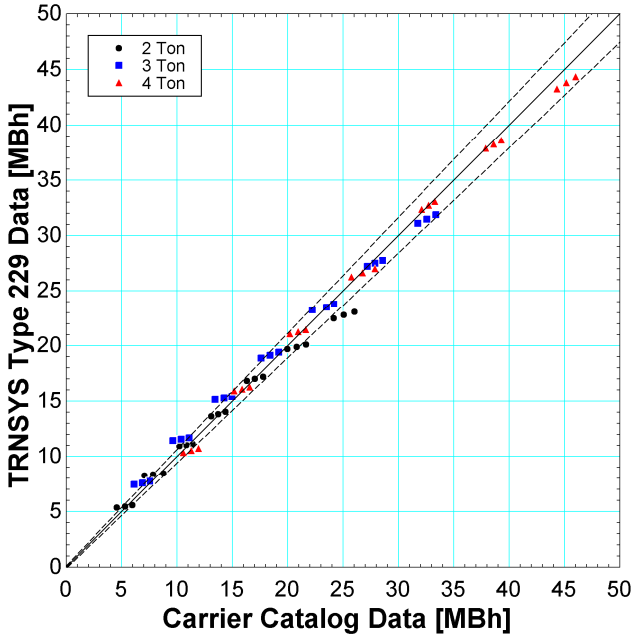

Figure A.26: Heating capacity results using original Type 229 data file for the SEER 16.5 heat pump. Each point represents a specific operating condition specified by the indoor and outdoor drybulb temperatures. The dashed lines represent a 5% error.

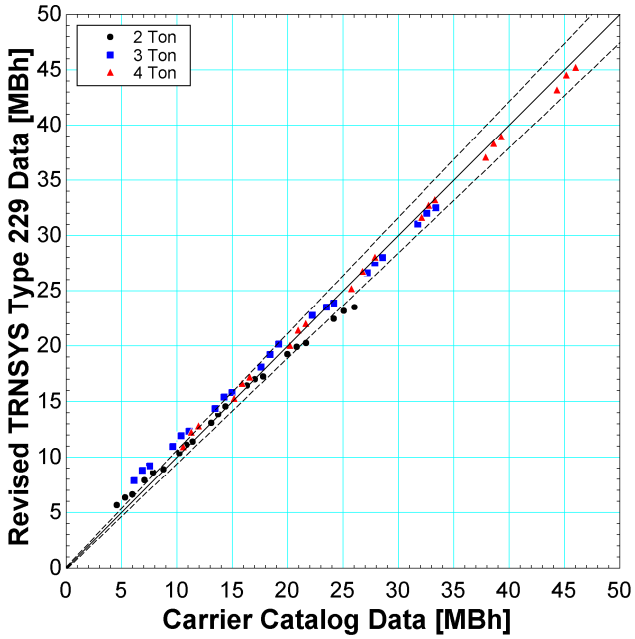

Figure A.27: Heating capacity results using revised Type 229 normalized data file for the SEER 16.5 heat pump. Each point represents a specific operating condition specified by the indoor and outdoor drybulb temperatures. The dashed lines represent a 5% error.

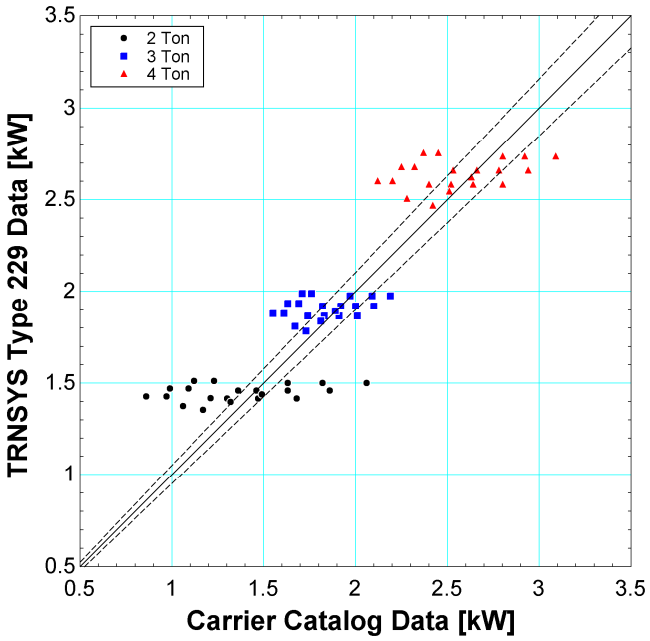

Figure A.28: Heating power consumption results using original Type 229 data file for the SEER 16.5 heat pump. Each point represents a specific operating condition specified by the indoor and outdoor drybulb temperatures. The dashed lines represent a 5% error. Again, the original normalized data file does not accurately reproduce the manufacturer's data.

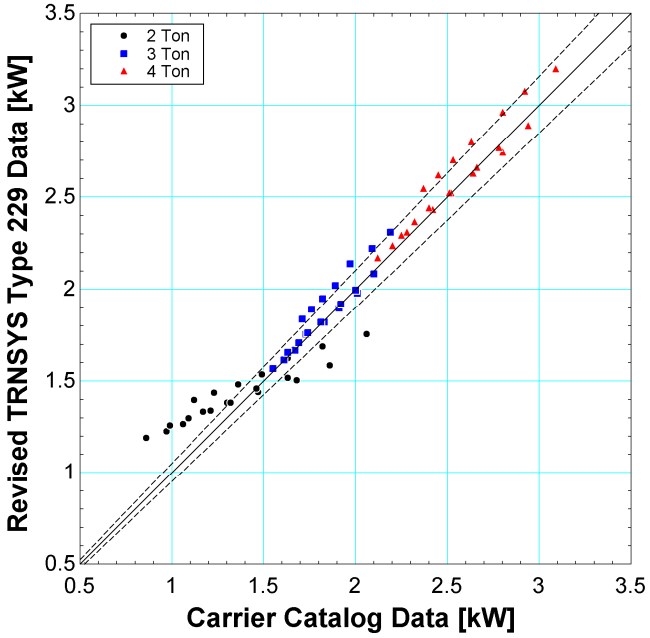

Figure A.29: Heating power consumption results using revised Type 229 normalized data file for the SEER 16.5 heat pump. Each point represents a specific operating condition specified by the indoor and outdoor drybulb temperatures. The dashed lines represent a 5% error.

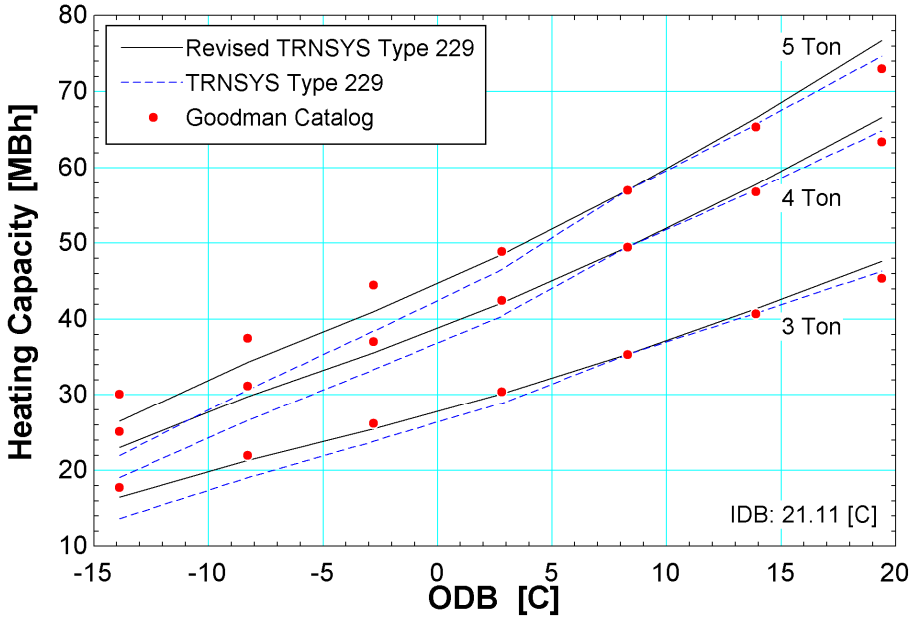

Figure A.30: Heating capacity results for the SEER 18 heat pump in the high stage vs. outdoor drybulb temperature. The indoor dry bulb temperature is 21.11 [C]. Improvements in reproducing the manufacturer's trends are made by using revised normalized file.

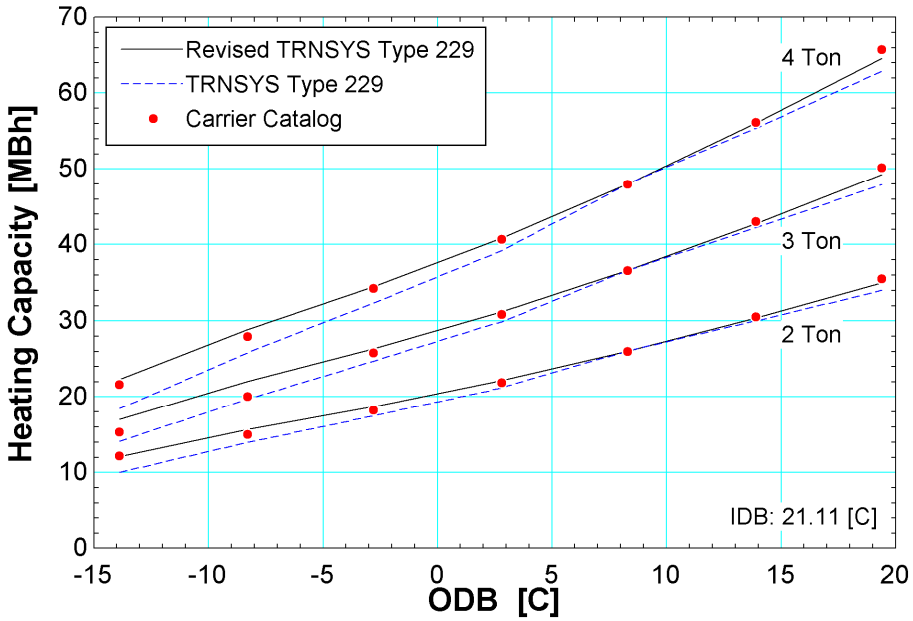

Figure A.31: Heating capacity results for the SEER 16.5 heat pump in the high stage vs. outdoor drybulb temperature. The indoor dry bulb temperature is 21.11 [C]. Improvements in reproducing the manufacturer's trends are made by using revised normalized file.

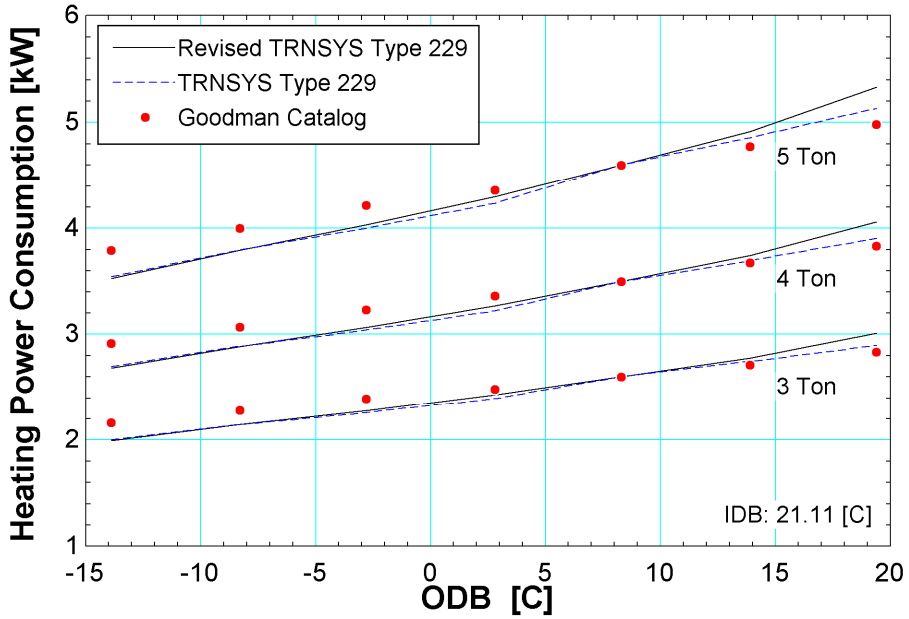

Figure A.32: Heating power consumption results for the SEER 18 heat pump in the high stage vs. outdoor drybulb temperature. The indoor dry bulb temperature is 21.11 [C]. In this case, the old normalized file is more accurate than the revised file.

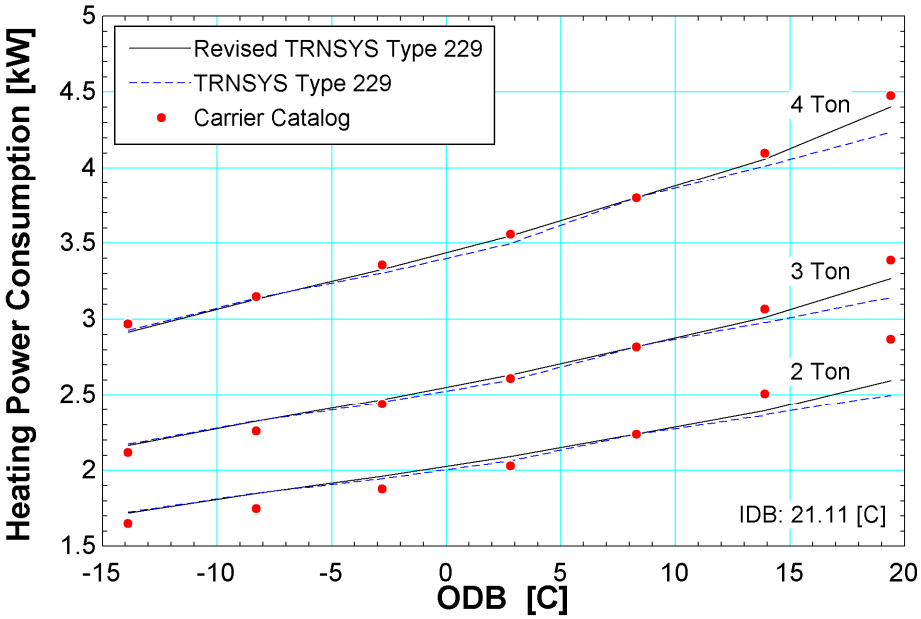

Figure A.33: Heating power consumption results for the SEER 16.5 heat pump in the high stage vs. outdoor drybulb temperature. The indoor dry bulb temperature is 21.11 [C]. Here, the revised Type 229 data file more accurately represents the manufacturer's data.

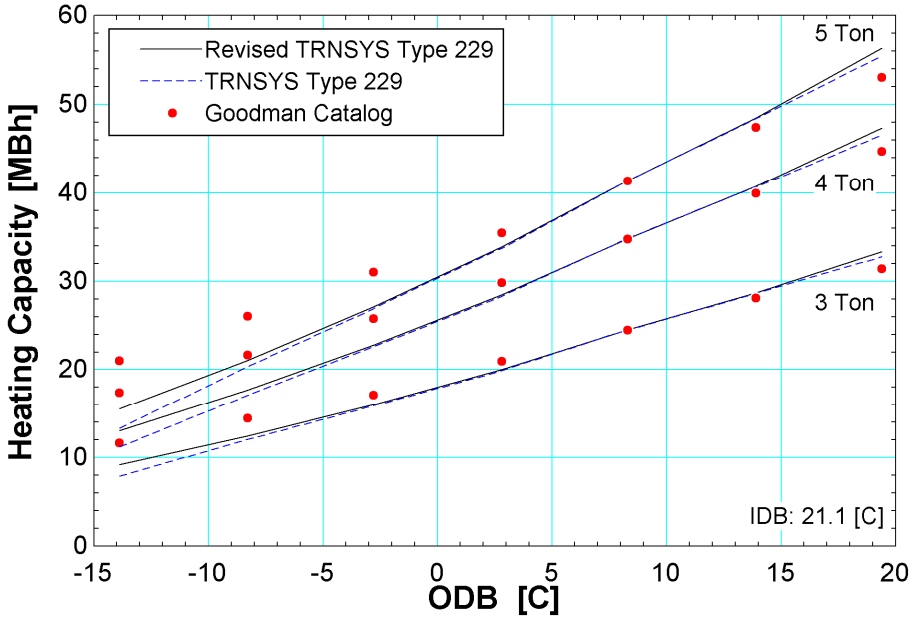

Figure A.34: Heating capacity results for the SEER 18 heat pump in the low stage vs. outdoor dry bulb temperature. The indoor dry bulb temperature is 21.11 [C]. In this case, both normalized files struggle to reproduce the manufacturer's data at cold outdoor temperatures. This is a possibility as shown before it is difficult to normalize many heat pumps to a single number.

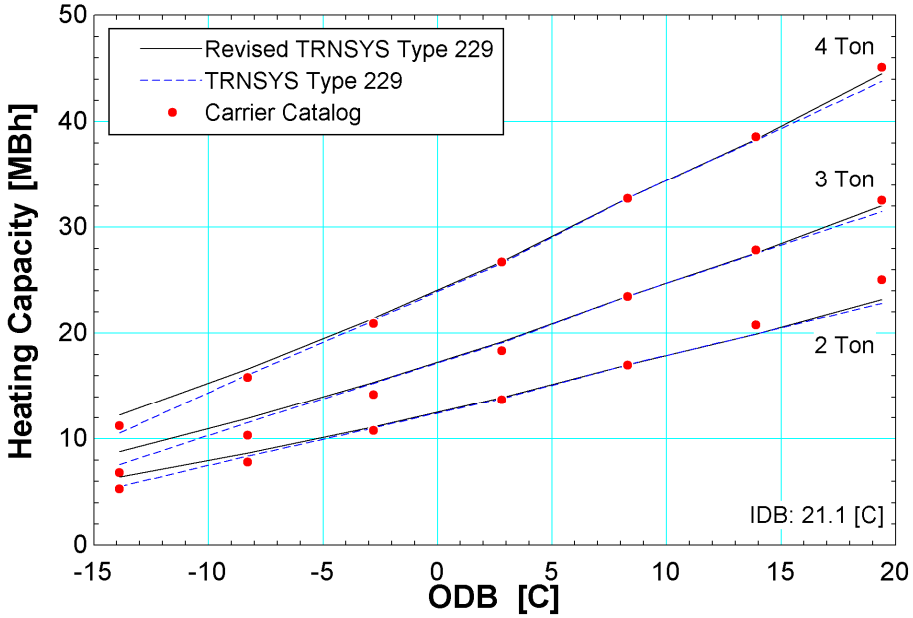

Figure A.35: Heating capacity results for the SEER 16.5 heat pump in the low stage vs. outdoor dry bulb temperature. The indoor dry bulb temperature is 21.11 [C].

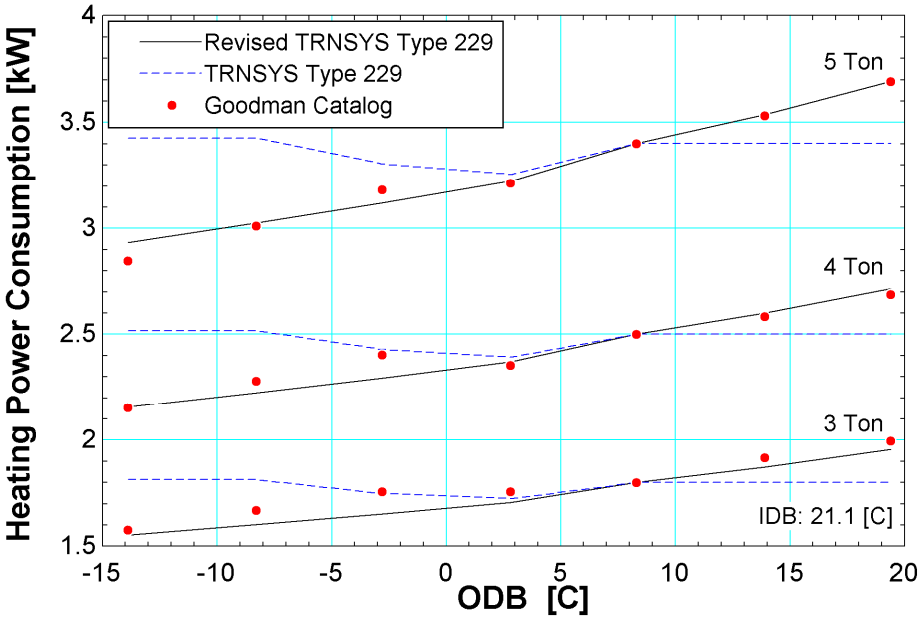

Figure A.36: Heating power consumption results for the SEER 18 heat pump in the low stage vs outdoor drybulb temperature. The indoor dry bulb temperature is 21.11 [C]. Vast improvements are made by using the revised normalized file.

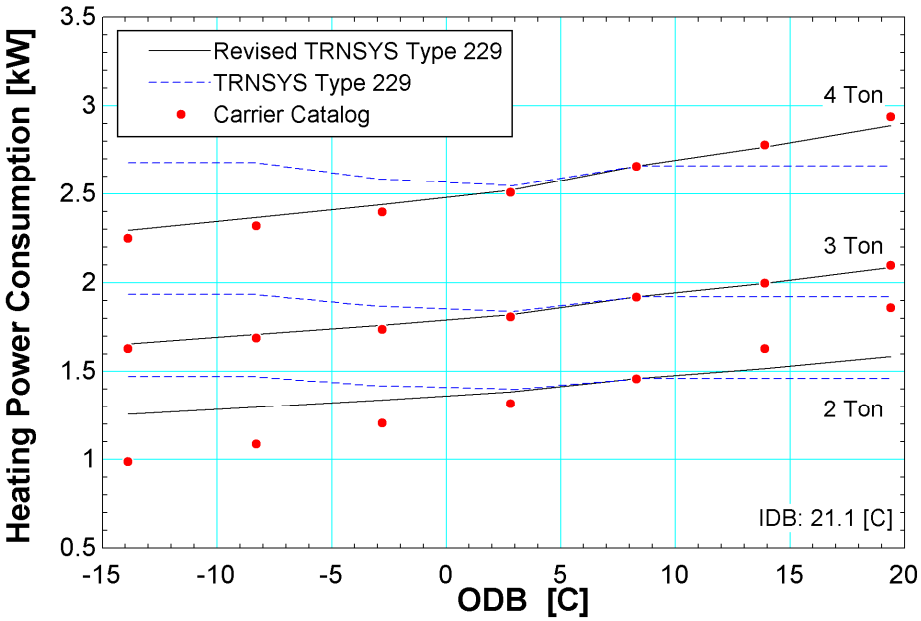

Figure A.37: Heating power consumption results for the SEER 16.5 heat pump in the low stage vs. outdoor dry bulb temperature. The indoor dry bulb temperature is 21.11 [C]. Again, vast improvements are made by using the revised data file.

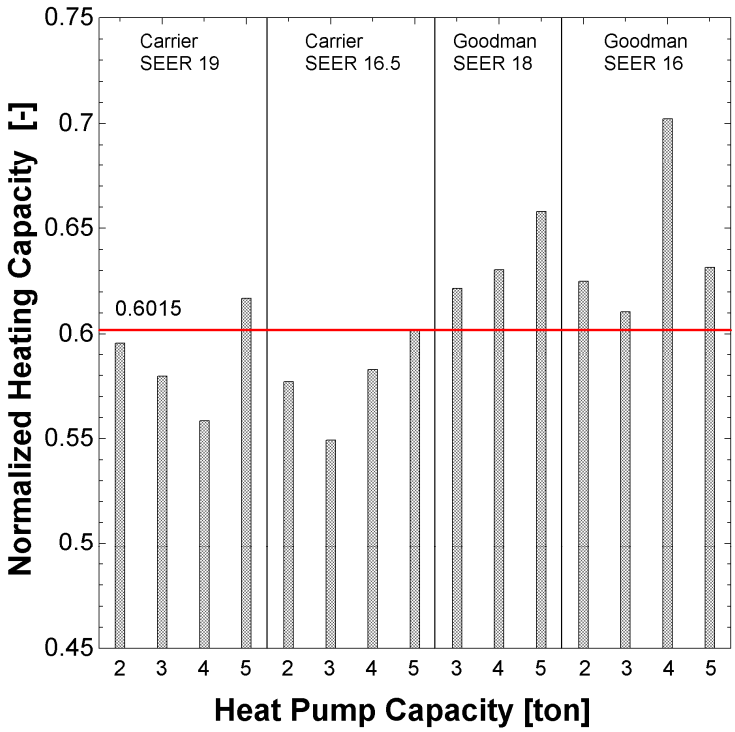

Figure A.38: Comparing normalized values for capacity. Operating conditions: IDB - 26.67, ODB - 46.1, IWB - 21.67. The red line signifies normalized value used in data file at this operating condition. This plot indicates the difficulty in using a single value to represent the heating capacity for various manufacturers, capacities and efficiencies at a single operating point.

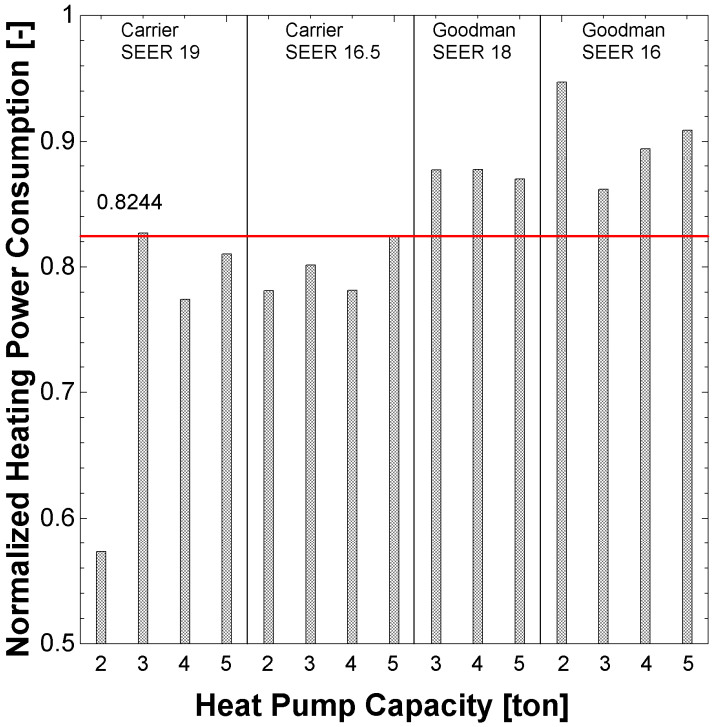

Figure A.39: Comparing normalized values for heating power. Operating conditions: IDB - 26.67, ODB - 46.1, IWB - 21.67. The red line signifies normalized value used in data file at this operating condition. This plot indicates the difficulty in using a single value to represent the heating power consumption for various manufacturers, capacities and efficiencies at a single operating point.

Appendix B

SOLAR COLLECTOR CERTIFICATION AND RATING	CERTIFIED SOLAR COLLECTOR	
SRCC OG-100	SUPPLIER:	Alternate Energy Technologies 851 Energy Cove Court Green Cove Springs, FL 32043 USA
	MODEL:	Alternate Energy AE-50
	COLLECTOR TYPE:	Glazed Flat-Plate
	CERTIFICATION#:	2002001H
	Original Certification Date:	05-AUG-05

COLLECTOR THERMAL PERFORMANCE RATING

Kilowatt-hours Per Panel Per Day				Thousands of BTU Per Panel Per Day			
CATEGORY (Ti-Ta)	CLEAR DAY (6.3 kWh / m^2.day)	MILDLY CLOUDY (4.7 kWh / m^2.day)	CLOUDY DAY (3.1 kWh / m^2.day)	CATEGORY (Ti-Ta)	CLEAR DAY (2000 Btu / ft^2.day)	MILDLY CLOUDY (1500 Btu / ft^2.day)	CLOUDY DAY (1000 Btu / ft^2.day)
A (-5 °C)	19.2	14.5	9.8	A (-9 °F)	65.5	49.5	33.6
B (5 °C)	17.5	12.8	8.1	B (9 °F)	59.6	43.5	27.6
C (20 °C)	14.6	10.0	5.5	C (36 °F)	49.9	34.2	18.6
D (50 °C)	8.8	4.7	1.0	D (90 °F)	30.0	15.9	3.5
E (80 °C)	3.4	0.5	0.0	E (144 °F)	11.6	1.7	0.0

A- Pool Heating (Warm Climate) B- Pool Heating (Cool Climate) C- Water Heating (Warm Climate) D- Water Heating (Cool Climate) E- Air Conditioning

COLLECTOR SPECIFICATIONS

Gross Area: 4.664 m^2 50.20 ft^2
Net Aperture Area: 4.40 m^2 47.36 ft^2
Dry Weight: 82.5 kg 182. lb
Fluid Capacity: 6.4 liter 1.7 gal
Test Pressure: 1103. KPa 160. psig

COLLECTOR MATERIALS

Frame: Anodized Aluminum
Cover (Outer): Low Iron Tempered Glass
Cover (Inner): None

Pressure Drop

Flow		ΔP	
ml/s	gpm	Pa	in H_2O

Absorber Material: Tube - Copper / Plate - Copper Fin
Insulation Side: Polyisocyanurate
Absorber Coating: Selective Coating
Insulation Back: Polyisocyanurate

TECHNICAL INFORMATION

Efficiency Equation [NOTE: Based on gross area and (P)=Ti-Ta]

				Y INTERCEPT	SLOPE
SI Units:	η= 0.691	-3.39600 (P)/I	-0.01968 $(P)^2/I$	0.706	-4.910 $W/m^2.°C$
IP Units:	η= 0.691	-0.59821 (P)/I	-0.00193 $(P)^2/I$	0.706	-0.865 $Btu/hr.ft^2.°F$

Incident Angle Modifier [(S)=1/cosθ - 1, 0°<θ<=60°]

Kτα = 1	-0.194 (S)	-0.006 $(S)^2$	
Kτα = 1	-0.20 (S)	Linear Fit	

Test Fluid: Water
Test Flow Rate: 20.1 ml /s.m^2 0.0296 gpm/ft^2

REMARKS:

March, 2012
Certification must be renewed annually, For current status contact:
SOLAR RATING & CERTIFICATION CORPORATION
400 High Point Drive, Suite 400 ♦ Cocoa, Florida 32926 ♦ (321) 213-6037 ♦ Fax (321) 821-0910